Wolfgang Lubitz

Max Planck Institute for Chemical Energy Conversion
Mülheim/Ruhr, Germany

Light-Induced Water Splitting and Hydrogen Production in Nature:
Blueprints for the Design of Chemical Catalysts

Weizmann Institute of Science

Alternative Energy Seminar,
Weizmann Institute, Rehovot, Israel – 24 February 2013

Chemical Energy Storage - Solar Fuel Production

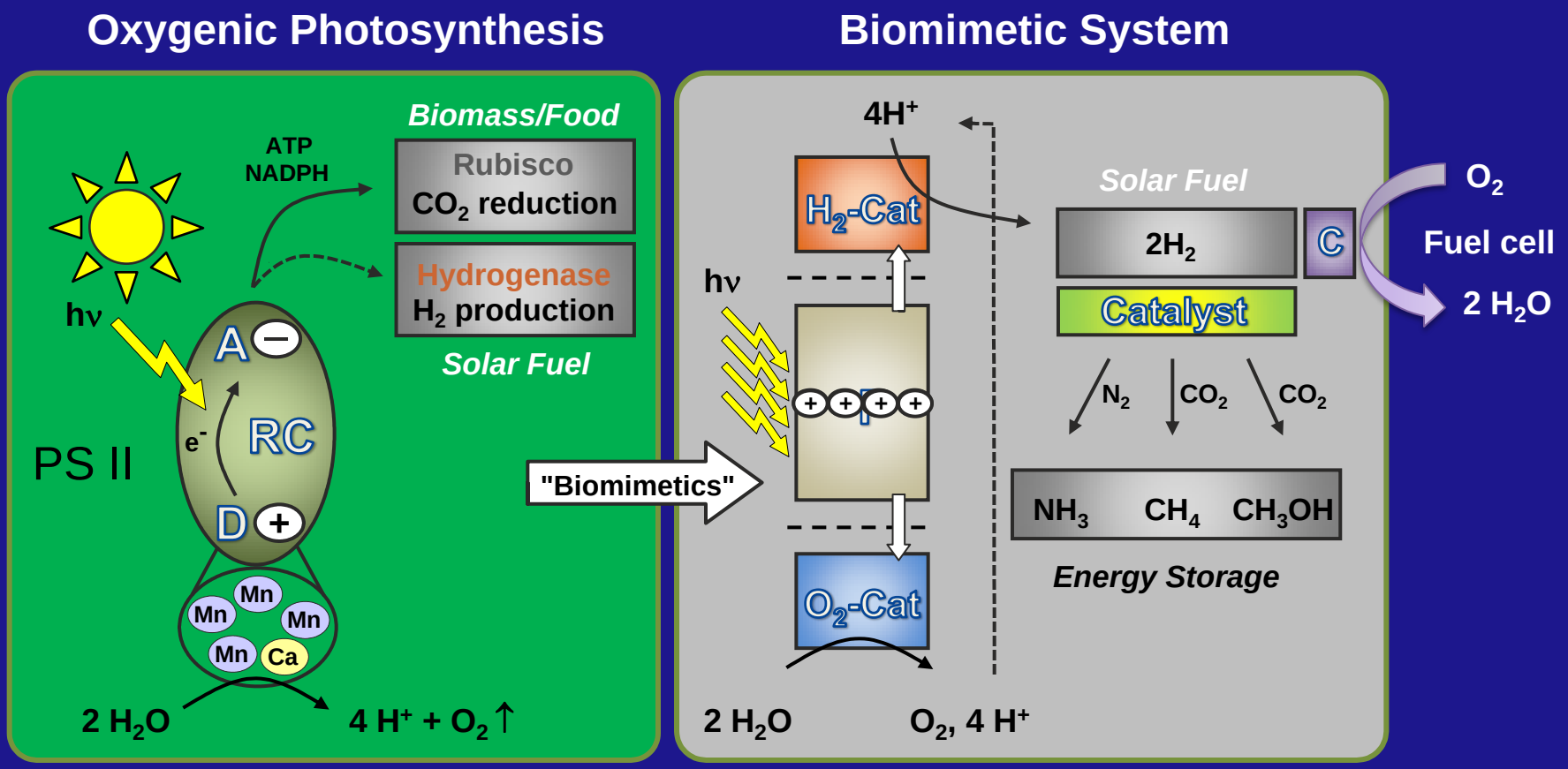

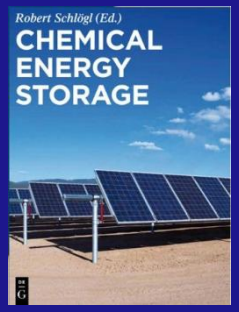

Molecular Concepts of Water Splitting: Nature's Approach

Nicholas Cox, Wolfgang Lubitz, MPI for Chemical Energy Conversion, Mülheim/Ruhr

Hydrogen: Energy Carrier of the Future

Basic material for production of other energy carriers (e. g. methanol) other chemicals and other uses (e. g. ammonia)

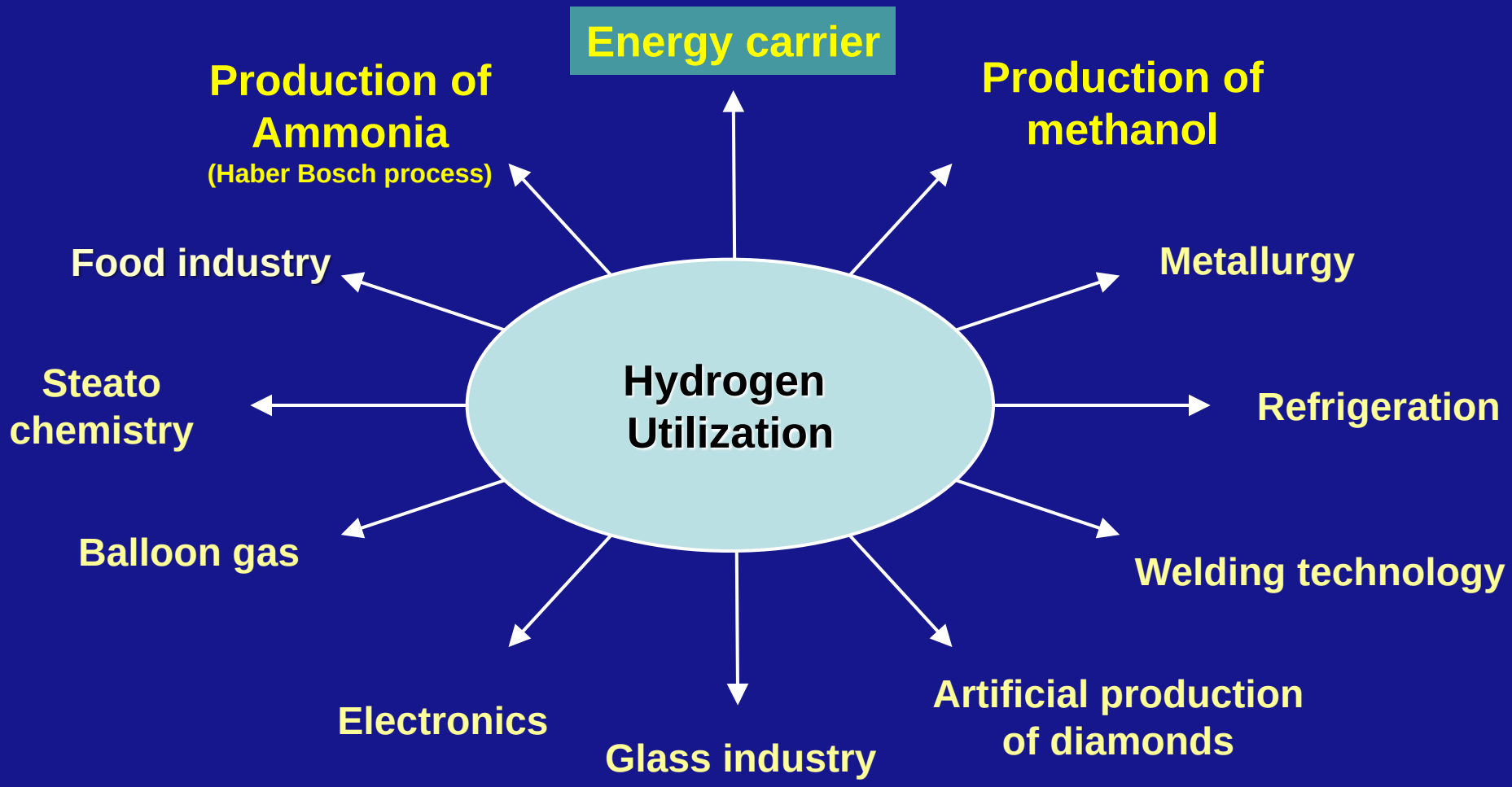

Karamanolis: Wasserstoff, Energieträger der Zukunft, 2001, Elektra Verlag

HYDROGEN PRODUCTION

1. Hydrocarbons
   Reformation of natural gas, coal

2. Water electrolysis
   Electricity from nuclear power or fossil resources
   Renewable energy (photovoltaics, wind ….)

3. Thermal methods
   Waste heat (nuclear power)
   Solar-Tower

4. Biological / Biomimetic Methods
   A. Modified natural systems (biophotolysis / photosynthesis)
   B. Semiartificial systems (enzymes on electrodes)
   C. Biomimetic systems (artificial photosynthesis, catalysis)

Photosynthesis:

Structure and Function of Photosystem II and the Water Oxidizing Complex

Oxygenic Photosynthesis

sunlight + carbon dioxide  water → 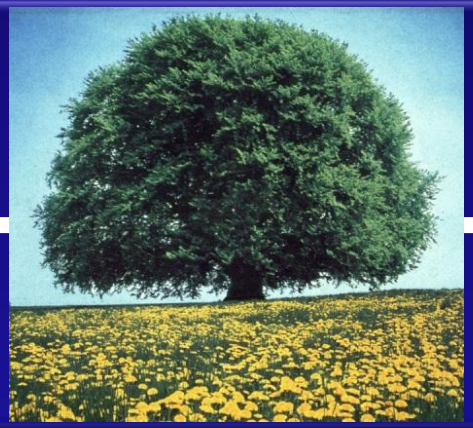 → biomass  carbo-hydrates + oxygen

$$H_2O + CO_2 \xrightarrow[\text{chlorophyll}]{\text{light}} (CH_2O) + O_2 \uparrow$$

carbohydrates

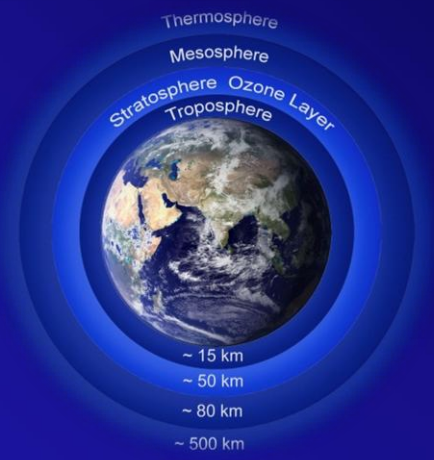

oxygen atmosphere
ozone layer

food
renewable raw materials

fossil fuels
oil, coal, gas

Photosynthesis: Light & Dark Reactions

O_2

CO_2

H_2O

section of a leaf

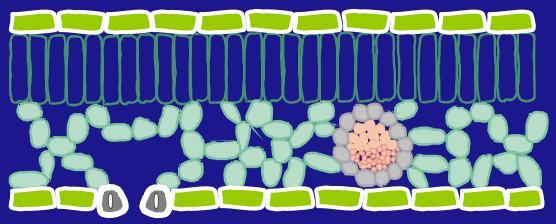

chloroplast

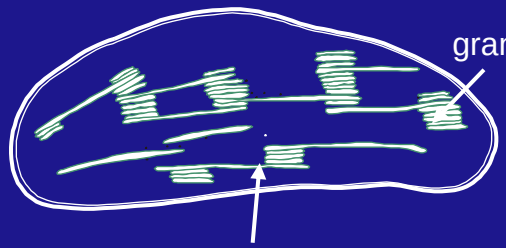

Photosynthetic membrane

dark reactions
Calvin cycle

CO_2-fixation to carbohydrates (CH_2O) enzyme Rubisco

CO_2

NADPH

ATP

ADP+Pi

hν

hν

Antenna (Lhcb)

Stroma

Membrane

Lhcb1+2+3

Lhcb4 Lhcb5 Lhcb6

C(CP43) B(CP47)

Q_A Fe Q_B

D (D2) A (D1)

Phe

E F (cyt b_{559})

P680

Y_Z Y_D

Mn Mn Mn Mn

P O T Q R

(CP43) (CP47)

$^1/_2PQH_2$

PQ-pool

H^+

cyclic e transport

b_6 IV FeS

Q

cyt b_{563HP}

cyt b_{563LP}

QH_2

FeS

cyt *f*

Fe

PC

Fd

Fx A_1 A_0

Lhca 1-4

Lhca 1-4

P700

PC

$3H^+$

α β γ δ ε

oscp

CF_1

d

F_6

a b

I II III IV

CF_0

$^1/_2$ H_2O

1/4 O_2 + H^+

PS II **Cyt b_6f** **PS I** **ATP synthase**

Electron Transport in Oxygenic Photosynthesis

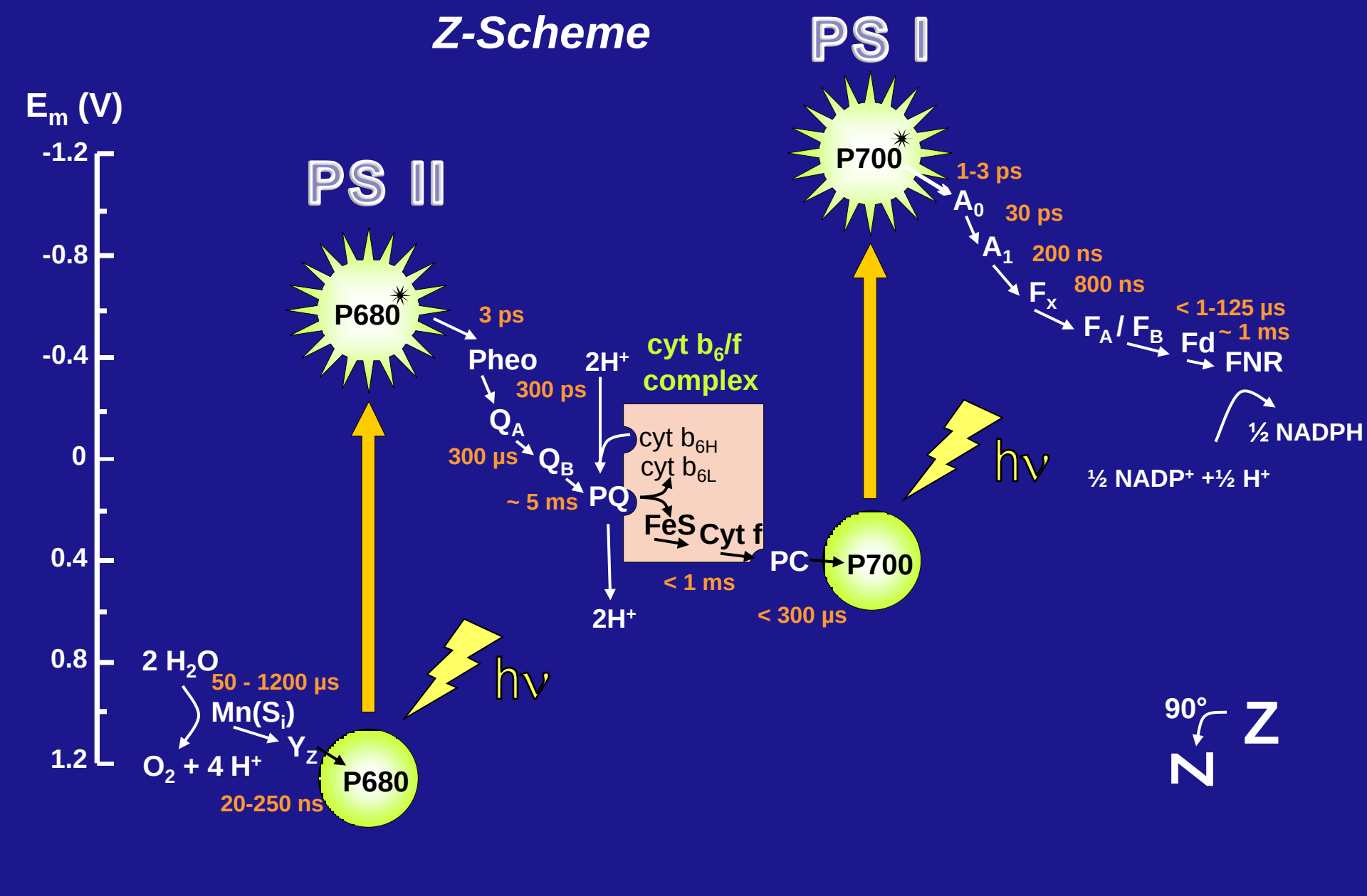

X-Ray Crystallography: Structure of Photosystem II

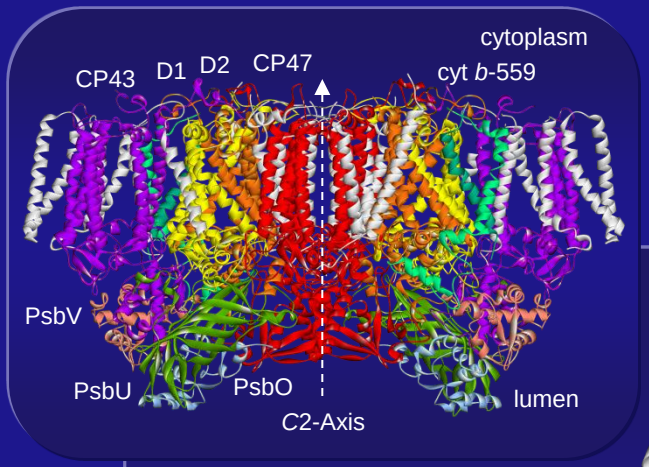

20 subunits
35 Chlorophylls
2 Pheophytins
11 Carotens
>20 lipids
2 plastoquinones
1 Fe, 2 hemes
Mn_4Ca-cluster

1300 water molecules in one monomer

T. vulcanus

Arrangement of water molecules

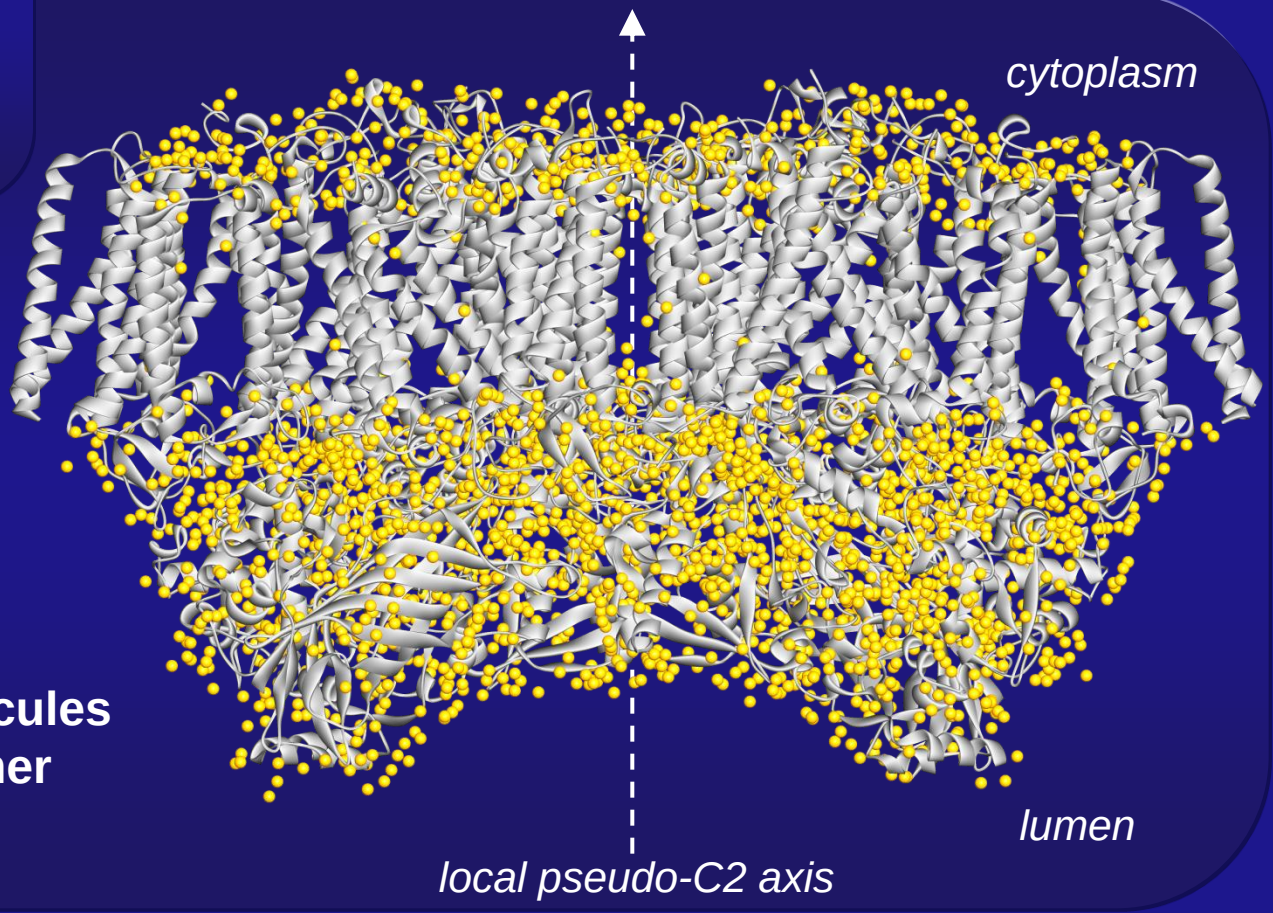

Umena, Kawakami, Shen, Kamiya, Nature 473, 55-60 (2011)

Resolution 1.9 Å

X-Ray Crystallography: Structure of Photosystem II

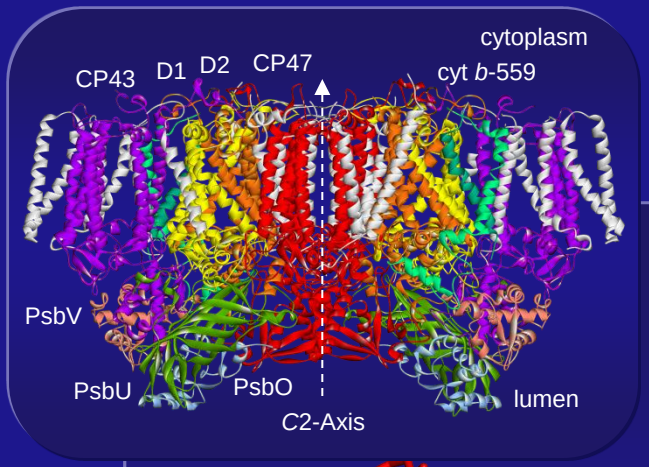

Cofactor Arrangement : Reaction Center

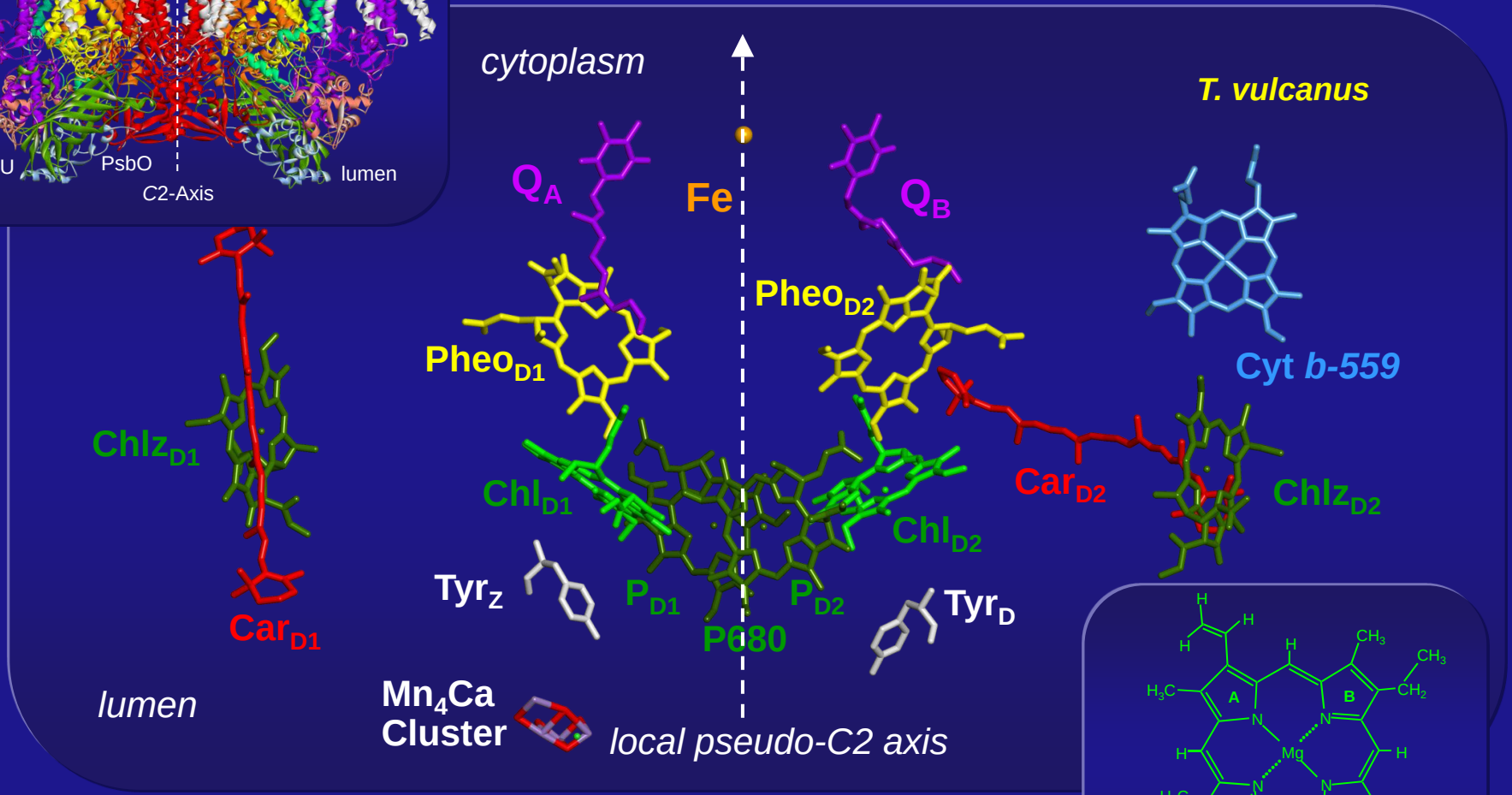

Resolution 1.9 Å

Umena, Kawakami, Shen, Kamiya, Nature 473, 55-60 (2011)

Model Structures of the Mn_4O_xCa Cluster

X-Ray-Crystallography

3.5 Å Resolution

(radiation damage)

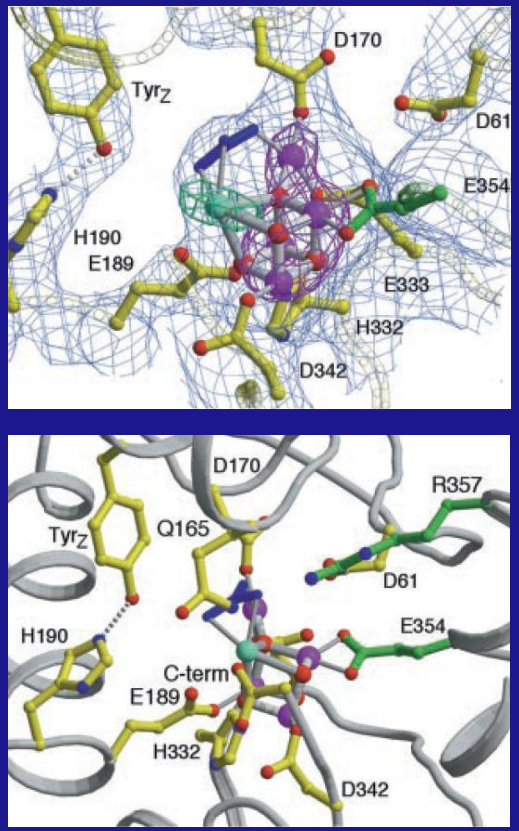

Ferreira et al.,
Science 303, 1831 (2004)

X-Ray-Crystallography

2.9 Å Resolution

(radiation damage)

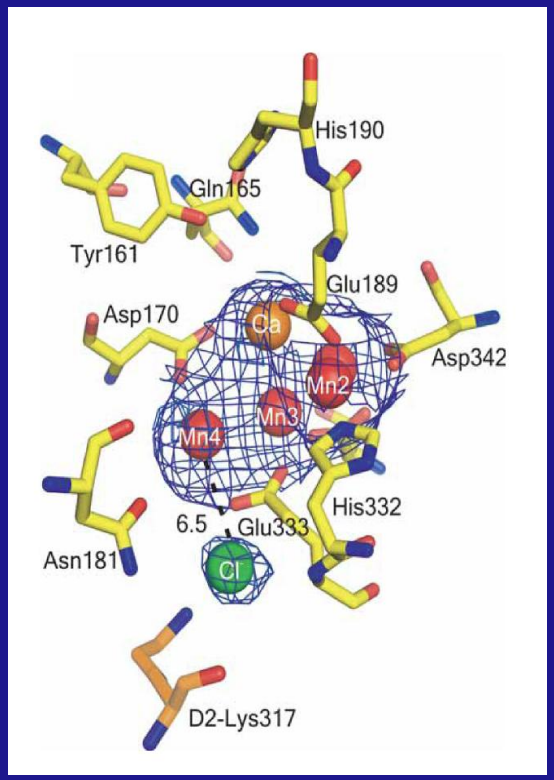

Gusko et al.,
Nat. Struct. Mol. Biol. (2009)

X-Ray-Crystallography

1.9 Å Resolution

(„little“ radiation damage)

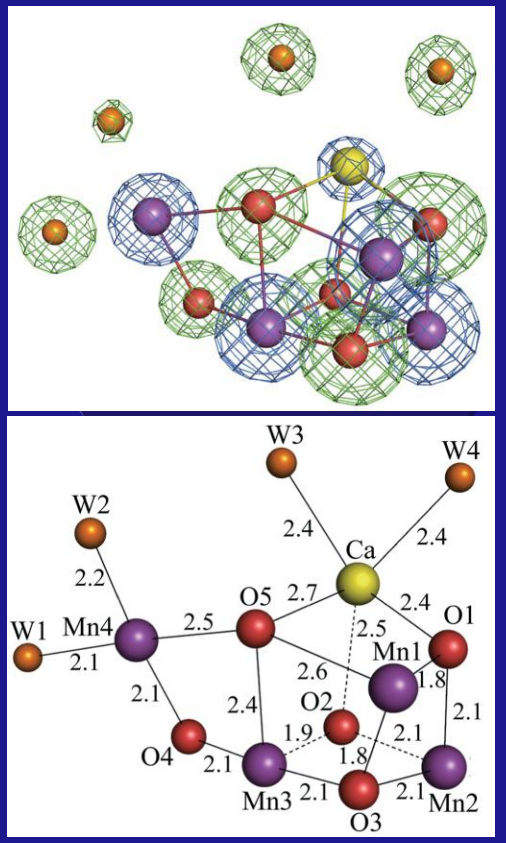

Umena et al.,
Nature (2011)

XANES and EXAFS at Different X-ray Doses

Mn XANES of PS II Crystal

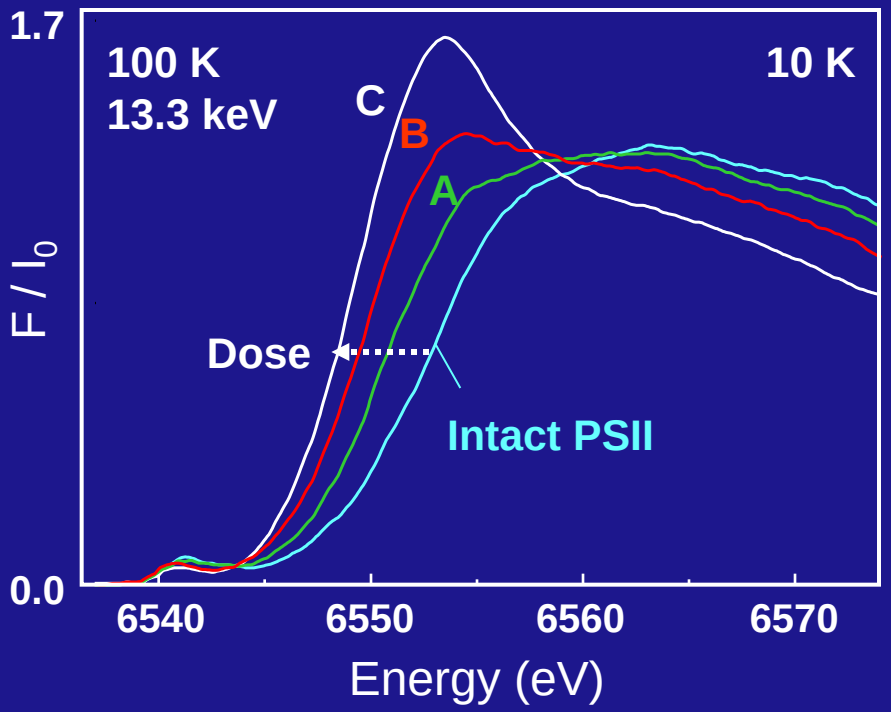

Mn Models

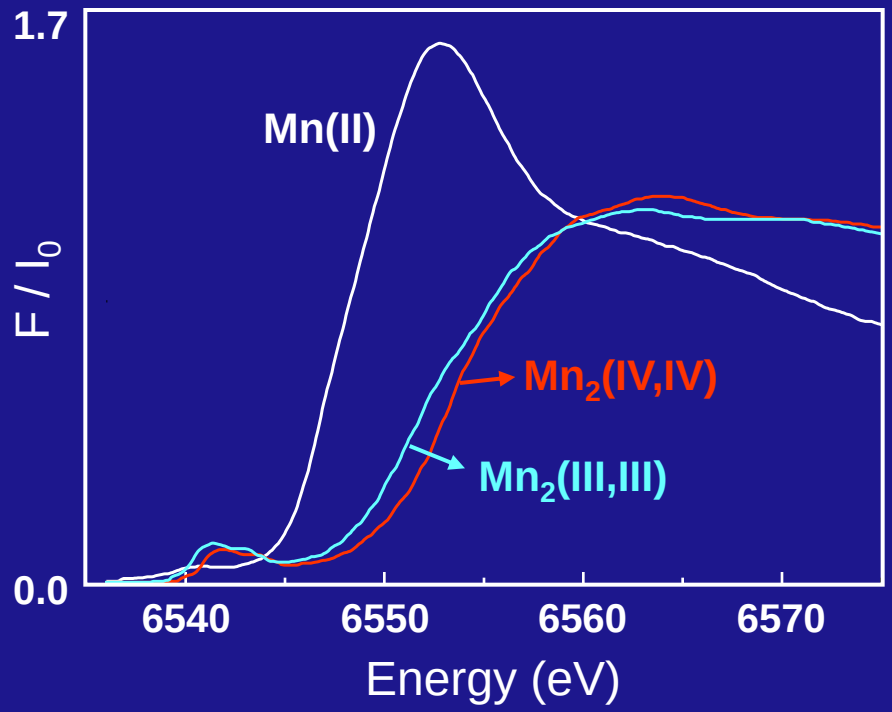

- X-ray damage reduces the $Mn_4(III_2IV_2)$ cluster (S_1 State) to Mn(II) and alters the geometric and electronic structure significantly

Yano et al. 2005 PNAS
102, 12047-12052

Yachandra, Messinger et al. 2005

Radiation Damage in X-Ray Diffraction: Photoreduction

Photoreduction of higher metal oxidation states

Mn K-edge

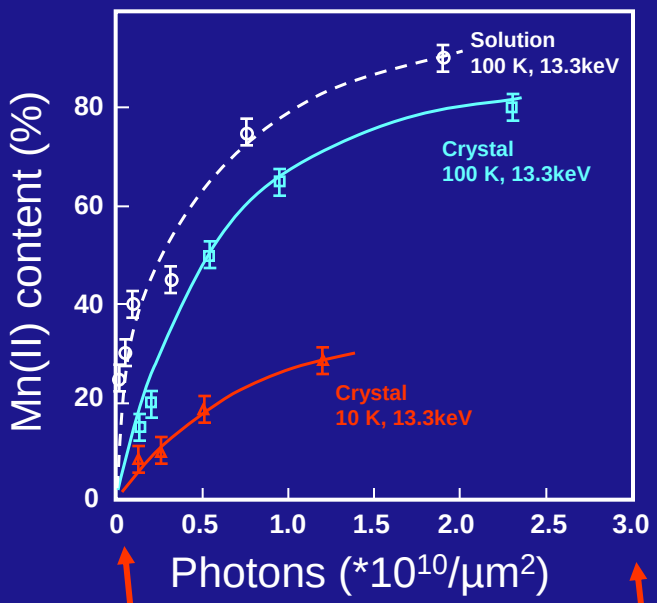

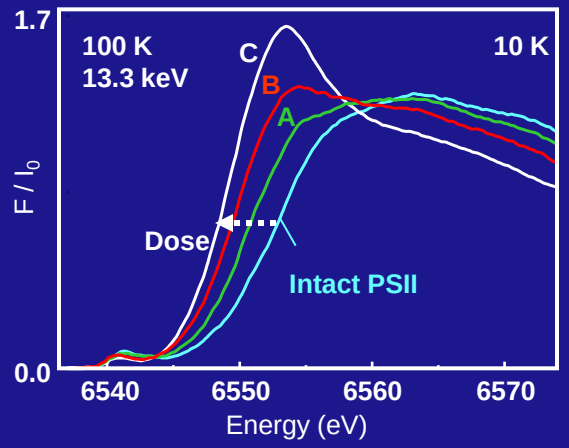

A: 25% Mn(II); 3% total dose
B: 45% Mn(II); 15% total dose
C: 75% Mn(II);~50% total dose

XAS at 10K, 6.6keV
$1*10^7$photons

XRD at 100K, 13.3 keV
$3.5*10^{10}$ photons

Mn EXAFS

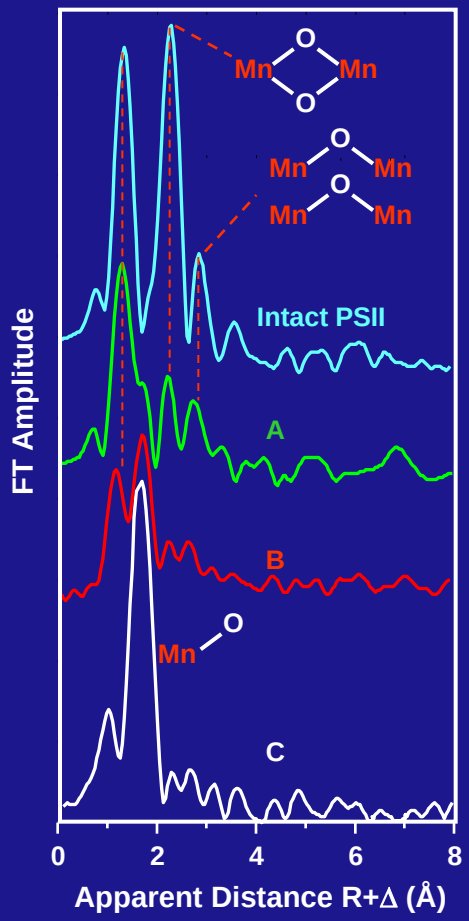

- **X-ray damage reduces the $Mn_4(III_2IV_2)$ cluster (S_1 State) to Mn(II) and alters the geometric and electronic structure significantly**

Yano et al. 2005 PNAS 102, 12047-12052

Imaging Biomolecules

Free Electron Laser

- $10^{12\text{-}13}$ photons
- 10 keV
- 10 fs pulse

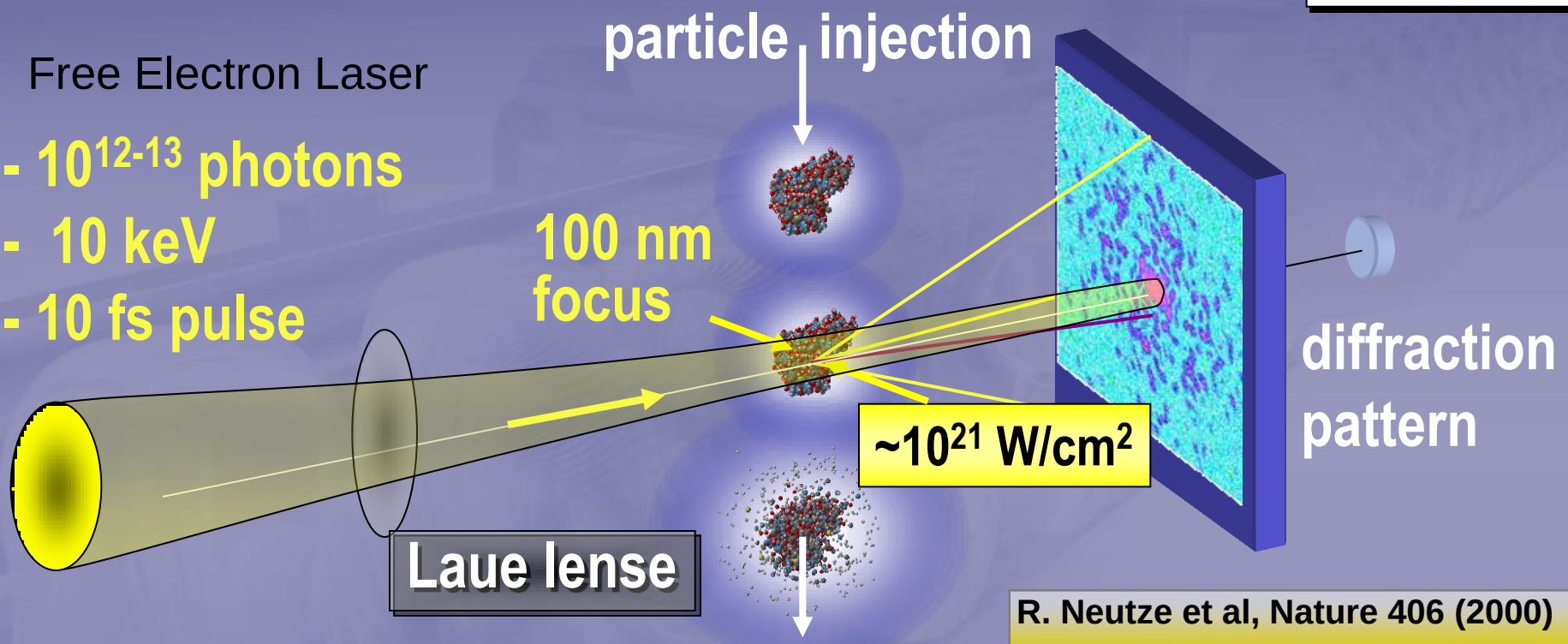

R. Neutze et al, Nature 406 (2000)

→ Avoid radiation damage (even at RT)

→ Explore time resolution

→ Structure of short-lived intermediates

Room temperature femtosecond X-ray diffraction of photosystem II microcrystals

Jan Kern[a,b], Roberto Alonso-Mori[b], Julia Hellmich[c], Rosalie Tran[a], Johan Hattne[a], Hartawan Laksmono[d], Carina Glöckner[c], Nathaniel Echols[a], Raymond G. Sierra[d], Jonas Sellberg[e,f], Benedikt Lassalle-Kaiser[a], Richard J. Gildea[a], Pieter Glatzel[g], Ralf W. Grosse-Kunstleve[a], Matthew J. Latimer[e], Trevor A. McQueen[h], Dörte DiFiore[c], Alan R. Fry[b], Marc Messerschmidt[b], Alan Miahnahri[b], Donald W. Schafer[b], M. Marvin Seibert[b], Dimosthenis Sokaras[e], Tsu-Chien Weng[e], Petrus H. Zwart[a], William E. White[b], Paul D. Adams[a], Michael J. Bogan[b,d], Sébastien Boutet[b], Garth J. Williams[b], Johannes Messinger[i], Nicholas K. Sauter[a], Athina Zouni[c], Uwe Bergmann[b,1], Junko Yano[a,1], and Vittal K. Yachandra[a,1]

[a]Physical Biosciences Division, Lawrence Berkeley National Laboratory, Berkeley, CA 94720; [b]Linac Coherent Light Source, SLAC National Accelerator Laboratory, Menlo Park, CA 94025; [c]Max-Volmer-Laboratorium für Biophysikalische Chemie, Technische Universität Berlin, D-10623 Berlin, Germany; [d]PULSE Institute, SLAC National Accelerator Laboratory, Menlo Park, CA 94025; [e]Stanford Synchrotron Radiation Lightsource, SLAC National Accelerator Laboratory, Menlo Park, CA 94025; [f]Department of Physics, AlbaNova, Stockholm University, S-106 91 Stockholm, Sweden; [g]European Synchrotron Radiation Facility, BP 220, F-38043 Grenoble Cedex, France; [h]Department of Chemistry, Stanford University, Stanford, CA 94025; and [i]Institutionen för Kemi, Kemiskt Biologiskt Centrum, Umeå Universitet, S-901 87 Umeå, Sweden

Edited by* Edward I. Solomon, Stanford University, Stanford, CA, and approved May 2, 2012 (received for review March 20, 2012)

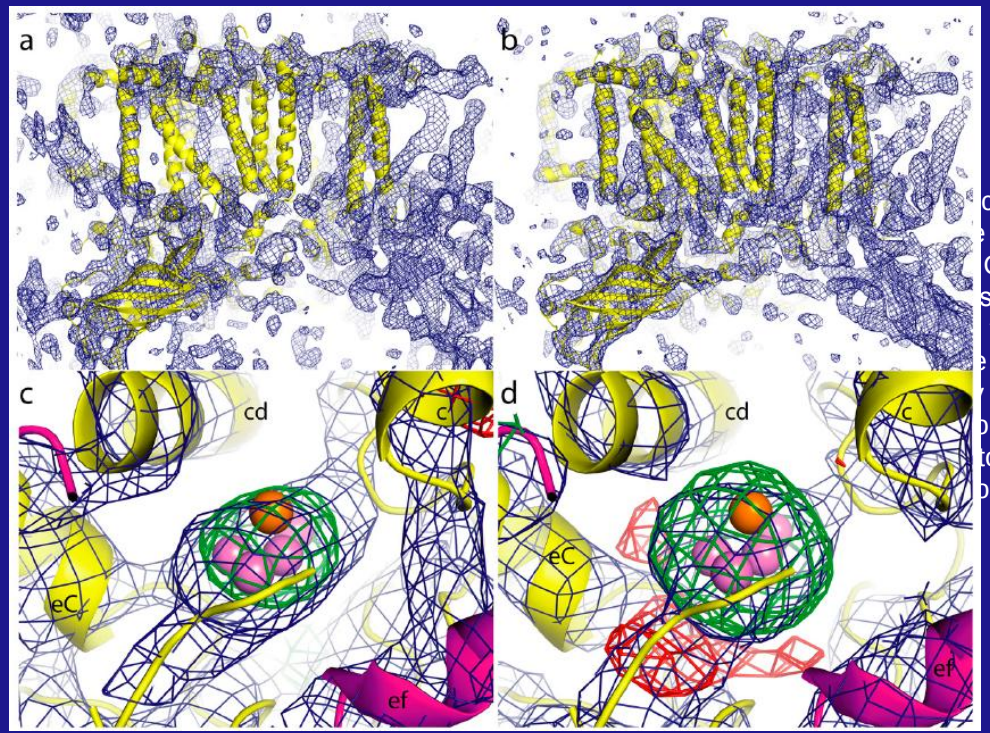

Comparison of electron density computed from CXI data with SR data truncated to 6.5 Å resolution. Overview of the electron density (blue mesh) for one monomer of PS II computed from the CXI data (A) and from the truncated SR data (B). Protein is shown as cartoon in yellow; 2mFo-DFc electron density is contoured at 1σ, view is along the membrane plane with cytoplasm at top. Electron density in the region of the Mn4CaO5 cluster computed from the CXI data (C) or from the truncated SR data (D), respectively. View direction is approximately 90 deg rotated with respect to Fig. 2B and is along the membrane plane, with cytoplasm at the top, lumen at the bottom. Protein is shown as cartoon in yellow (D1) and magenta (CP43), Mn as violet spheres and Ca as orange sphere. The lumenal end of TMH c as well as helix cd and the C-terminal helix (eC) of D1 and the ef helix of CP43 are labeled. The 2mFo-DFc electron density map is contoured at 1σ (blue mesh); the difference density (mFo-DFc map) is shown at þ3σ (green mesh) and at −3σ (red mesh).

croscope image of crystals (average size of 10 um) of PS II
XRD measurements. (B) X-ray diffraction pattern of PS II
CXI using a pulse width of <50 fs and a flux of 3.4×10^{11}
se at 9 keV. Resolutions of some highlighted Bragg spots
yellow and resolution at edges of the selected area of the
e indicated by white dashed circles. The background was
y subtracting the average image of 1,052 misses recorded
ore and after the crystal diffraction. (C) Enlarged view of an
op left corner of the diffraction pattern shown in B (marked
ox) to show highest resolution spots observed.

PNAS (2012)

Refinement of the OEC Structure

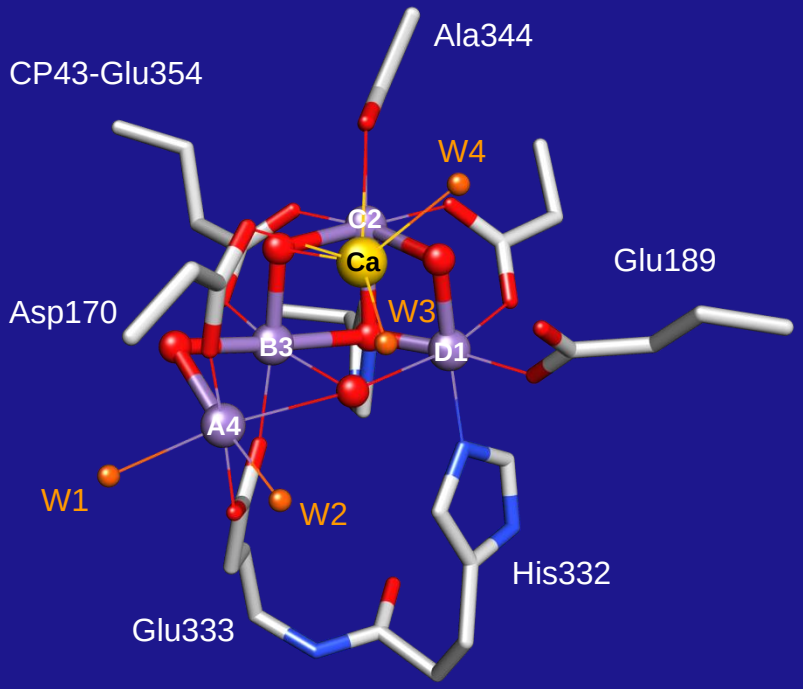

4 Mn
1 Ca
5 oxygen bridges
4 water molecules W1 – W4
Protein: carboxylates and 1 His

Umena et al., Nature (2011)

x-tal structure *DFT-optimized structures*

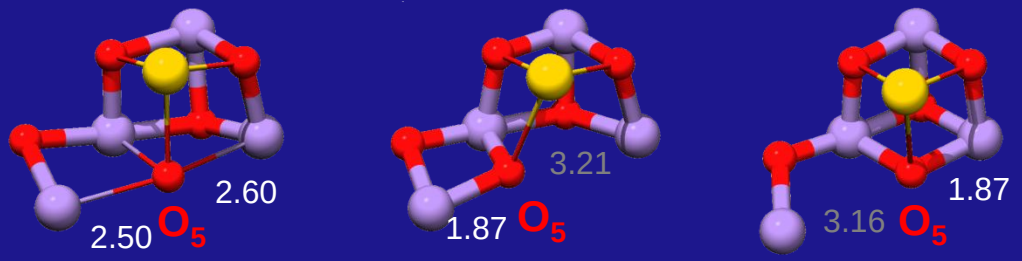

S_2: S_{eff} = ½ ground state 1

S_{eff} = 5/2 ground state 2 (+1 kcal/mol)

Upon geometry optimization O(5) relaxes to form Mn-Mn μ-oxo bridge.

Now Mn-Mn and Mn-O distances comparable with EXAFS.

Cooperation Frank Neese

Ames et al., JACS (2011)
Pantazis et al. Angew. Chem. (2012)

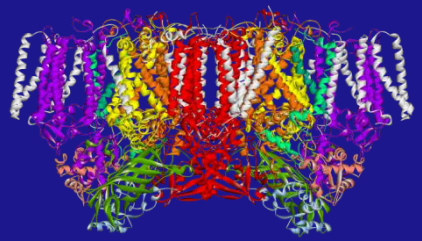

PS II - Functional Model

Photosystem II

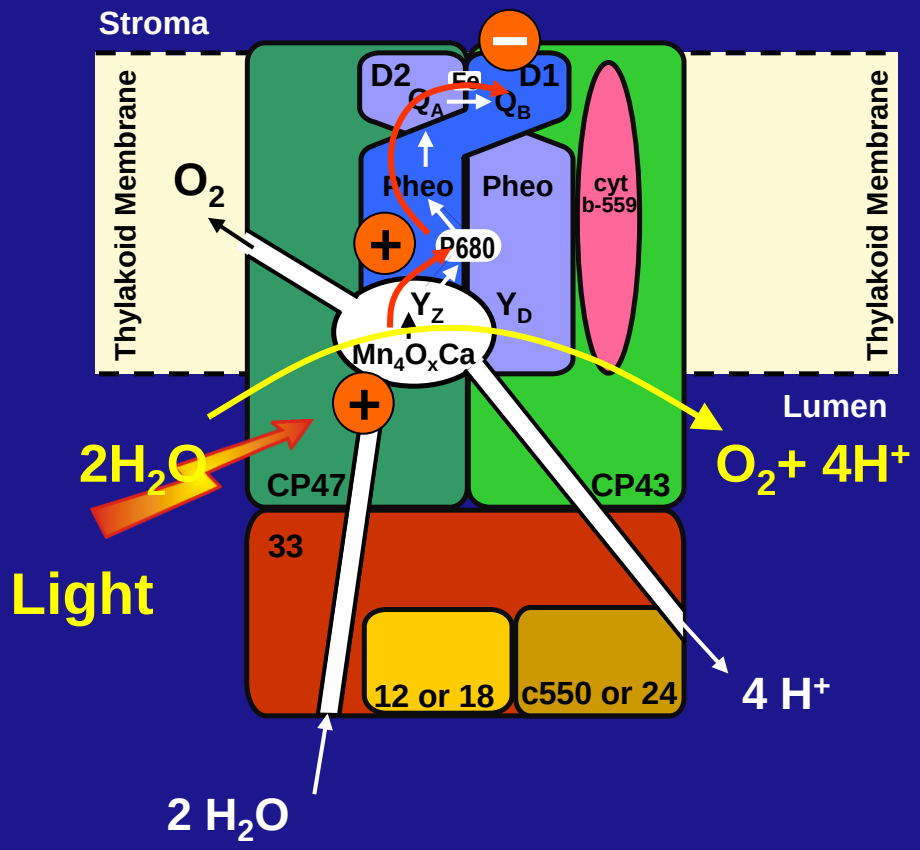

Activity Measurement:
O_2 release via **Clark Electrode**

Functional Test:
O_2 release after 1-4 µs-light flashes:
Joliot-Type Electrode

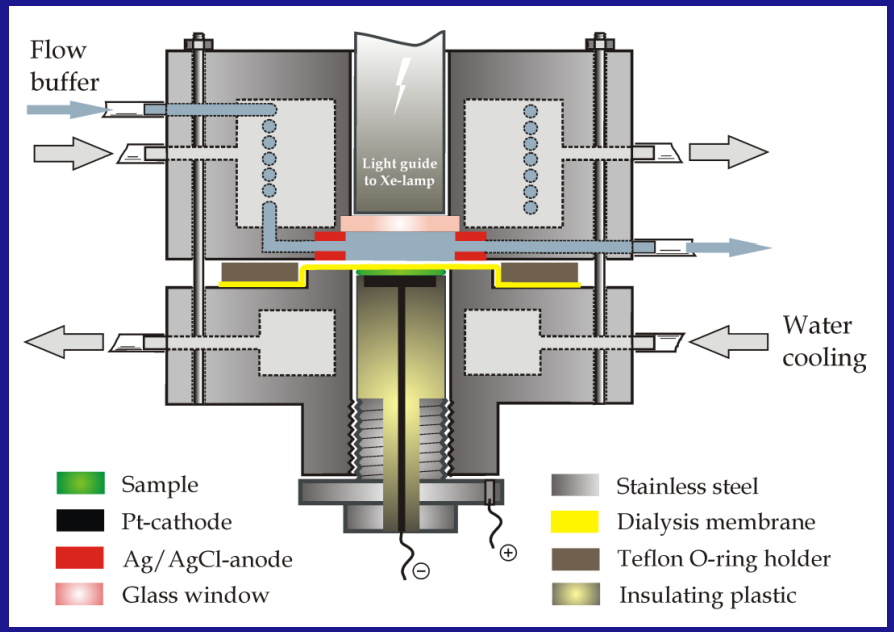

$$2\,H_2O \xrightarrow{4\,h\nu} O_2\uparrow + 4\,H^+ + 4\,e^-$$

PS II - Functional Model

Oxygen Evolution in PS II

induced by μs light flashes in spinach thylakoids

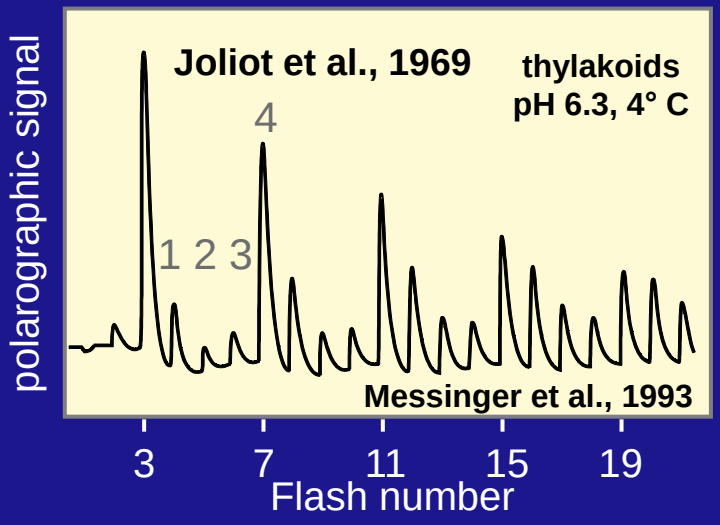

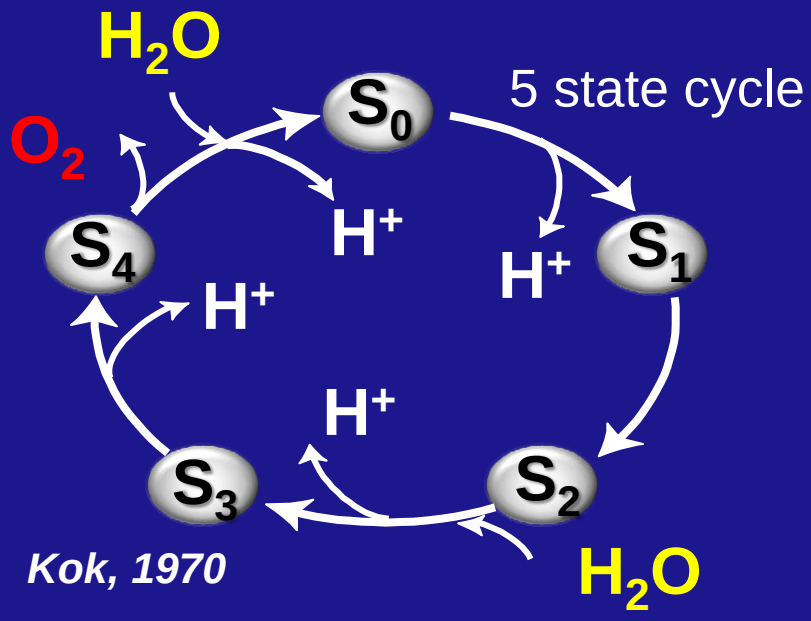

Activity Measurement:
O_2 release via **Clark Electrode**

Functional Test:
O_2 release after 1-4 μs-light flashes:
Joliot-Type Electrode

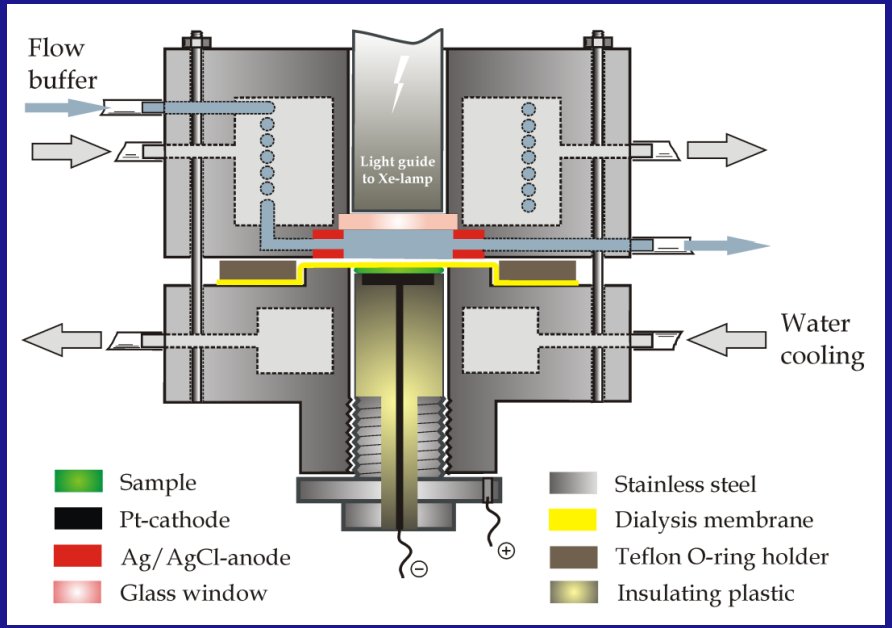

PS II - Functional Model

Oxygen Evolution in PS II

induced by μs light flashes in spinach thylakoids

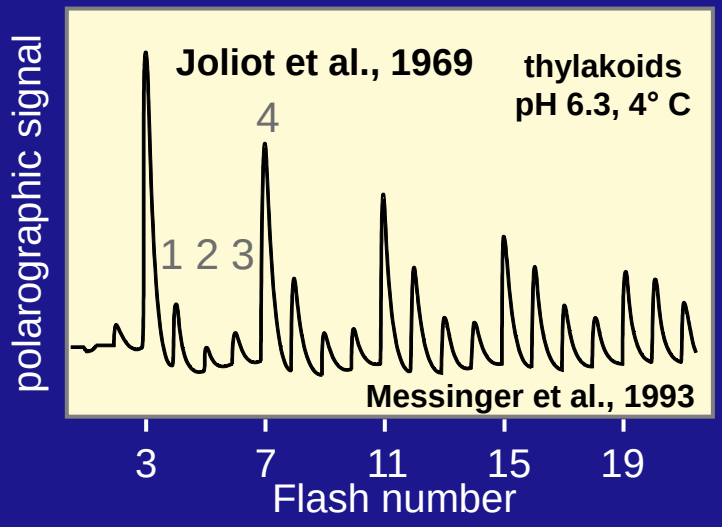

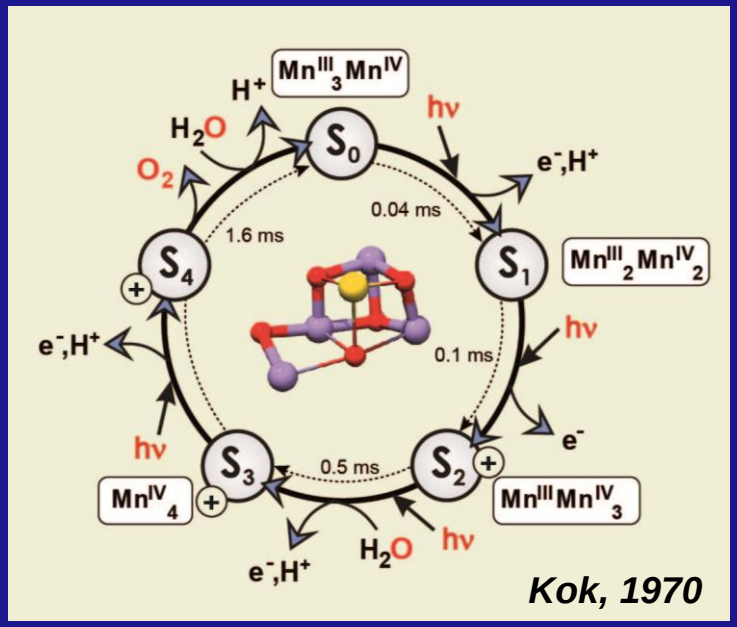

Activity Measurement:
O_2 release via **Clark Electrode**

Functional Test:
O_2 release after 1-4 μs-light flashes:
Joliot-Type Electrode

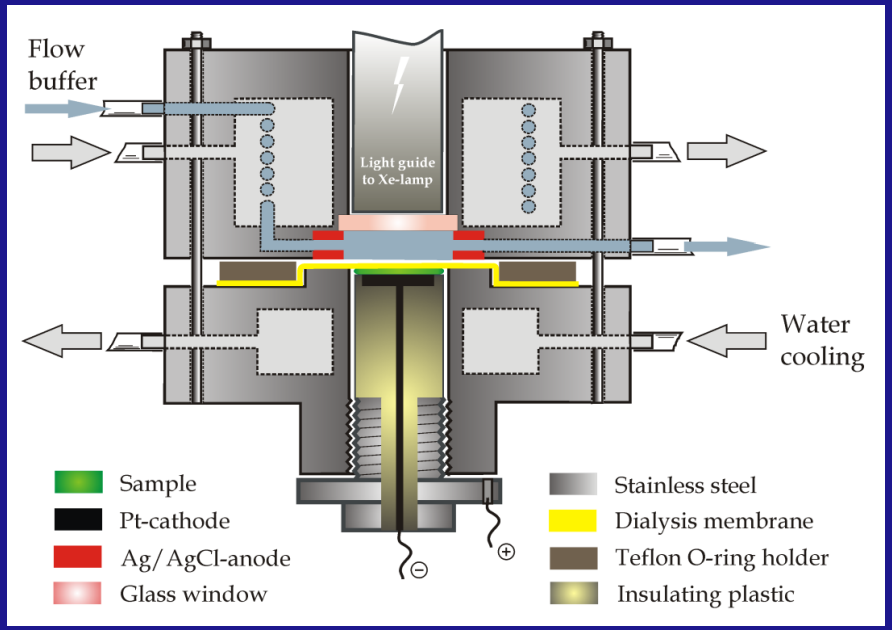

Water Oxidation in Aqueous Solution and in PS II: Function of Water-Splitting Complex

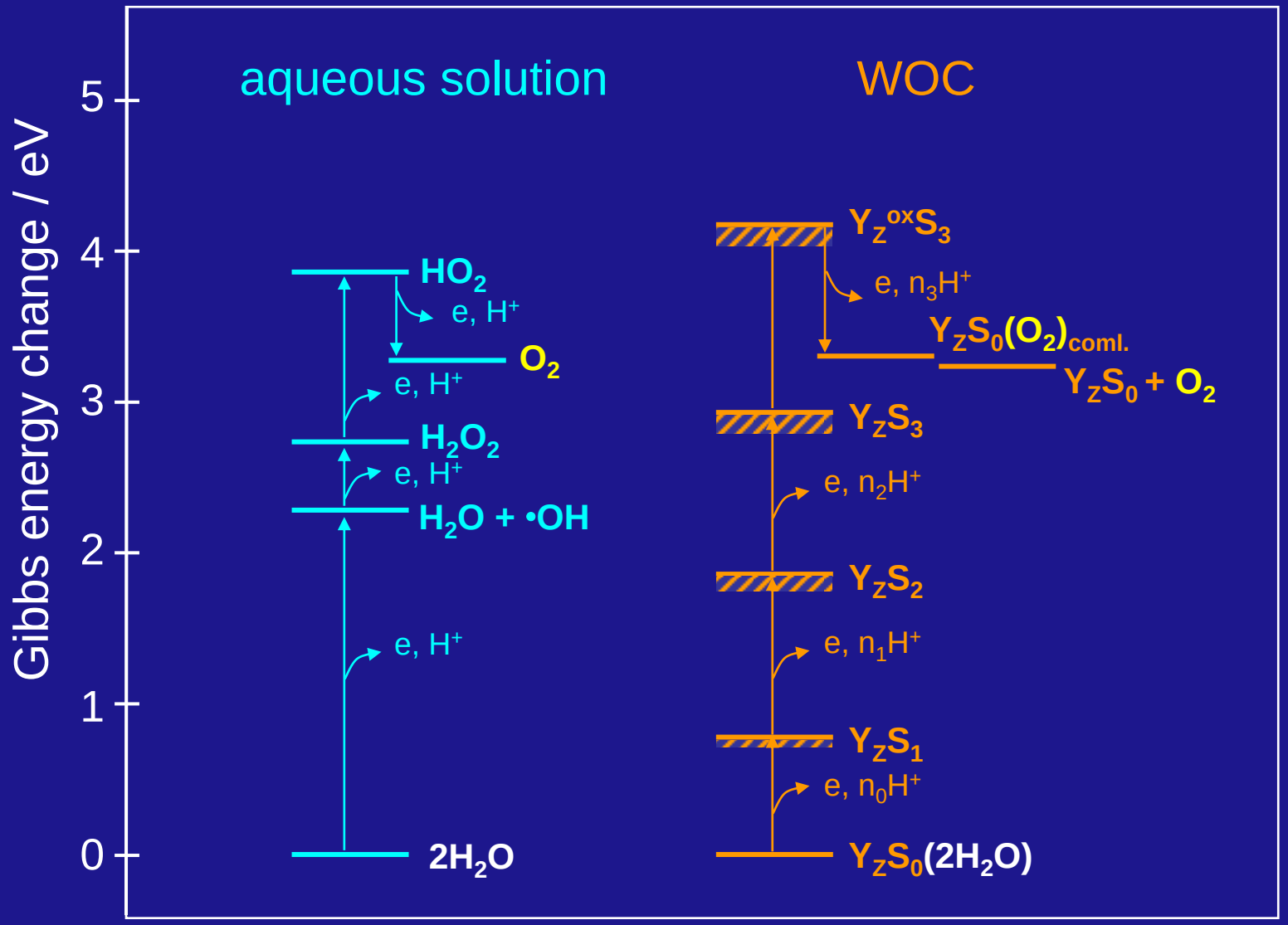

Messinger & Renger, 2008

PS II and Water Oxidase - Problems & Nature´s Solutions

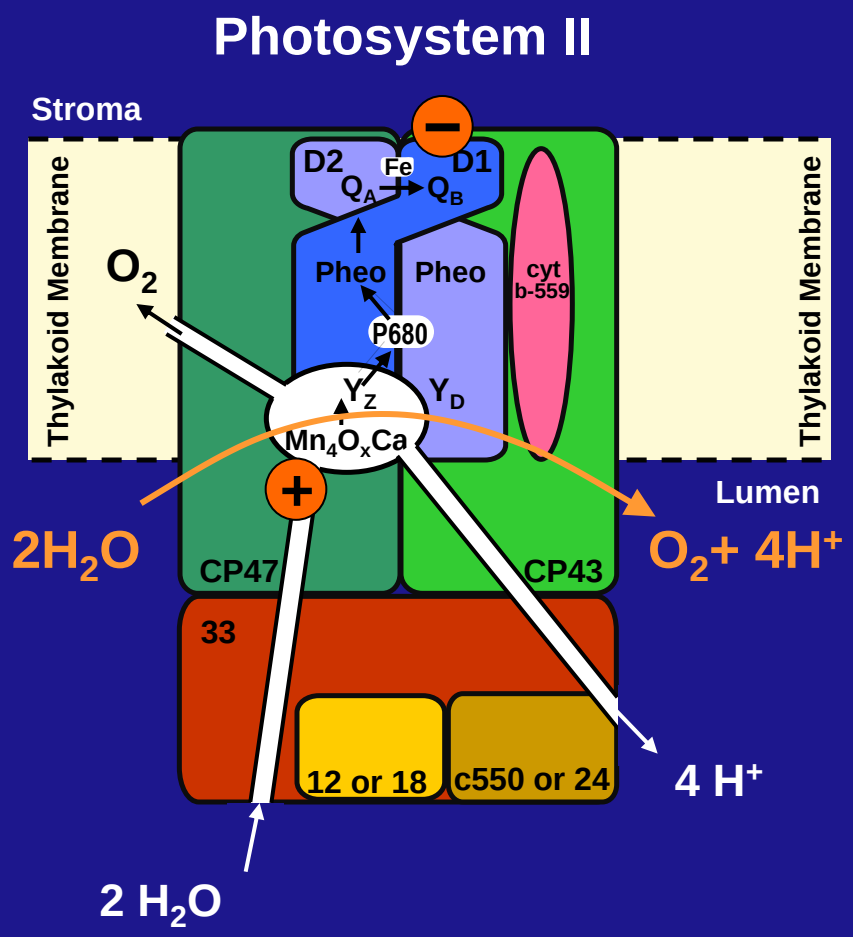

$$2\,H_2O \xrightarrow{4\,h\nu} O_2\uparrow + 4\,H^+ + 4\,e^-$$

1. Light-induced single electron transfer (*ps*) coupled to 4-electron water oxidation process (*ms*)- ***storage of oxidation equivalents***
2. Redox leveling at the catalyst: ***small and equal steps!***
3. Electron-proton coupling at the catalyst – ***charge balance***
4. Interfacing: ***via a redox-active tyrosine Y_z***
5. Water binding, orientation and O-O bond formation – ***catalysis mechanism***
6. High oxidative power of $P680^{\bullet+}$ - ***protection***
7. Chl triplets and singlet oxygen (D1 damage) - ***repair/replacement***

Assembly and Repair: Replacement of D1 Protein in PS II

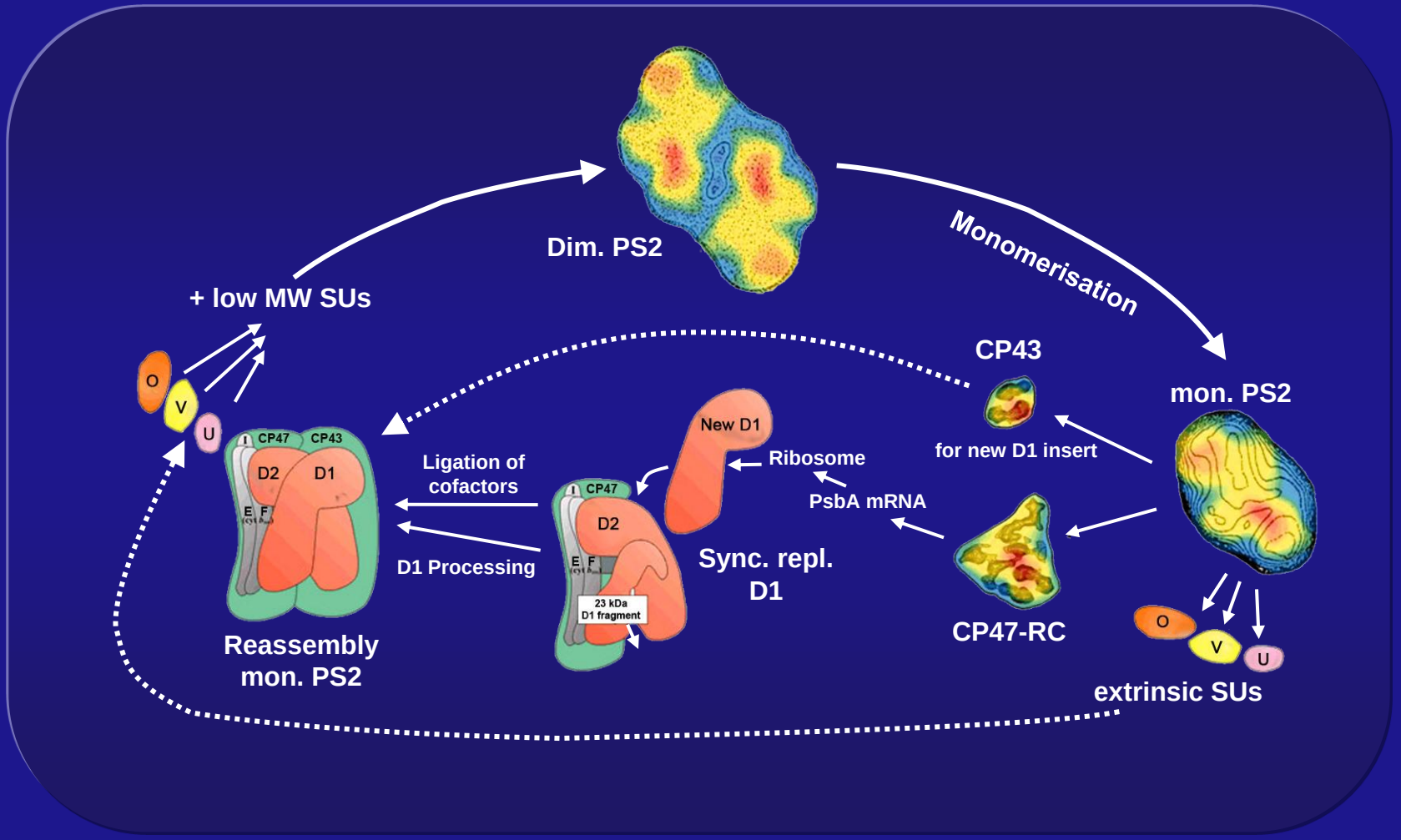

Peter Nixon, 2010

D1 half lifetime in the light 30 min!

Electronic Structure of the S-States: EPR

Mn(II) S=5/2
Mn(III) S=4/2
Mn(IV) S=3/2

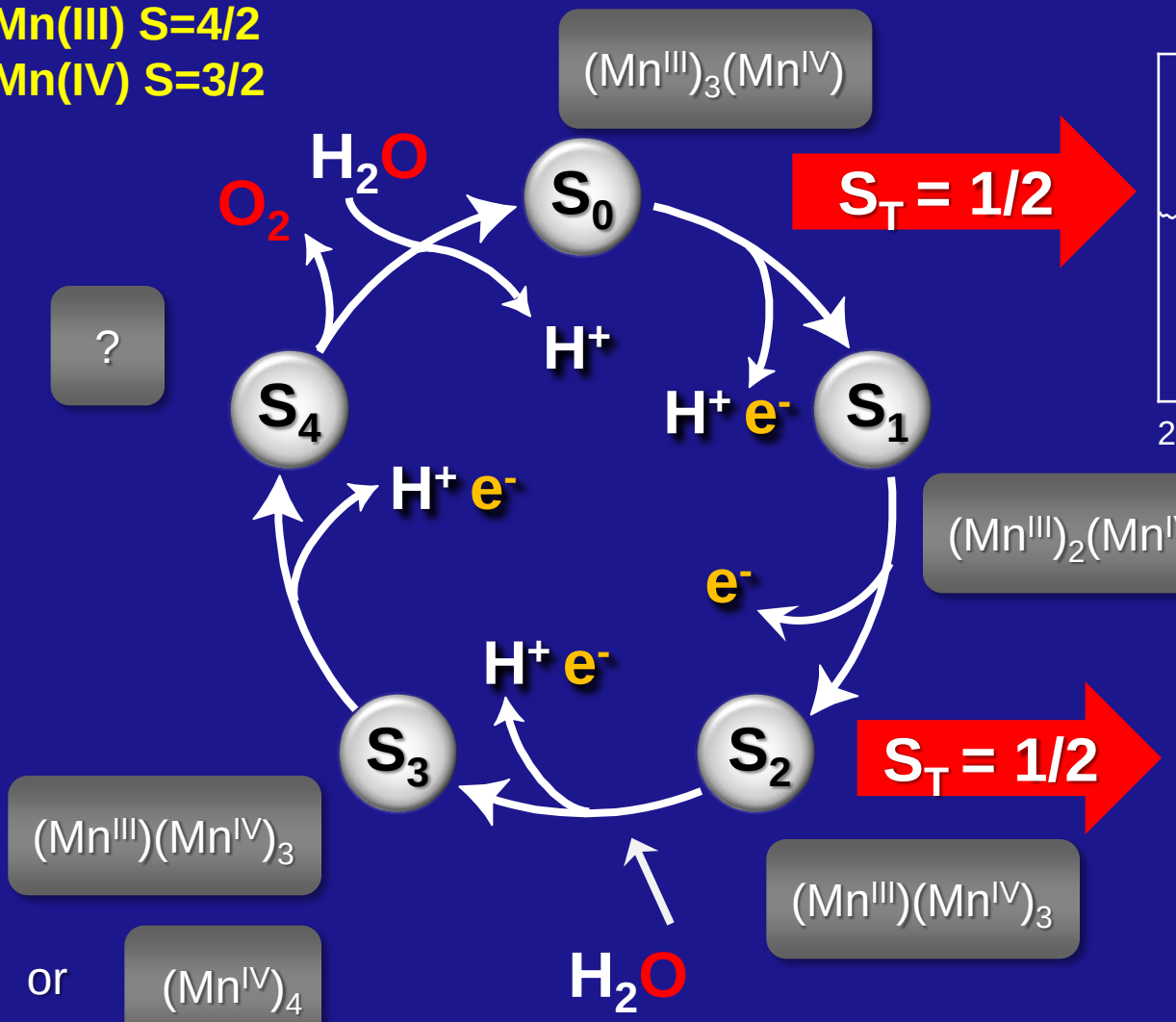

S-states differ by one electron oxidation

I (^{55}Mn)=5/2 → Hyperfine Structure

Messinger et al./Ahrling et al. 1997

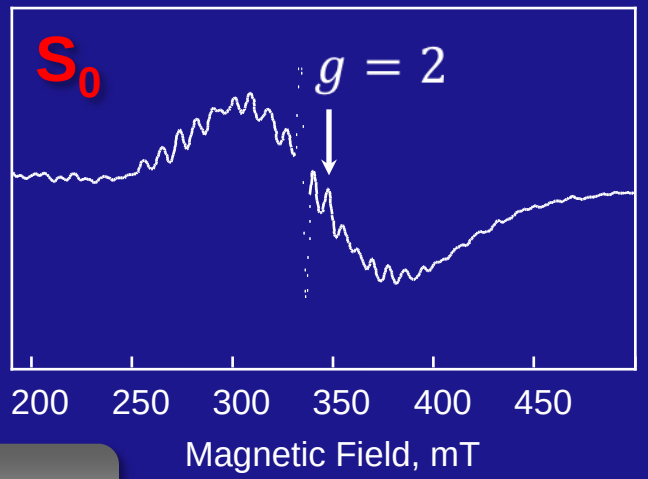

Dismukes and Siderer, 1981

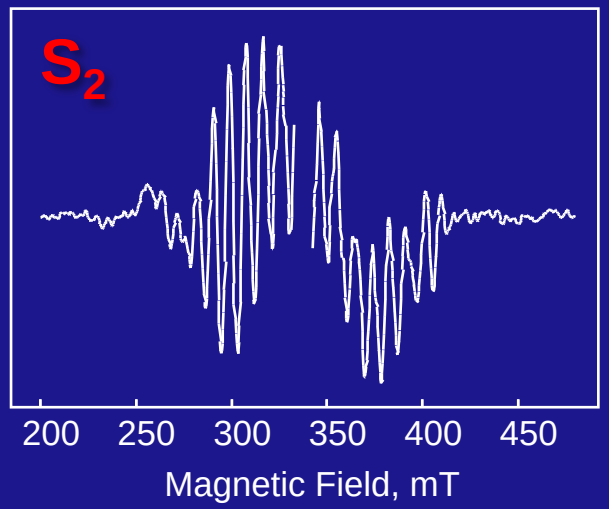

Pulse EPR & Multiresonance Techniques

Field-Swept Pulse EPR

High Frequency / High Field

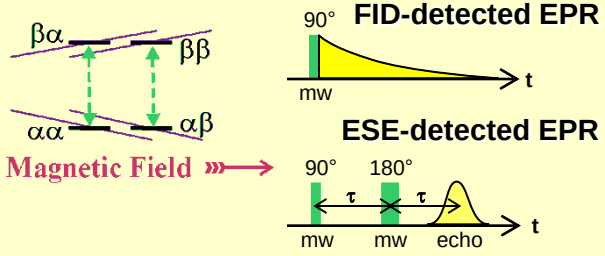

EPR spectra, ns time resolution

PELDOR-DEER

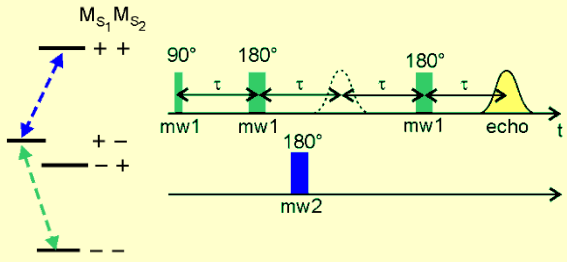

distance between electron spins

Echo Envelope Modulation

ESEEM

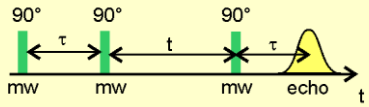

HYSCORE

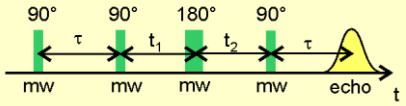

weakly coupled nuclei (hyperfine & quadrupole)

ELDOR-detected NMR

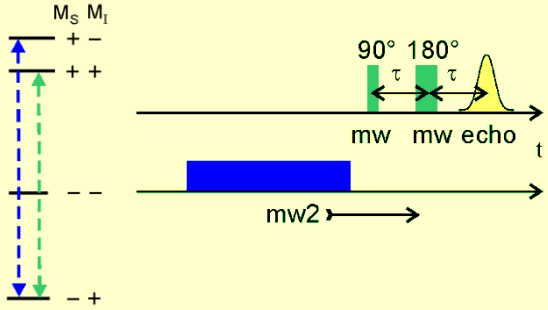

hfc of strongly coupled nuclei

Davies ENDOR

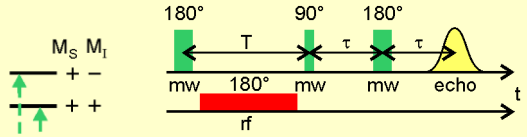

Mims ENDOR

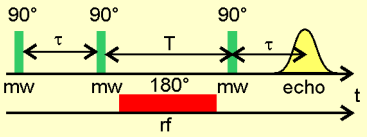

hfc and nqc determination

Electron-Nuclear-Nuclear Triple Resonance

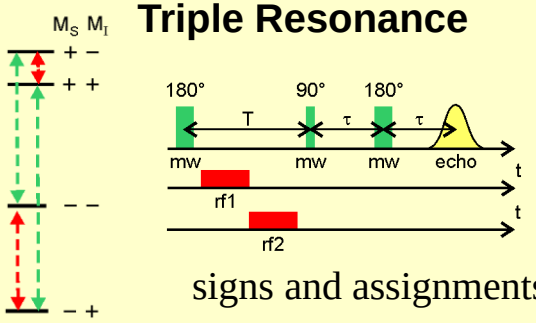

signs and assignments

^{55}Mn ENDOR at X- and Q-Band S_2-State of the WOC

- There are no ^{55}Mn ENDOR signals above ~180 MHz; all signals fall in the 60-180 MHz range
- Mn^{II} not present in the S states
- The spin projection coefficients must all be approximately 1 (ρ~1) (see also EPR simulation)

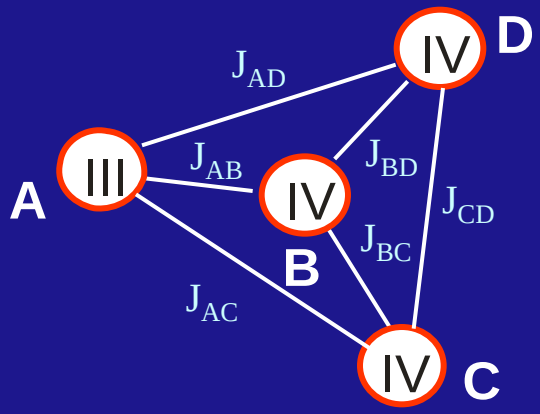

Peloquin et al,, JACS (2000)
Kulik et al., JACS (2005, 2007)

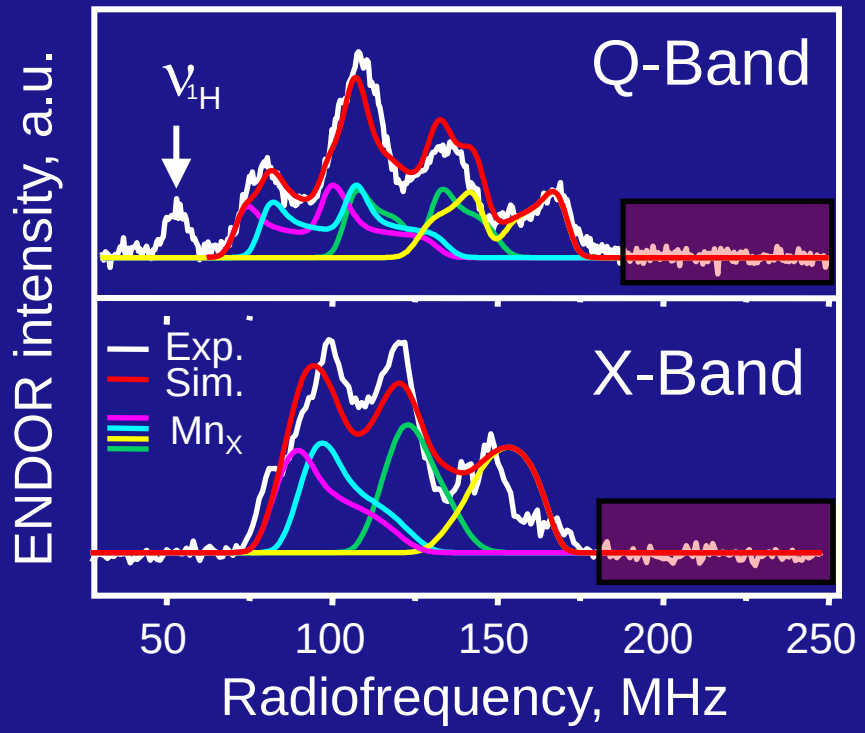

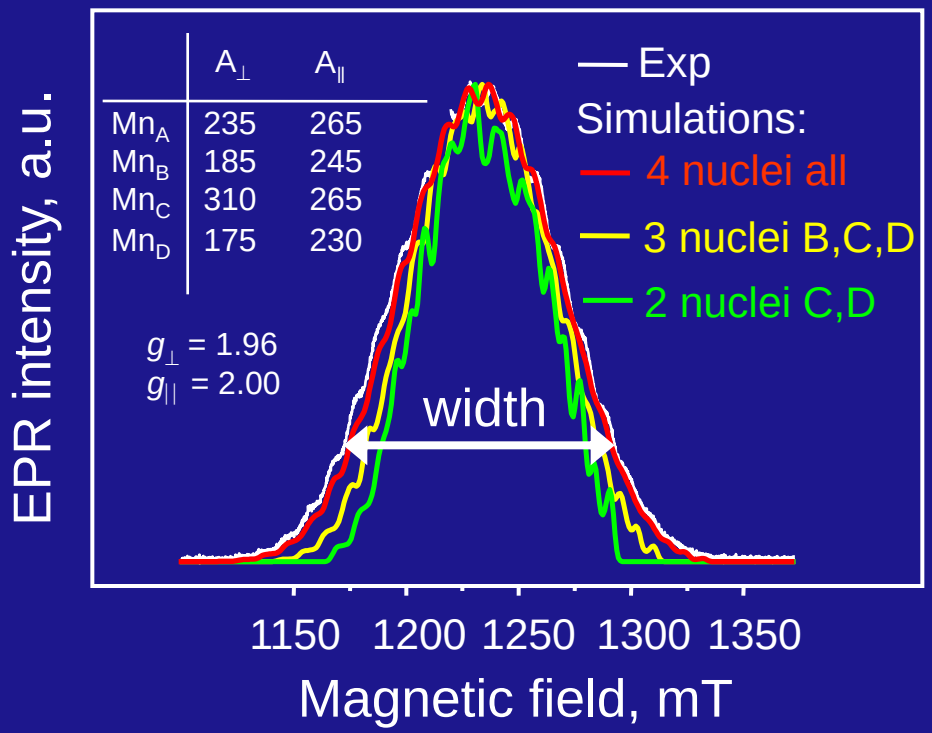

Electronic Structure: Multiline EPR and ^{55}Mn ENDOR

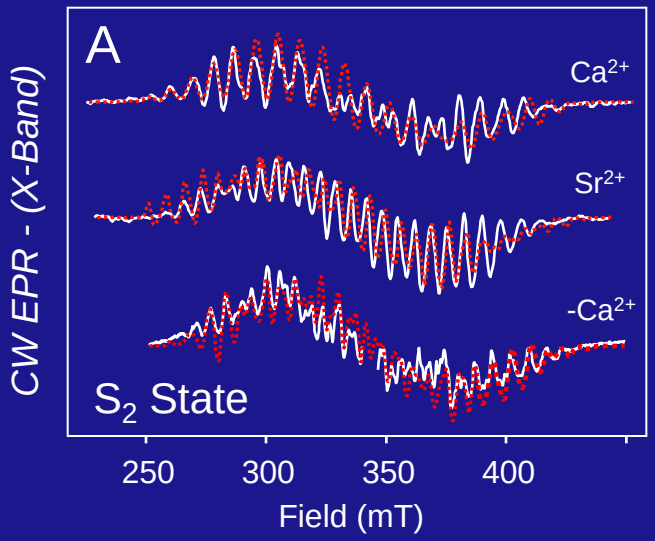

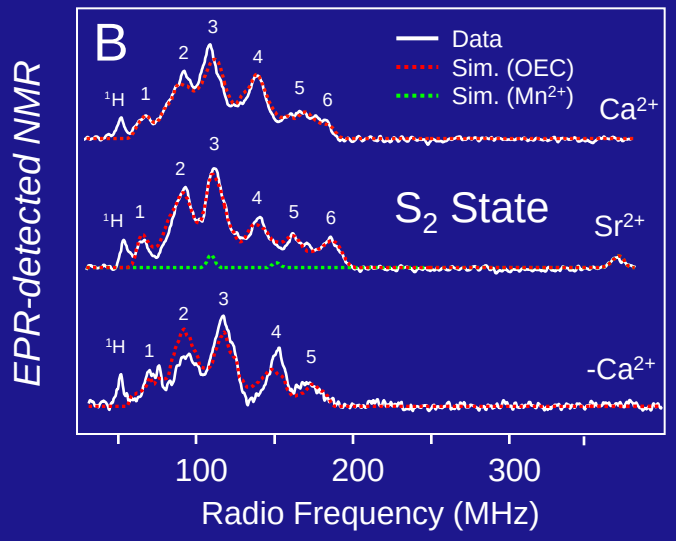

Electronic Structure

Exchange Coupling Scheme

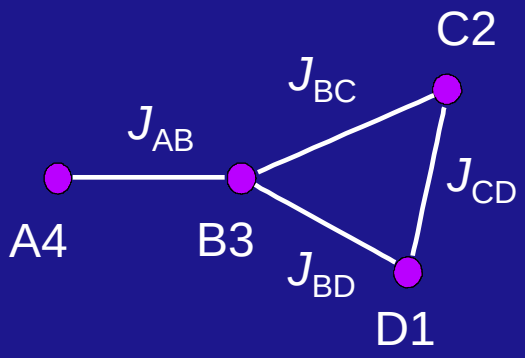

EPR

Oxidation States (S_2)

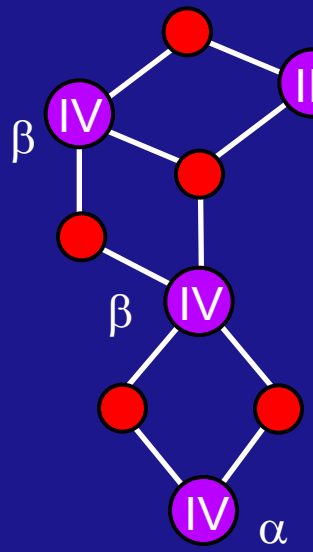

DFT

Structural Model (S_2)

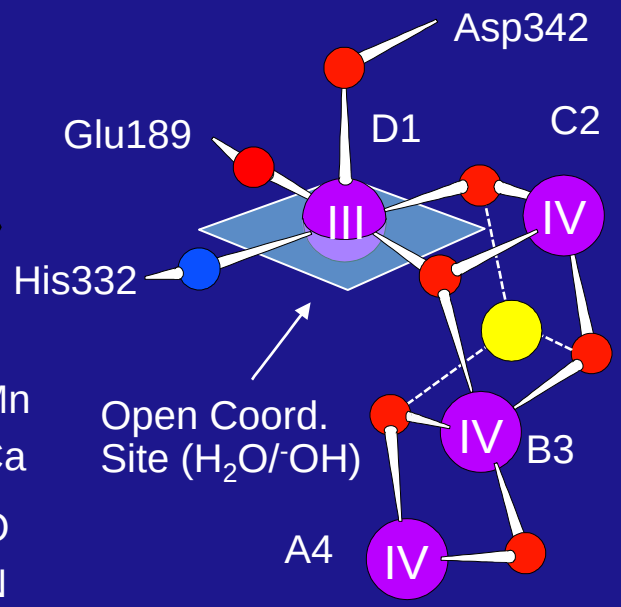

Pantazis et al. PCCP (2009)
Cox, Rapatskiy et al. JACS (2011)
Ames et al. JACS (2011)
Lohmiller et al. JBC (2012)

^{17}O Labelling of PSII

All oxygens (i.e. possible substrates) EPR/NMR silent

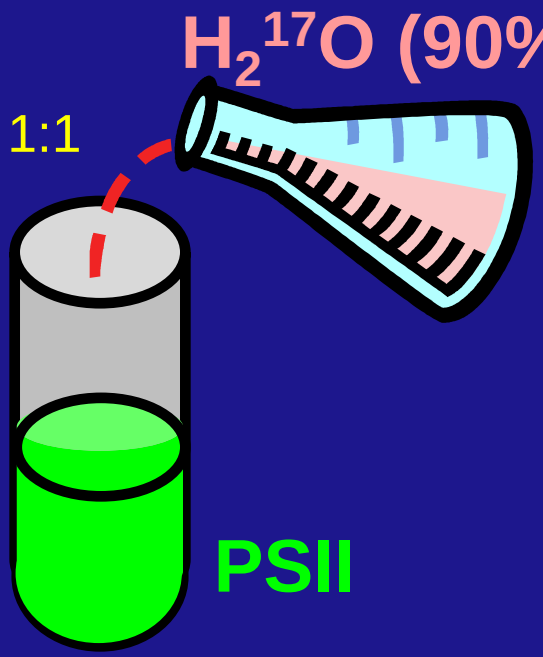

Exchanged sites now EPR/NMR active

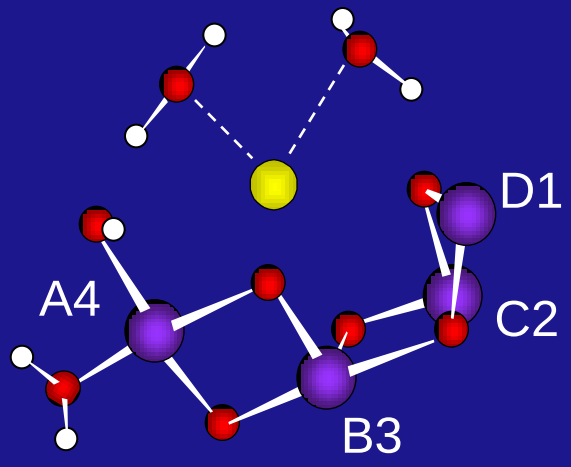

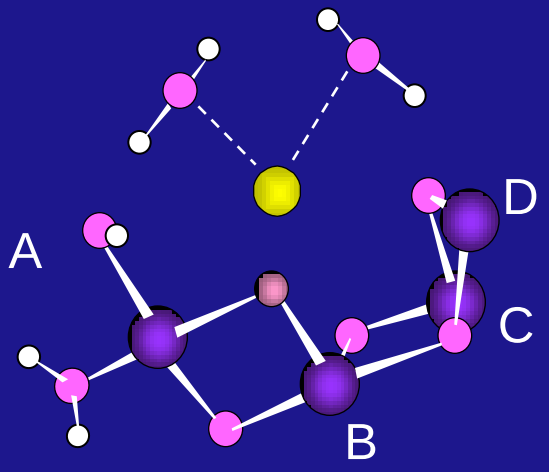

^{55}Mn
^{40}Ca
^{16}O
^{1}H

3x exchanged (in dark, S1 state)
1 hour
75% enrichment (final)

^{55}Mn
^{40}Ca
^{16}O
^{17}O
^{1}H

ENDOR *versus* ELDOR-detected NMR (EDNMR)

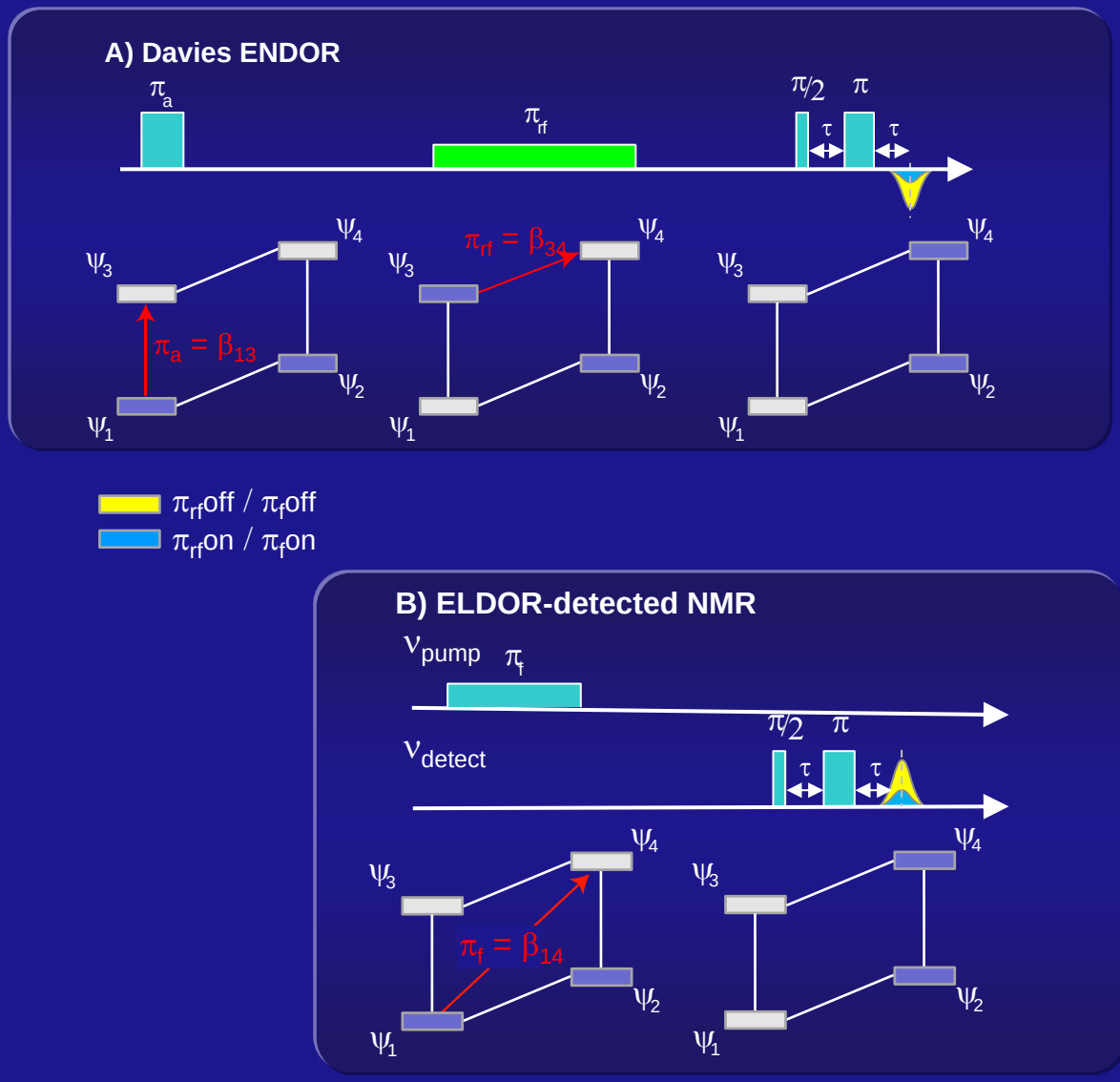

^{17}O EDNMR vs. ENDOR

W-band (94 GHz)

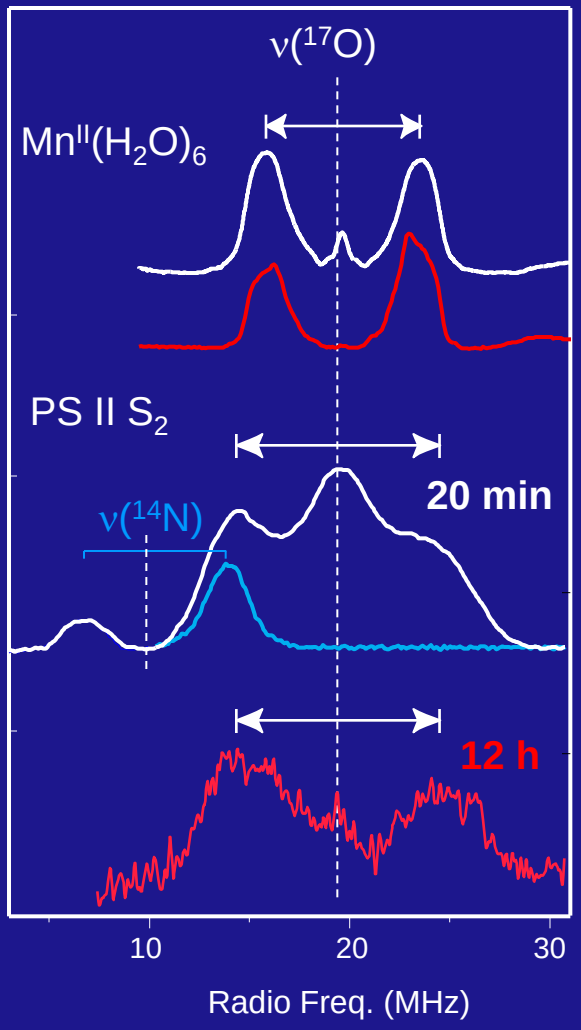

Rapatskiy et al., J. Am. Chem. Soc. in press

^{17}O ELDOR-detected NMR at 94 GHz - Simulations

Three ^{17}O species are required to reproduce the entire envelope

1. **Weakly coupled water (matrix) – Ca-W1/W3/W4**
2. **Intermediary coupled water (Mn bound) – Mn_{A4}-OH (W2)**
3. **Strongly coupled water (μ-oxo bridge)**

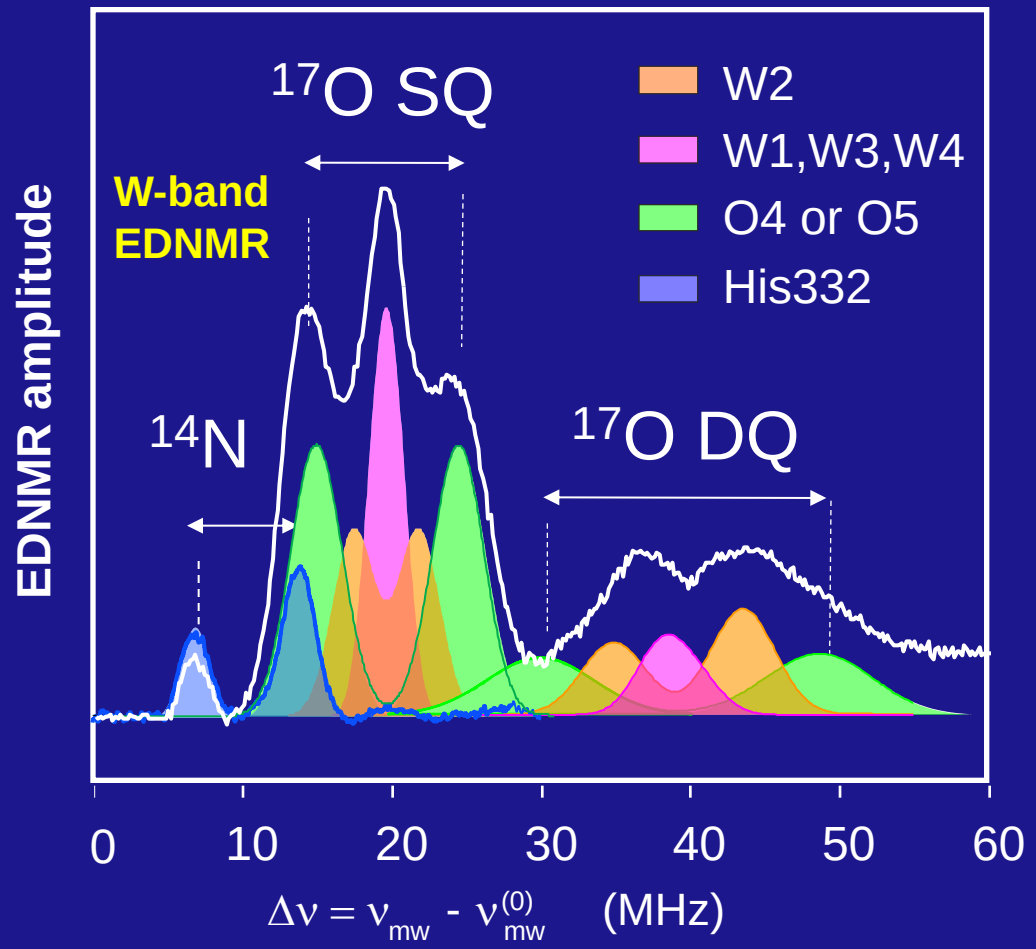

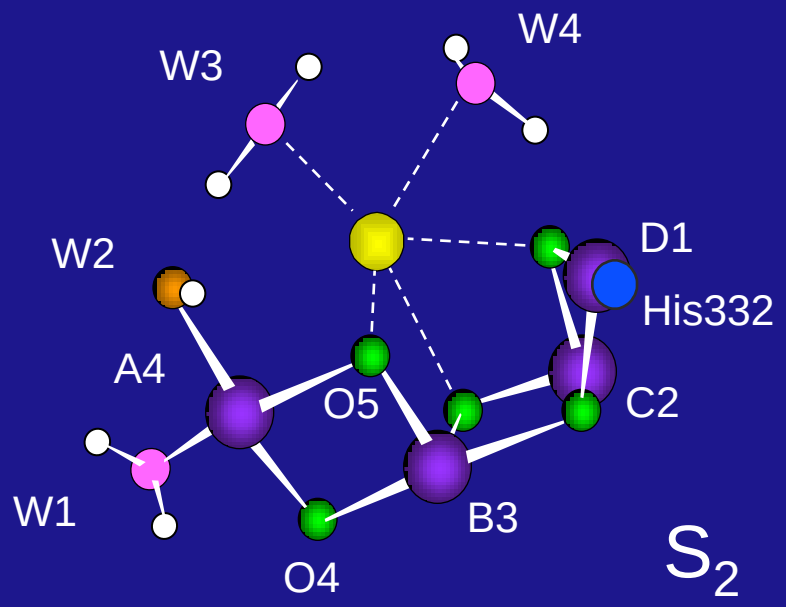

A_{iso}(μ-oxo) ~10 MHz

A_{iso}(OH) ~4 MHz

typical values seen in models agrees with DFT calculations

Rapid Dilution in $H_2{}^{17}O$; the same signal envelope is seen!

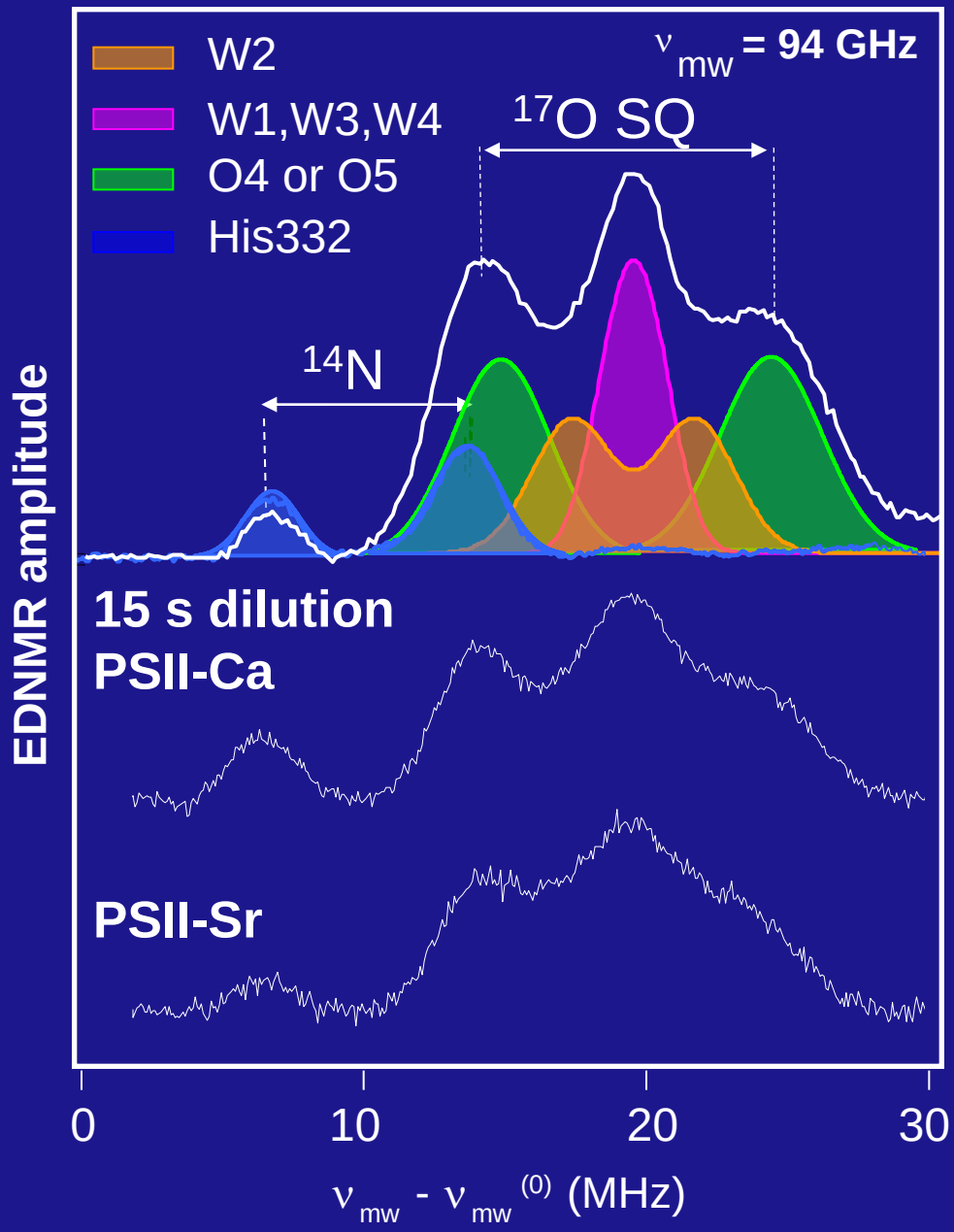

All three ^{17}O species are seen after dilution in $H_2{}^{17}O$ (1x) and rapid freezing (<15 s)

1. **Matrix – Ca-W3/W4 and W1**
2. **Mn bound – Mn_{A4}-OH/OH_2**
3. **μ-oxo bridge –O5**

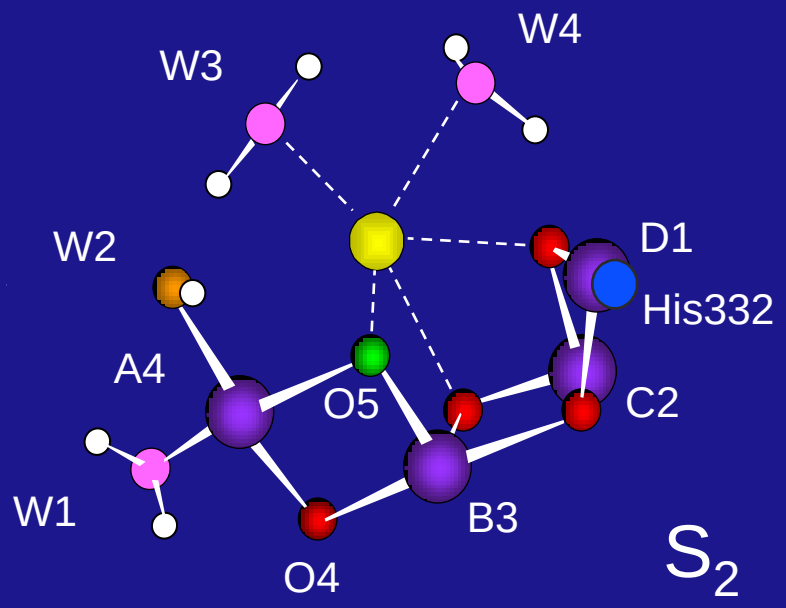

Possible Mechanism of Water Oxidation

I: Nucleophilic attack

$$\left[\begin{array}{c} Mn^{IV} = O^{\bullet} \\ \text{or} \\ Mn^{V} \equiv O \end{array}\right] \left[\begin{array}{c} H_2O\text{-}Ca \\ \text{or} \\ HO\text{-}Ca \end{array}\right]$$

S_1

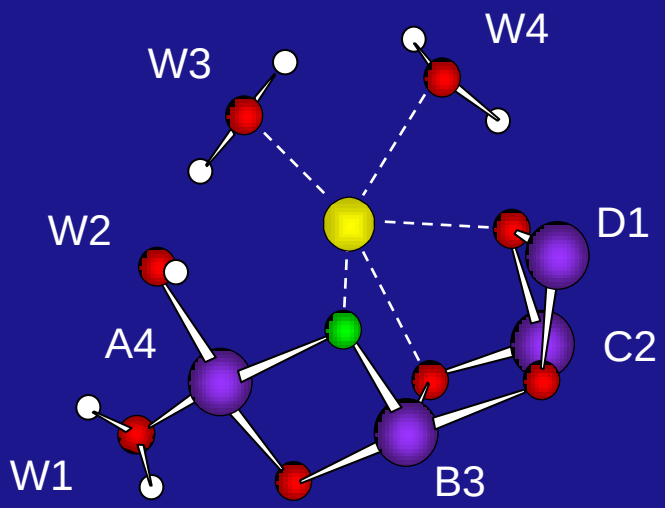

O5 + W3

***or O5 + W2**

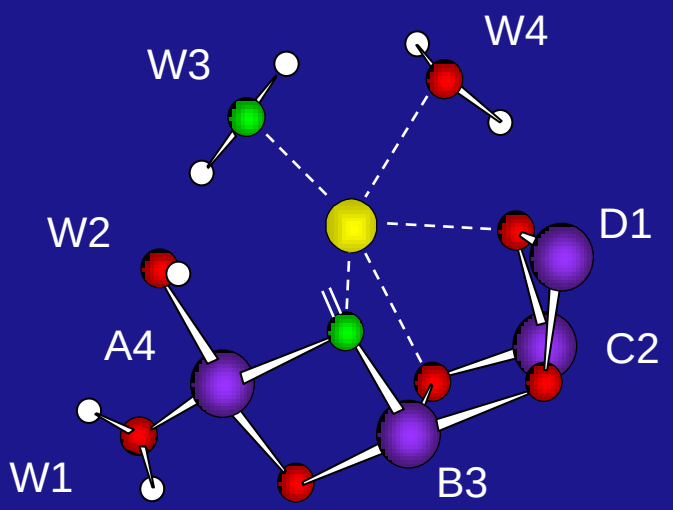

S_4

O5 + WX

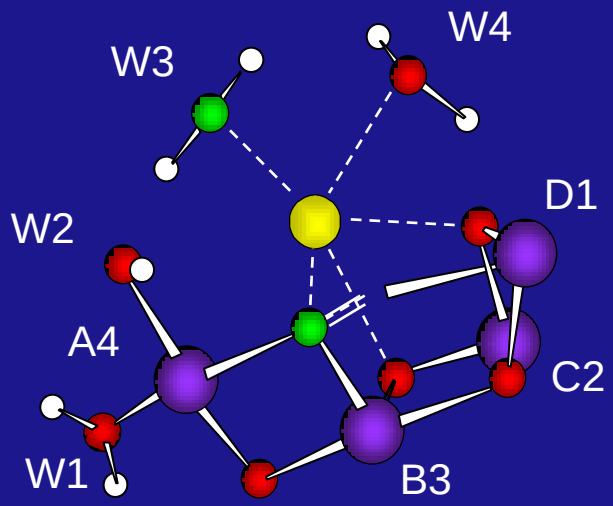

^{55}Mn ^{16}O
^{40}Ca ^{1}H
Substrate

II. Oxo/oxyl radial coupling

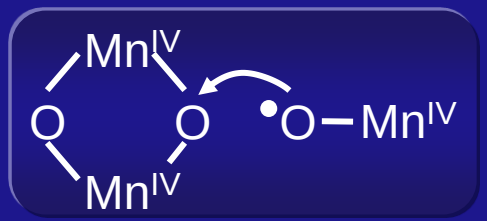

Why is O5 exchangeable on a seconds timescale?

- **O5 is a μ-oxo bridge to the Ca (Ca tunes pK_a of bound water(s))**
- **O5 has a flexible coordination sphere**

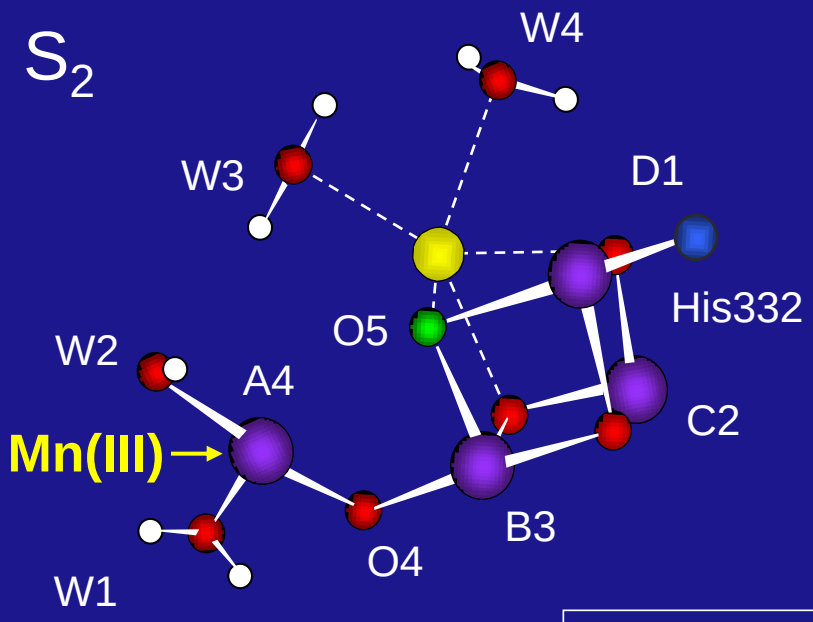

~200 K Anneal

~150 K IR illum.

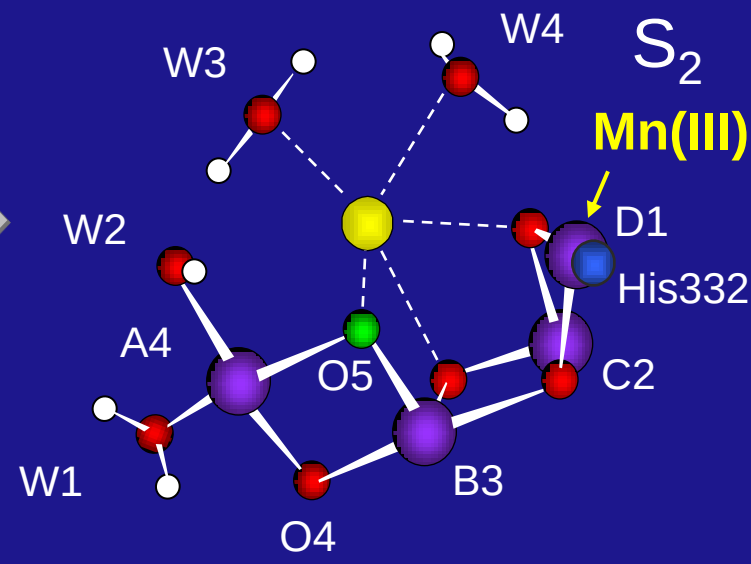

'g = 4.1 state'

$S_G = 5/2$

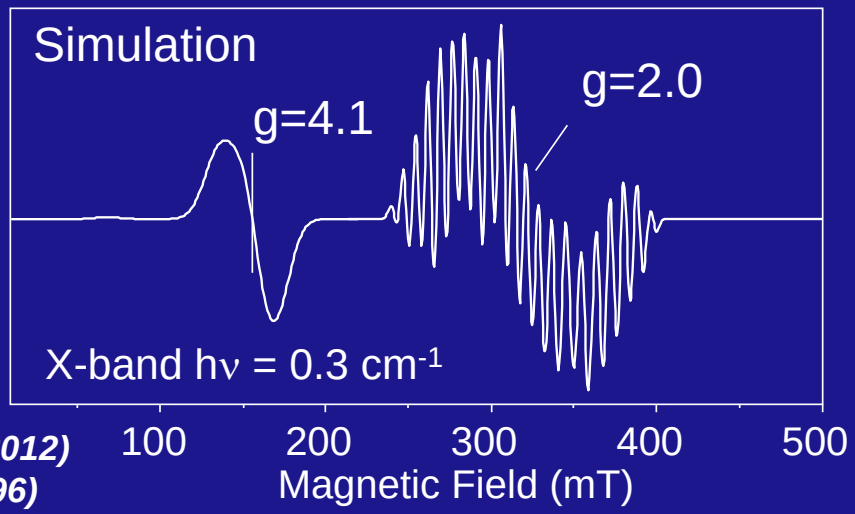

'multiline state'

$S_G = 1/2$

Pantazis et al. , Angew. Chem. (2012)
Boussac et al. Biochemistry (1996)

Neese Cooperation

Lessons from Nature: A light-driven water splitting machine

1. Choice of the catalyst: earth-abundant metals (Mn, Ca) with optimized physicochemical properties and simple (bridging) ligands (O) forming a cage-like/dangler structure
2. Nuclearity of cluster: 4 Mn for storage of oxidizing equivalents – charge accumulation: coupling of one-electron charge separation to four-electron water oxidation
3. Redox leveling at the catalyst: avoiding high-energy intermedites during the reaction
4. Co-metal: Ca for water binding/delivery
5. Correct and precise sequential substrate water binding in juxtaposition at the metals, deprotonation and preparation for O-O bond formation
6. Substrate water „integration“ in the cluster: active participation of the catalyst
7. Proton coupled electron transfer PCET: stepwise H^+ release for charge neutrality
8. Efficient interfacing of ET chain and catalyst via Y_z – lowering the overpotential
9. Smart Matrix: correct binding Mn_4Ca-cluster, channels for educts & products, proton management; electrostatic environment, ET and catalyst dynamics, protection - all that providing high efficiency (TOF) of the catalyst
10. Self assembly of the catalyst; efficient repair “self healing“ in case of damage – provides good stability and long lifetime

Hydrogenases:

Spectroscopy & Electrochemistry,

Structure, Function and Oxygen Sensitivity

Two Main Classes of Hydrogenases

[NiFe] Hydrogenase

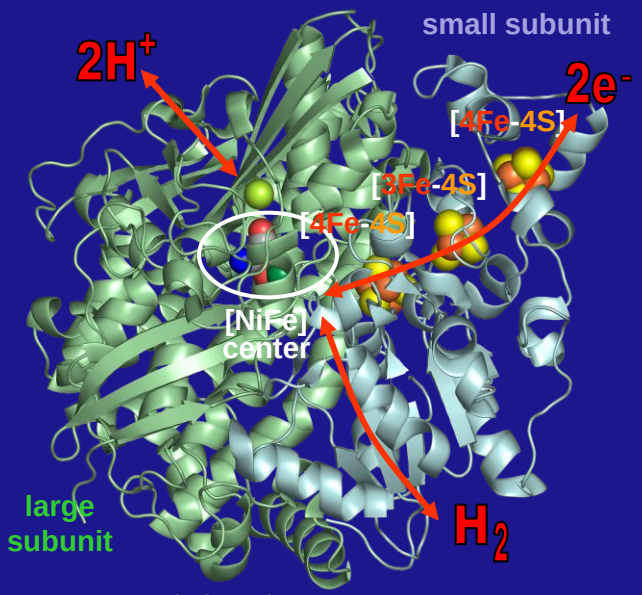

Ogata et al. (2005) Structure v13 pp. 1635-42

[FeFe] Hydrogenase

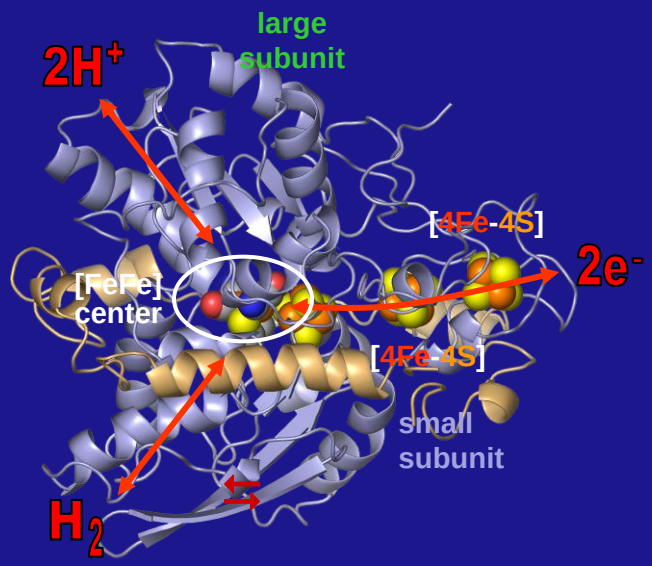

Nicolet et al. (1999) Structure Fold.Des. v7 pp. 13-23

Volbeda et al., 1995
Higuchi et al., 1997

$$H_2 \leftrightarrows H^- + H^+ \leftrightarrows 2H^+ + 2e^-$$

Peters et al., 1998
Nicolet et al., 1999

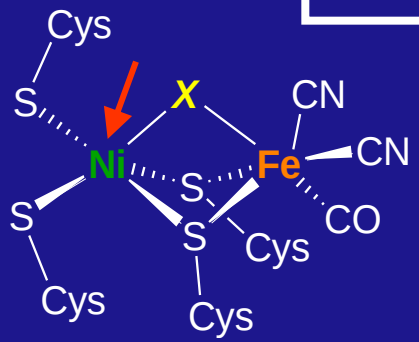

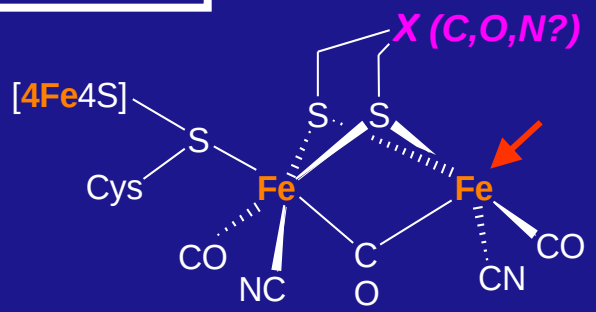

Desulfovibrio vulgaris Miyazaki F, PDB 1WUI

Desulfovibrio desulfuricans, PDB 1HFE

Biological Functions of Hydrogenases

Activity:

$10^2 – 10^3$ [µmol H_2/min* mg protein]

[NiFe]-hydrogenases

H_2 oxidation

- H_2 sensing (RH)
- Energy generation (MBH)
- Re-generation of reducing equivalents (SH)

H_2 evolution

disposal of reducing equivalents

[FeFe]-hydrogenases

H_2 evolution

Disposal of reducing equivalents

H_2 oxidation

(Re-)generation of reducing equivalents

Activity:

$10^3 – 10^4$ [µmol H_2/min* mg protein]

$$H_2 \underset{\text{evolution}}{\overset{\text{uptake}}{\rightleftharpoons}} 2\,H^+ + 2\,e^-$$

Hydrogenases: Catalytic Activity

The most active [FeFe] hydrogenases produce 10,000 molecules H_2 per second at 30°C

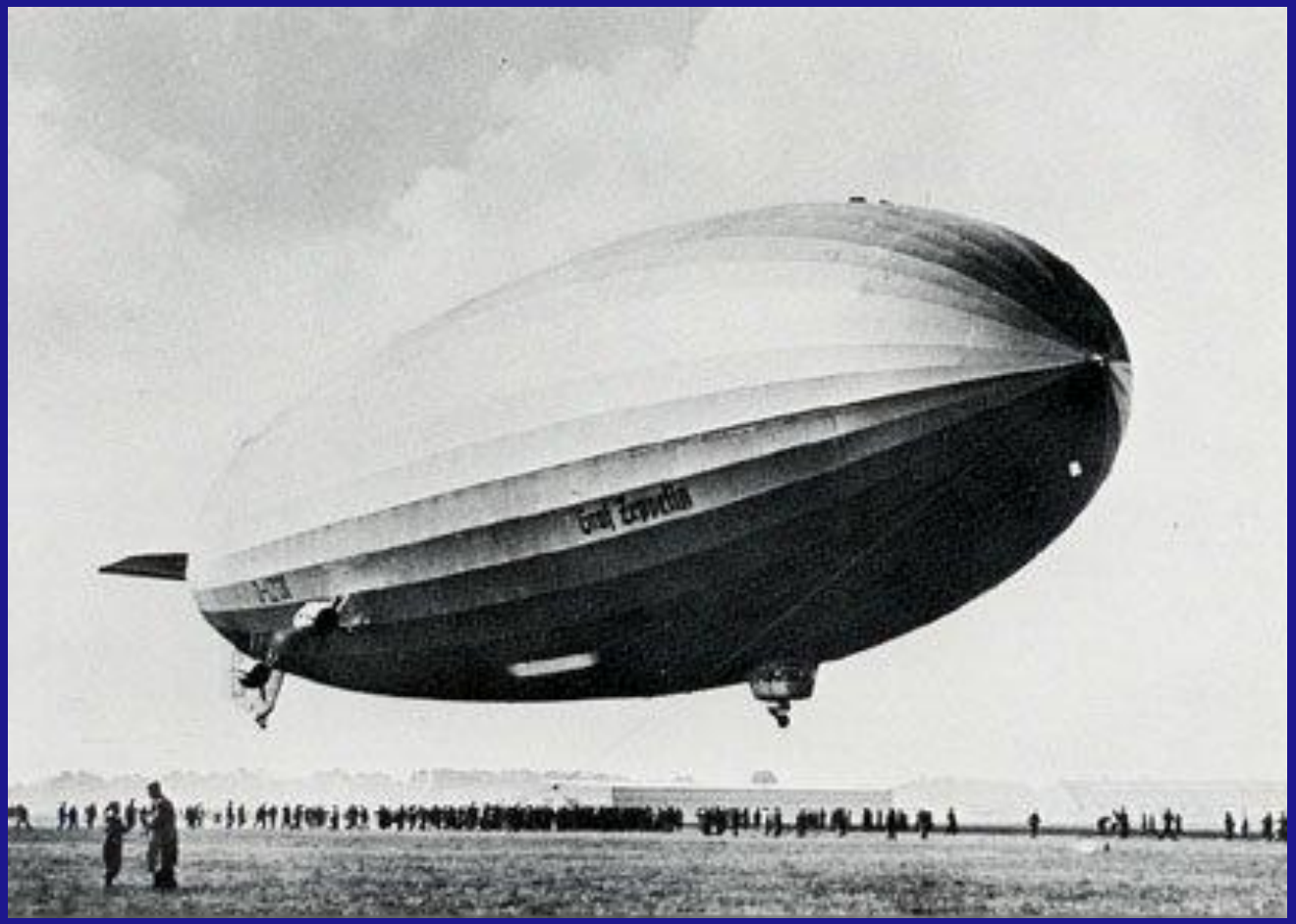

'... one mole of such a hydrogenase could produce enough hydrogen to fill the *Graf Zeppelin* in 10 minutes.....'

R. Cammack, Nature (1999)

Initial Questions (AC)

- intermediates of the reaction cycle: redox states of active site and ET components.
- Formal oxidation and spin states of the metal ions
  Electronic configurations of the ground states.
- Identification and function of the diatomic ligands at the Fe and the bridging ligand X.
- Intermediates in the reaction cycle and their geometry
- Binding site of the substrate hydrogen.
- Effect of light on the hydrogenase intermediary states.
- Impact of the protein surrounding.
- Mechanism of enzyme inhibition (e.g. by O_2 or CO) and oxygen tolerance.
- Mechanism of activation/deactivation and reversible hydrogen conversion by hydrogenases
- Structural basis for enzyme activity (TOF) and lifetime (TON)

[NiFe]- und [FeFe]-Hydrogenasen

[NiFe] Hydrogenase

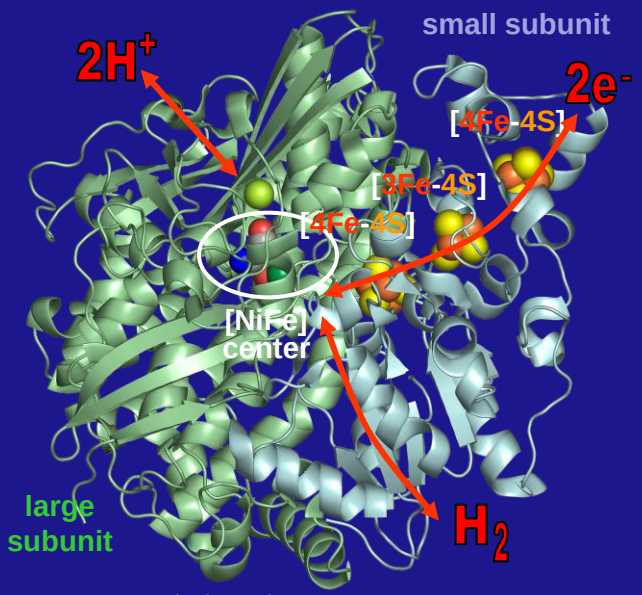

Ogata et al. (2005) Structure v13 pp. 1635-42

[FeFe] Hydrogenase

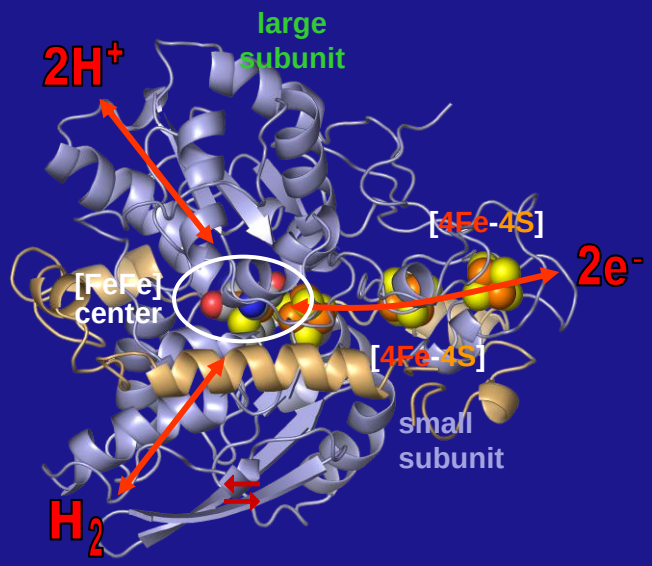

Nicolet et al. (1999) Structure Fold.Des. v7 pp. 13-23

Volbeda et al., 1995
Higuchi et al., 1997

$$H_2 \leftrightarrows H^- + H^+ \leftrightarrows 2H^+ + 2e^-$$

Peters et al., 1998
Nicolet et al., 1999

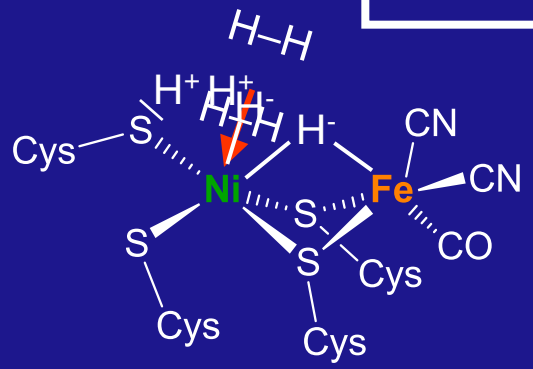

Desulfovibrio vulgaris Miyazaki F, PDB 1WUI

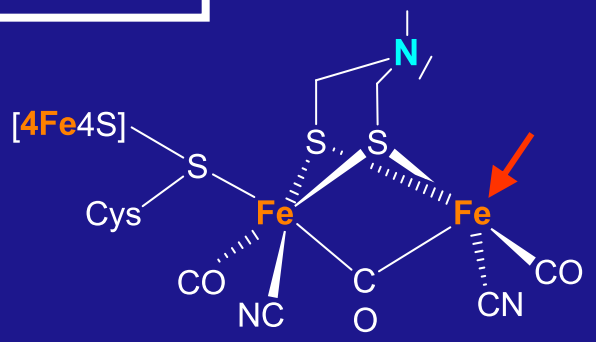

Desulfovibrio desulfuricans, PDB 1HFE

Hydrogenase Structure

$H^+ + H^- \rightleftharpoons H_2$

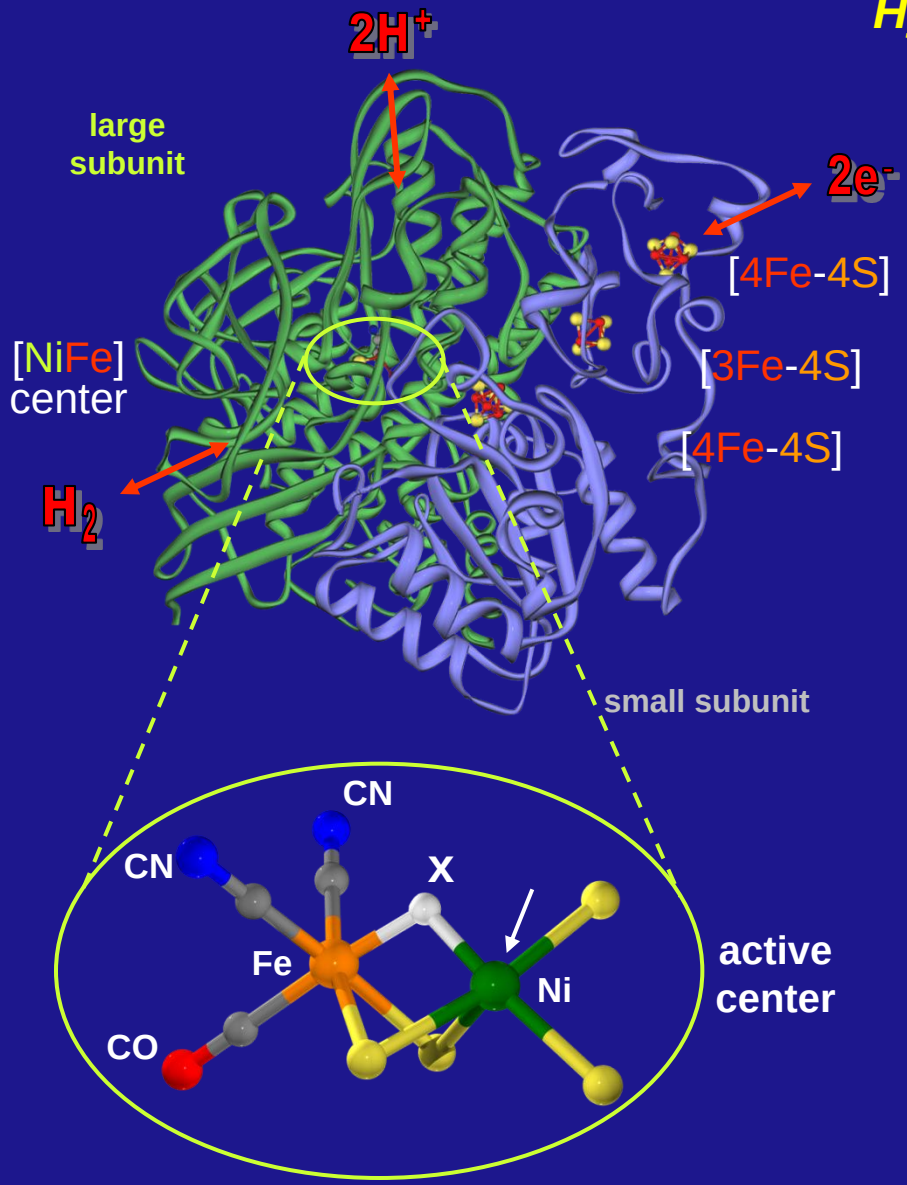

Structure of the active (hydrogen-carrying) intermediate

Hyperfine Spectroscopy: ENDOR & ESEEM

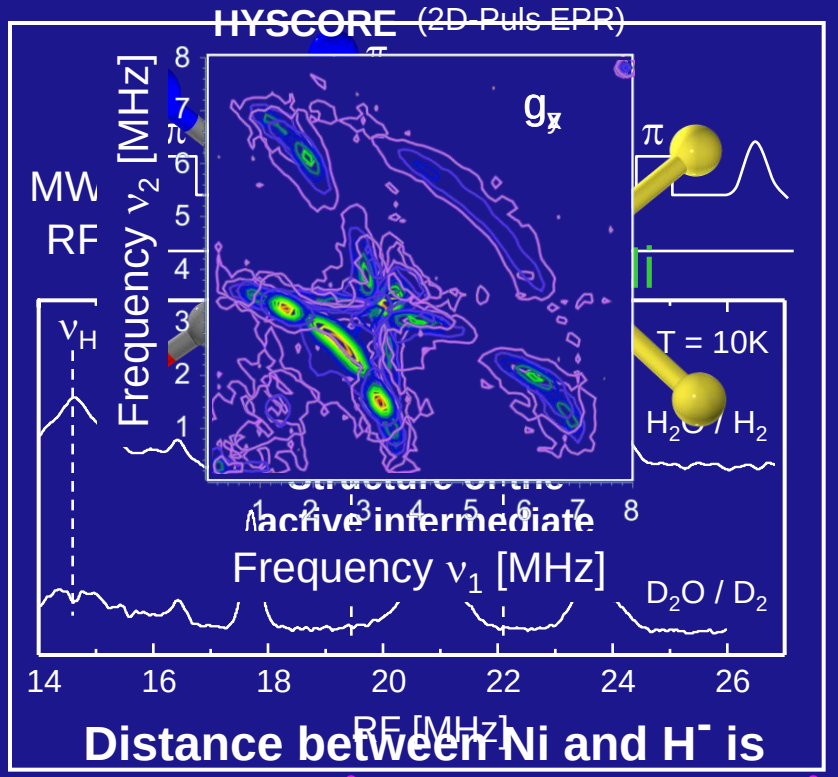

Distance between Ni and H^- is

d = (1.7 ± 0.1) Å and d = (1.8 ± 0.1) Å

between Fe and H^-

Ni-C (H/D exchange)

Brecht et al., JACS 2003

EPR and HYSCORE Spectra of Ni-C and Ni-L

H/D Exchanged NiFe-Hydrogenase RH of *R. eutropha*

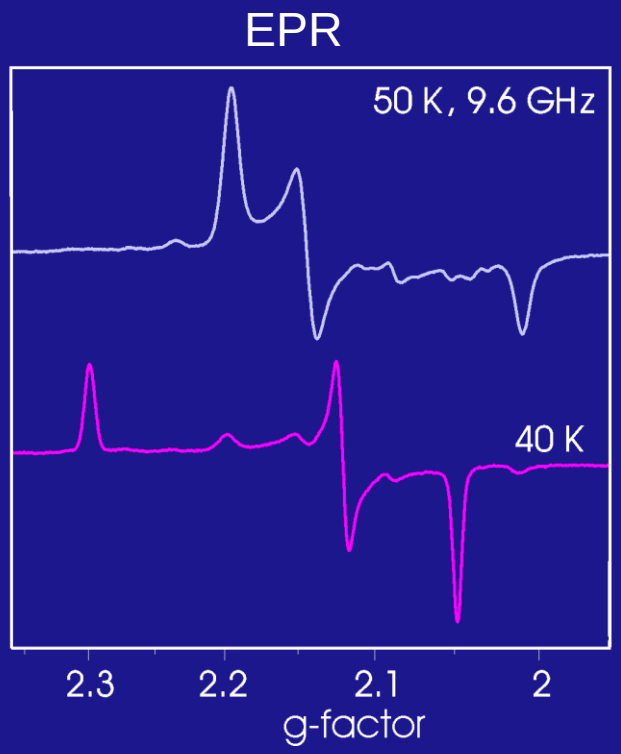

Ni-C

Ni-L

4-Pulse ESEEM

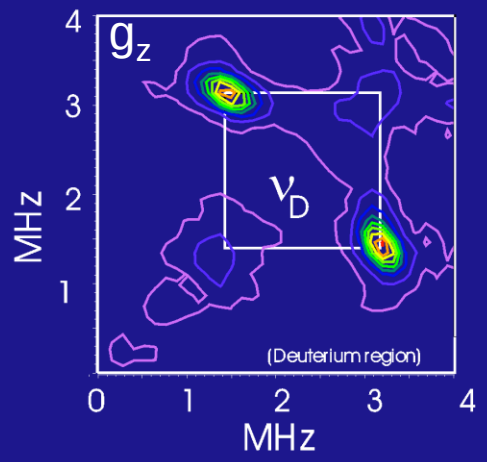

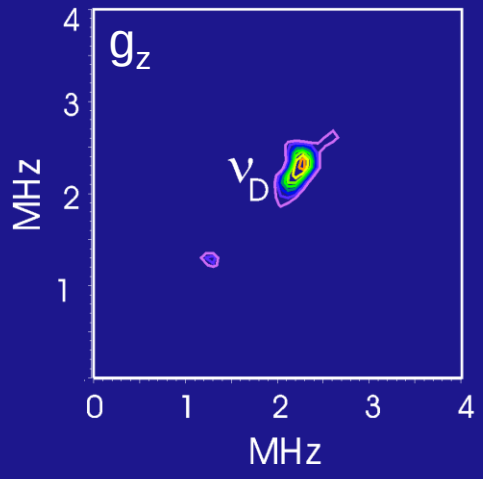

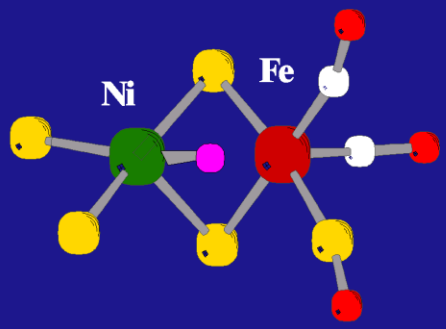

hν

20 min
white light

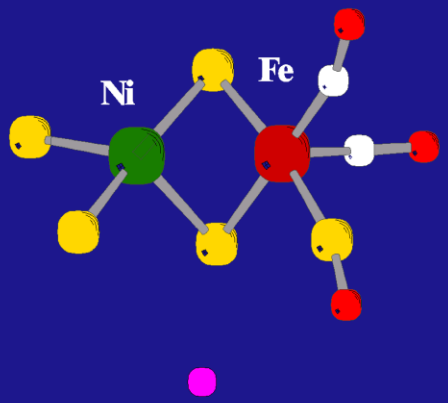

Brecht et al. JACS (2003)

ENDOR of Ni-L: H/D Exchanged, RH of *R. eutropha*

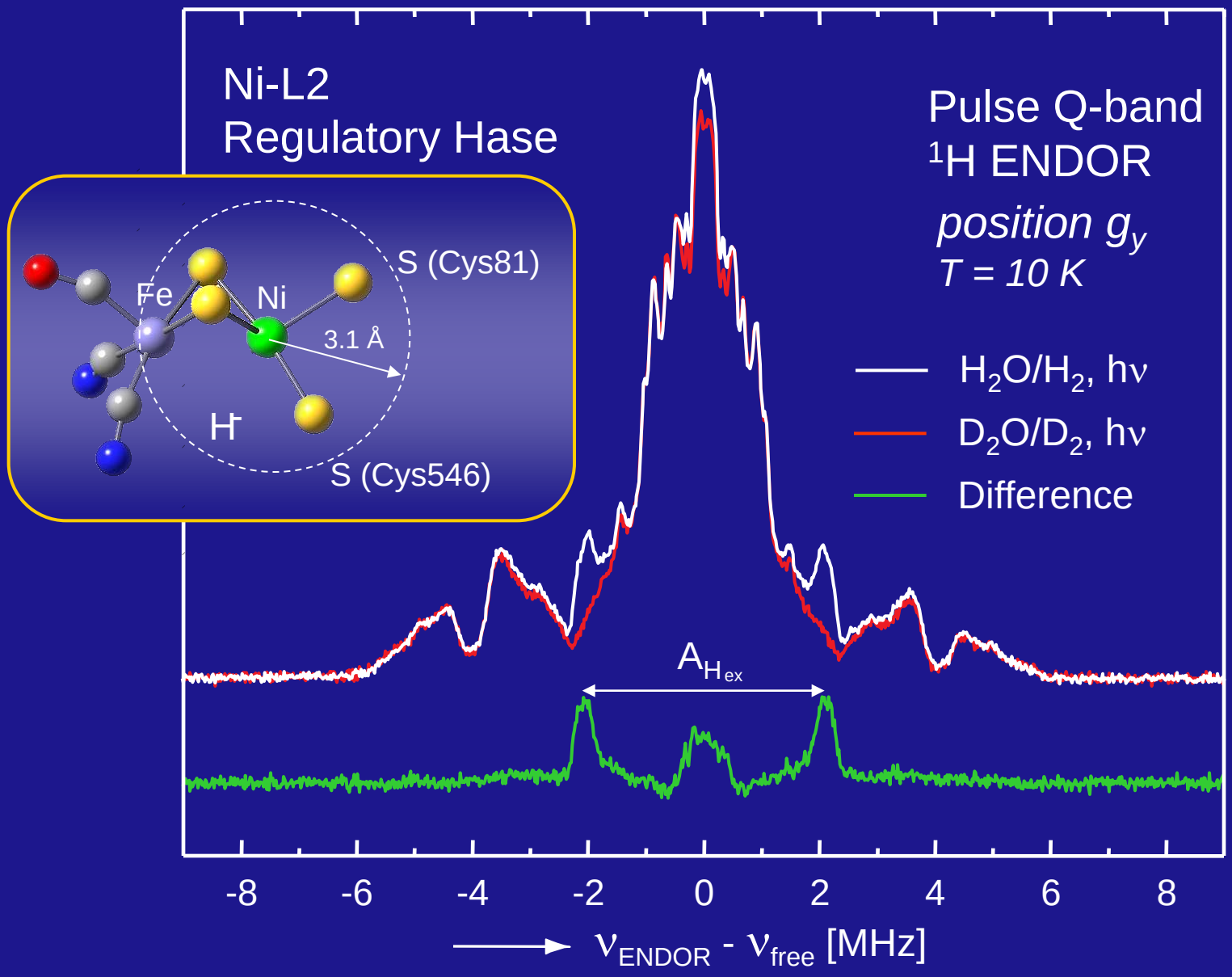

Flores et al. unpublished

Hydrogen Conversion Mechanism of [NiFe]-Hydrogenases

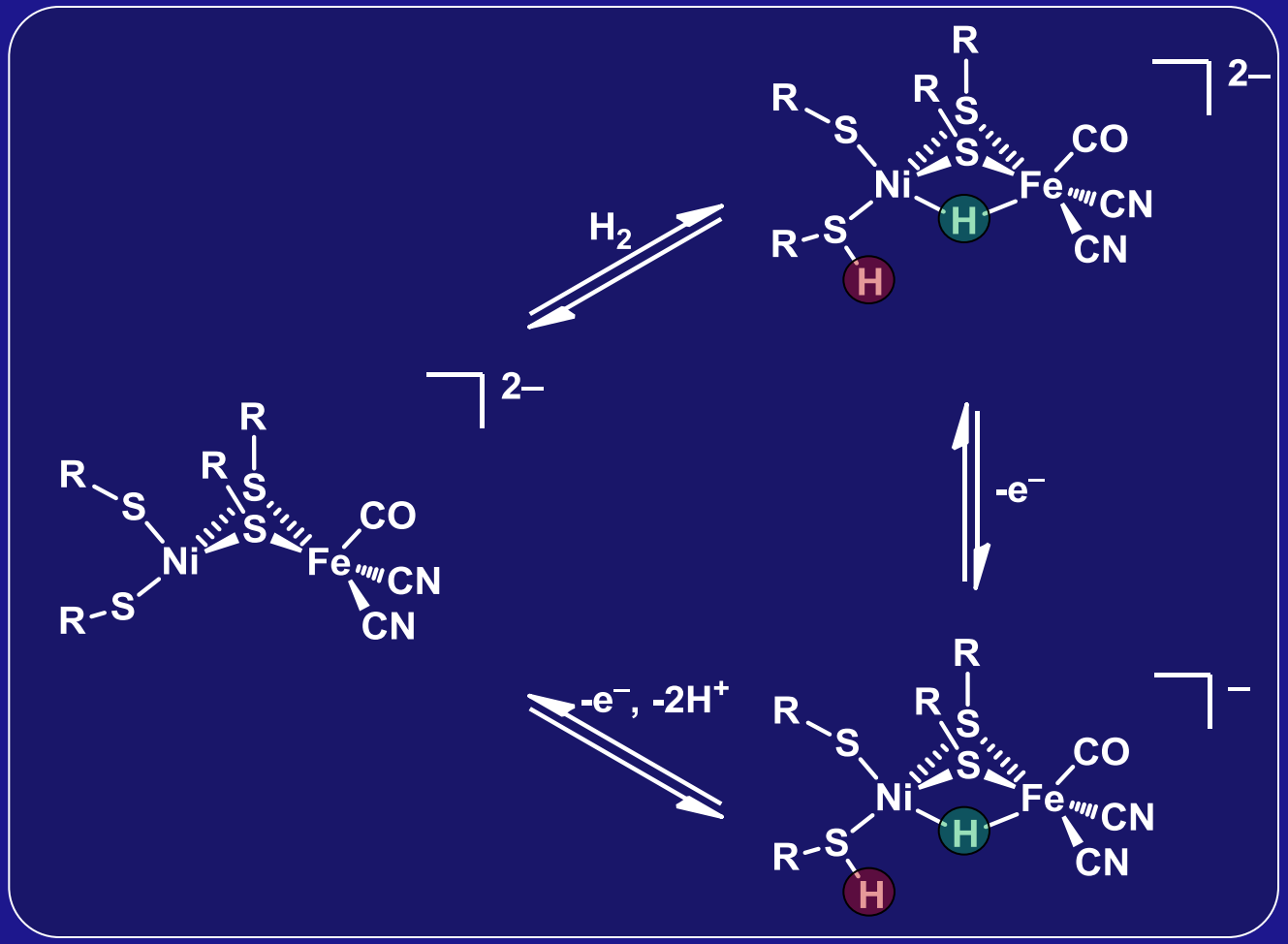

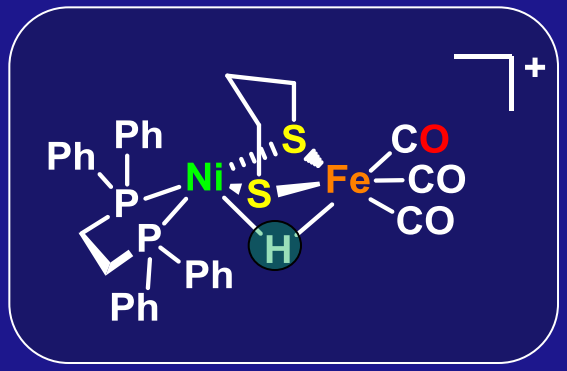

Rauchfuss et al. 2009
Shafaat et al. 2012

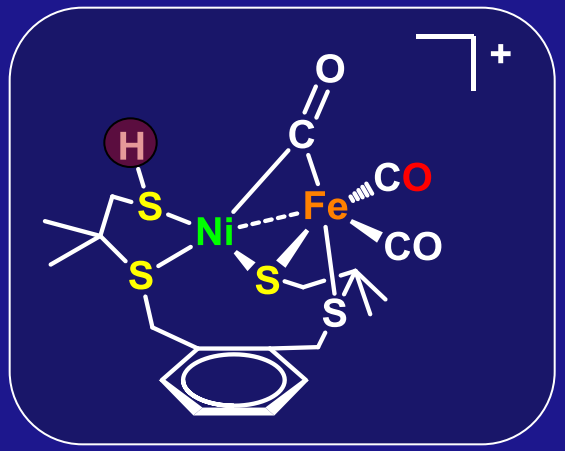

Weber et al. **2012, JACS**

L. De Gioia, P. Fantucci, B. Guigliarelli, P. Bertrand,Inorg. *Chem.* **1999**, *38*.

Reaction Scheme for Standard [NiFe] Hydrogenases

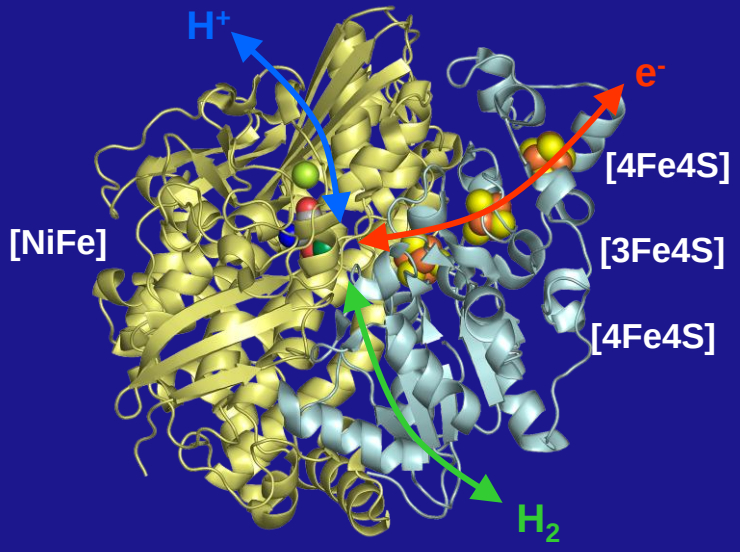

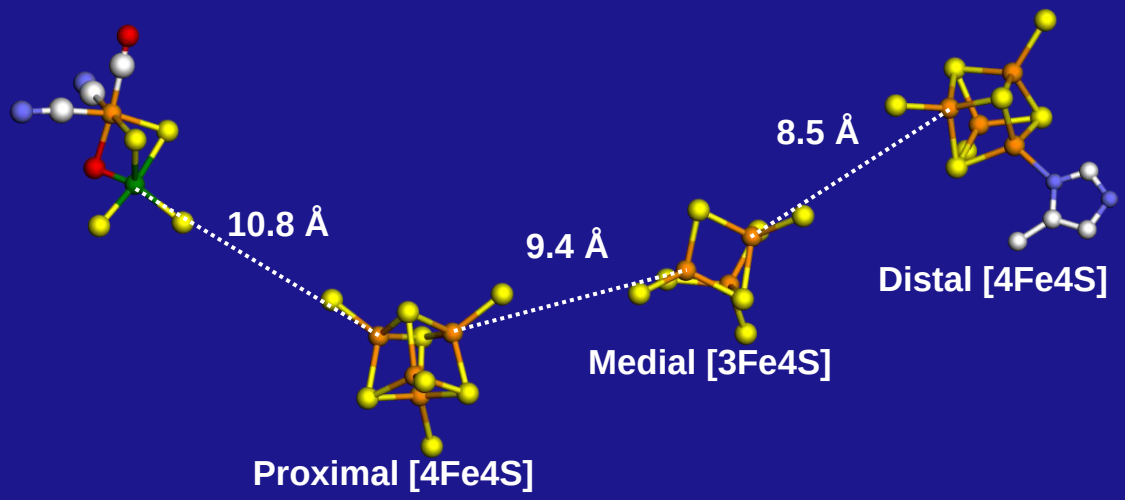

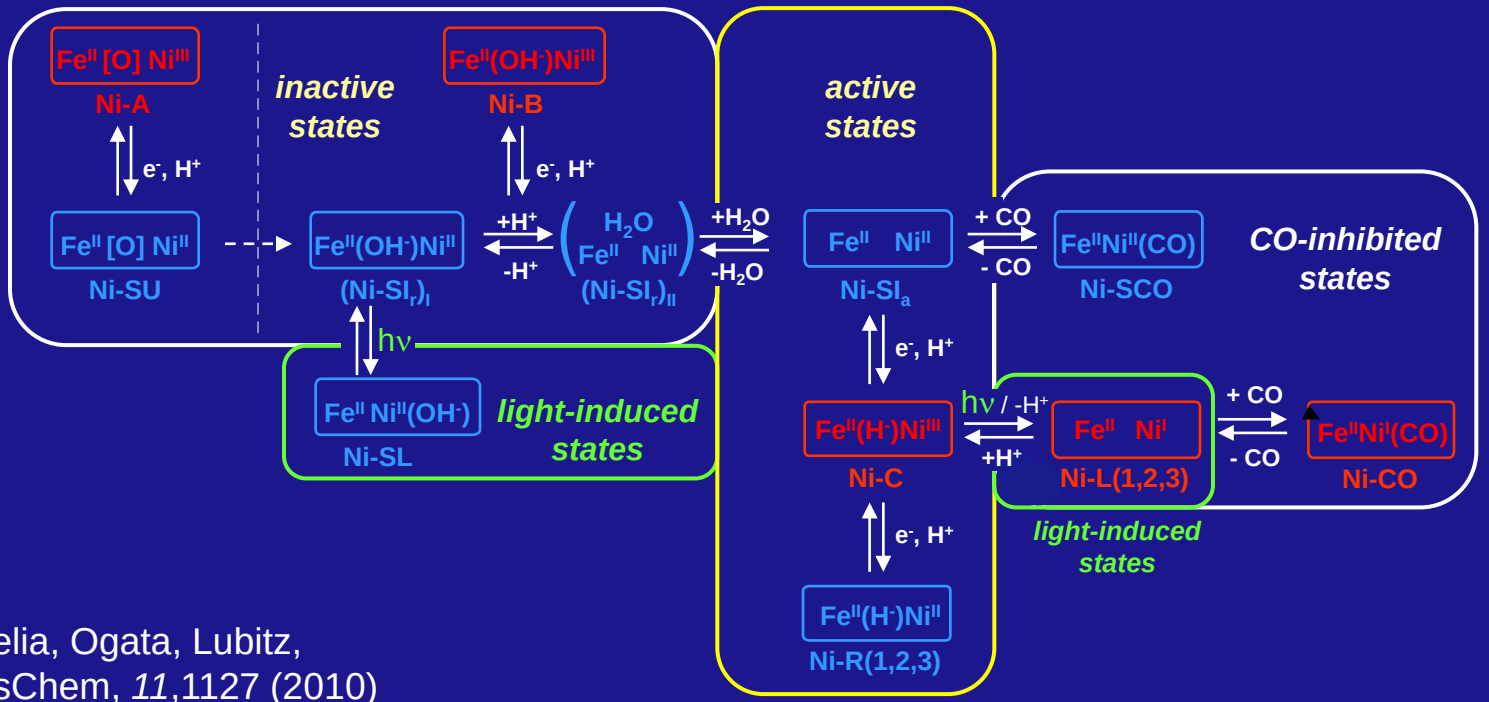

Pandelia, Ogata, Lubitz,
ChemPhysChem, *11*,1127 (2010)

[NiFe]- und [FeFe]-Hydrogenasen

[NiFe] Hydrogenase

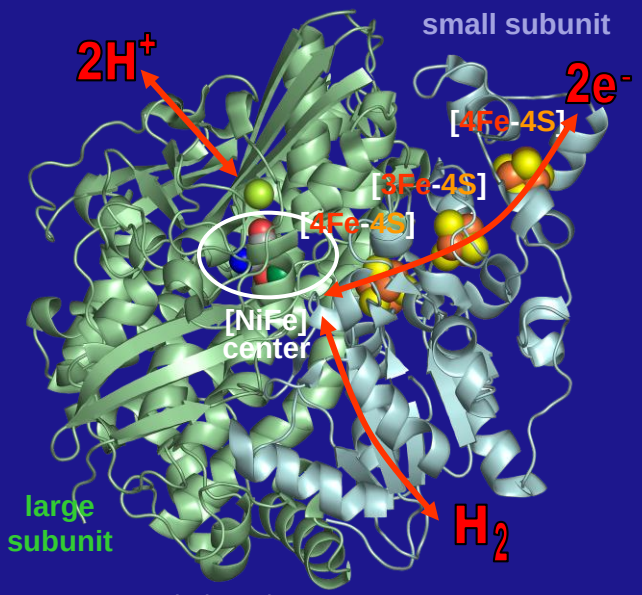

Ogata et al. (2005) Structure v13 pp. 1635-42

[FeFe] Hydrogenase

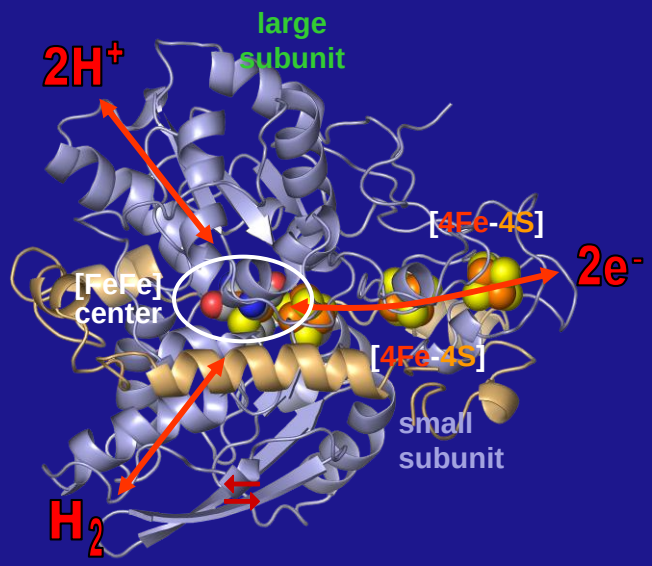

Nicolet et al. (1999) Structure Fold.Des. v7 pp. 13-23

Volbeda et al., 1995
Higuchi et al., 1997

$$H_2 \leftrightarrows H^- + H^+ \leftrightarrows 2H^+ + 2e^-$$

Peters et al., 1998
Nicolet et al., 1999

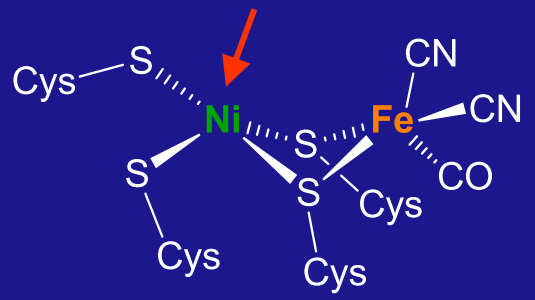

Desulfovibrio vulgaris Miyazaki F, PDB 1WUI

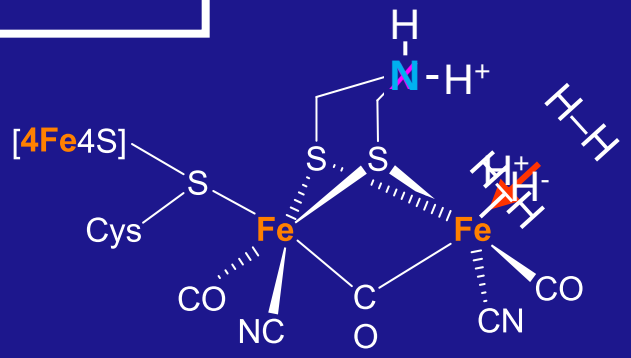

Desulfovibrio desulfuricans, PDB 1HFE

^{14}N in the dithiolate bridge:
Implications for the H_2 splitting mechanism

^{14}N HYSCORE

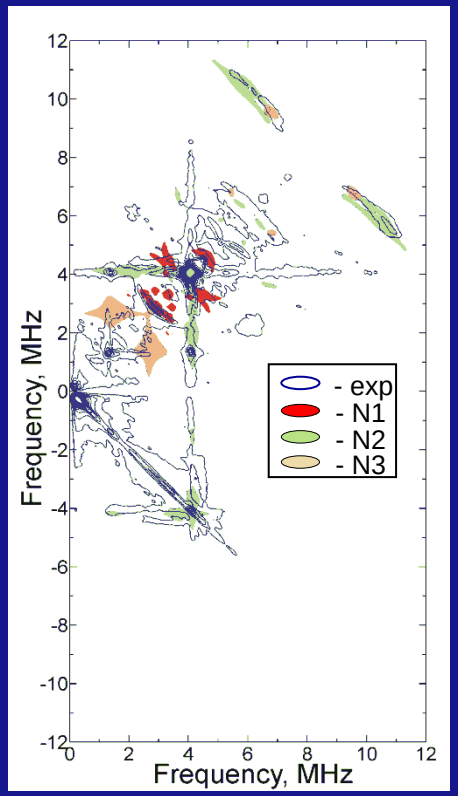

^{14}N detected via pulse EPR

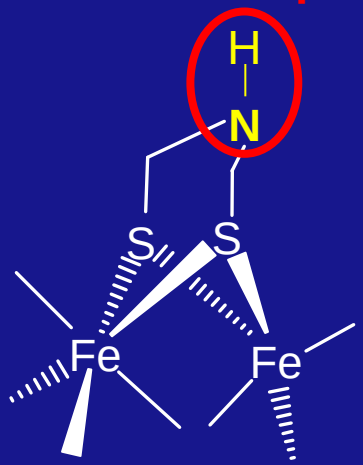

Silakov et al.
***PCCP* (2009)**

H_{ox}: $Fe(I)_pFe(II)_d$

H_{red}: $Fe(I)_pFe(I)_d$

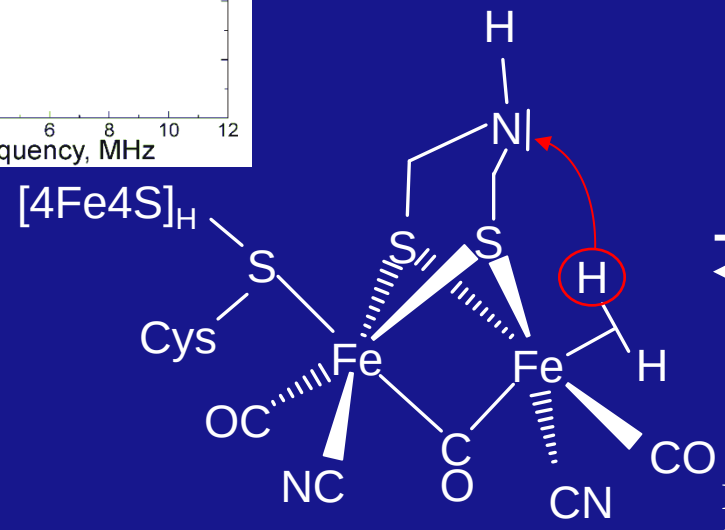

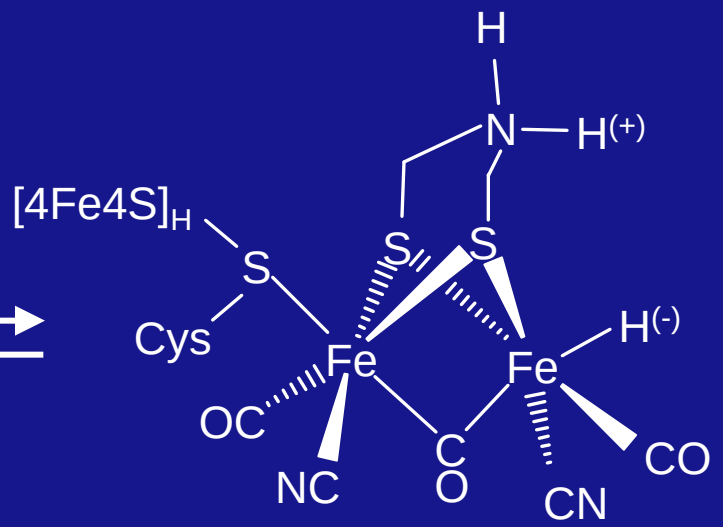

H.-J. Fan, M.B. Hall, J. Am. Chem. Soc. 123 (2001) 3828.
Z.-P. Liu, P. Hu, J. Am. Chem. Soc. 124 (2002) 5175.

[2Fe3S](PMe$_3$)$_2$ complex, ^{14}N & ^{15}N HYSCORE

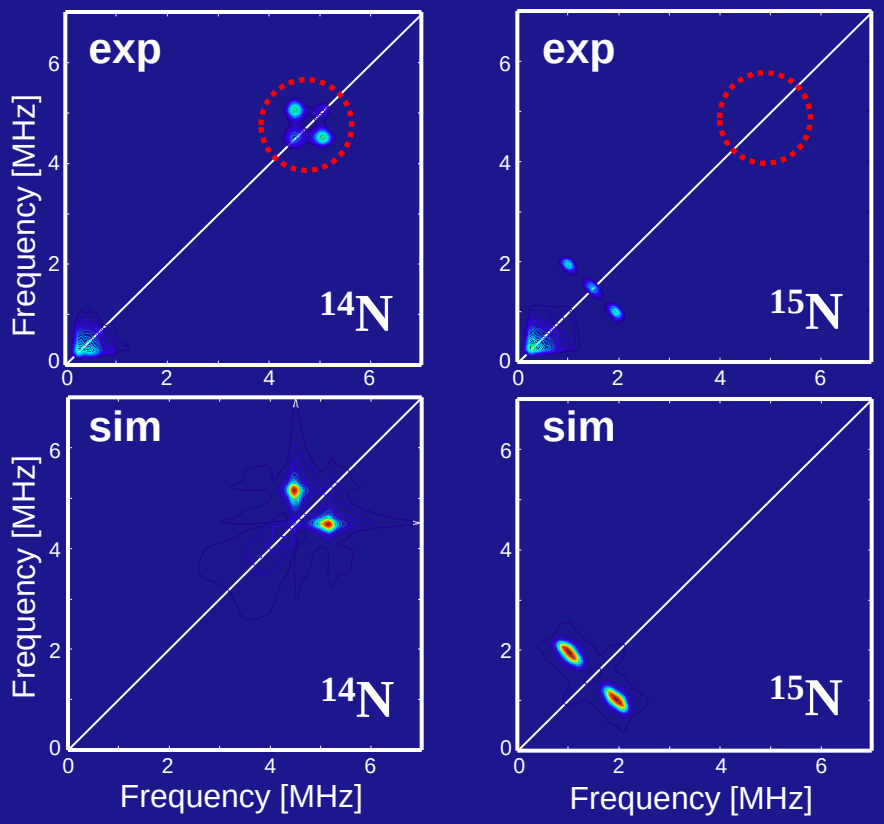

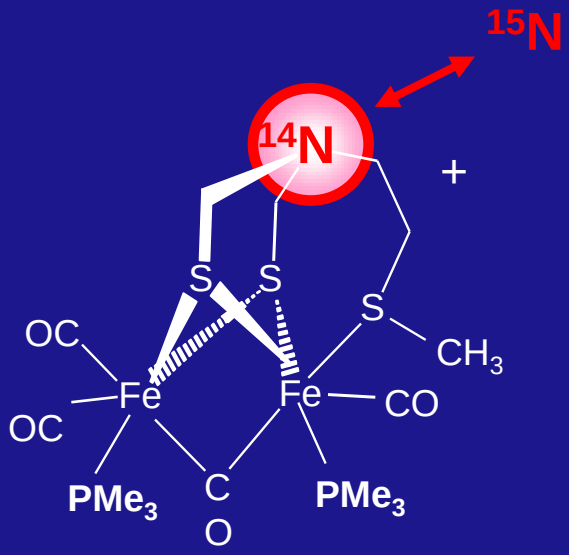

Ö Erdem, et al.
Angew. Chem. Int. Ed.
50, 1439 (2011)

Cooperation S. Ott (Uppsala)

	active site model compound	native system H_{ox} active site
A_N (x, y, z) [MHz]	(0.3, 0.8, 0.7)	(1.0, 1.9, 1.4)
A_{iso} [MHz]	0.6	1.43
K [MHz]	1.28	1.23
η	0.11	0.13

[FeFe] Hydrogenase: Proposed Catalytic Mechanism

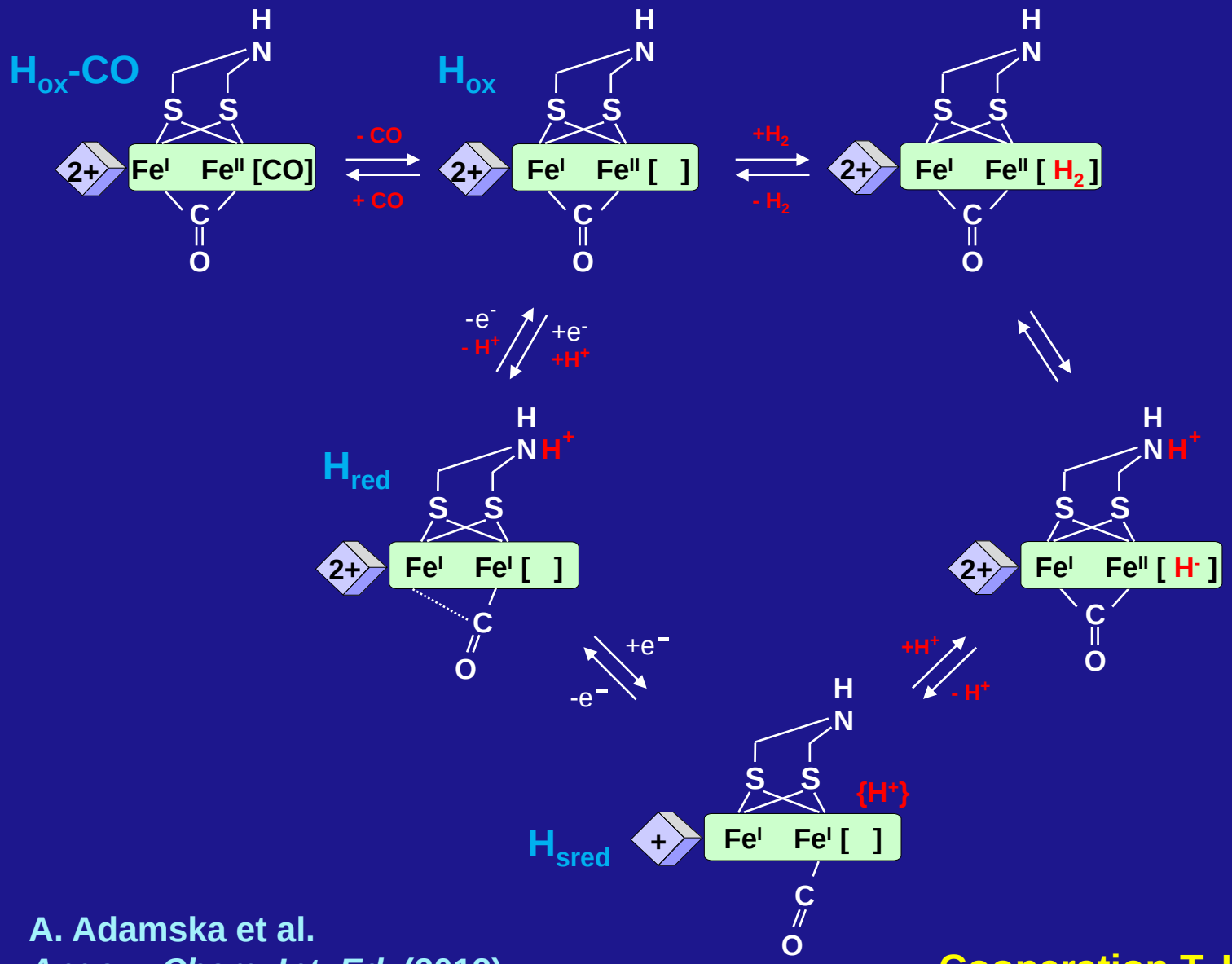

A. Adamska et al.
Angew. Chem. Int. Ed. (2012)

Cooperation T. Happe (Bochum)

Essential components of the hydrogen producing active site of [FeFe] hydrogenase:

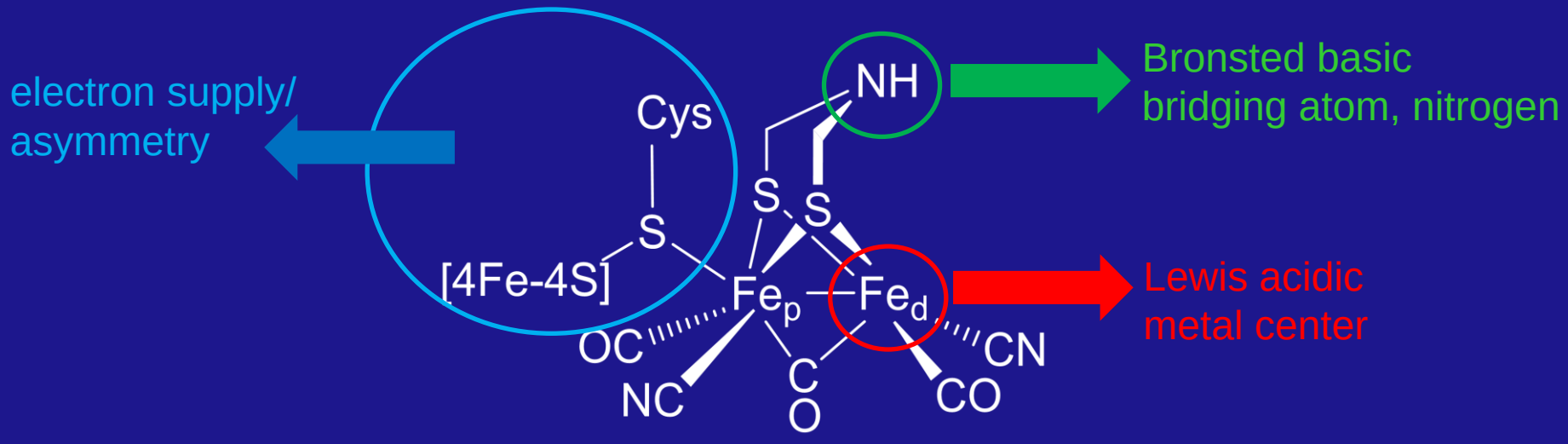

Design criteria for artificial hydrogenase catalysts:

Reaction: $H_2 \leftrightarrows H^- + H^+ \leftrightarrows 2H^+ + 2e^-$

A. **Metal center at optimal potential and spin state** (CN/CO ligands) to polarize H_2 for heterolytic splitting (open coordination site!) and accept hydride as ligand (hydride acceptor ability)

B. **Adjacent base** to accept proton (H^+ acceptor ability) in concert with metal

C. **Energetic matching** of metal and base acceptor reactions to ensure reversibility, avoid high energy intermediates and thereby achieve **higher rates** and **lower overpotentials** for both reactions

D. Provide efficient delivery of educts and transport of products (solvent; water; **smart matrix**) and efficient, optimized **electron transport** chain

E. Solve problem of **oxygen sensitivity**

F. Solve problem of degradation **(self-repair, self-healing, simplicity)**

F. Integrate into a **device** for (sun) light harvesting, charge separation/transport, water oxidation catalysis
– including a membrane system (H+, e-/h+ movement)

A Synthetic Nickel Electrocatalyst with a Turnover Frequency Above 100,000 s^{-1} for H_2 Production

Monte L. Helm,[1,2]* Michael P. Stewart,[1] R. Morris Bullock,[1]†
M. Rakowski DuBois,[1] Daniel L. DuBois[1]†

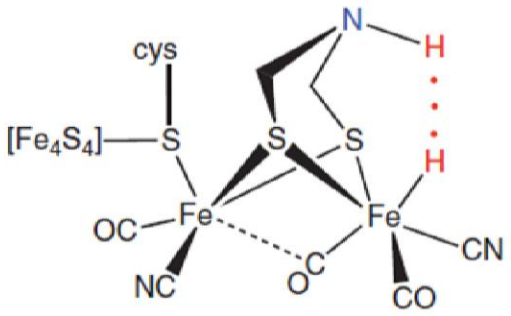

1

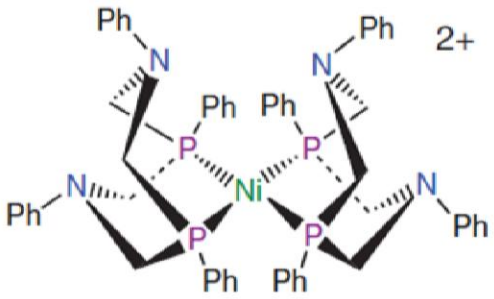

2

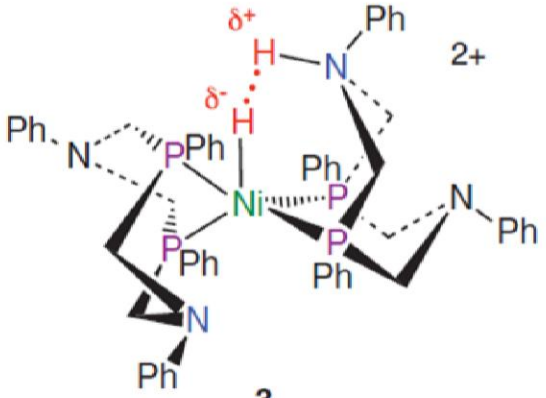

3

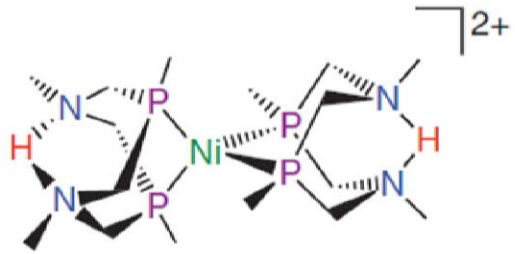

4

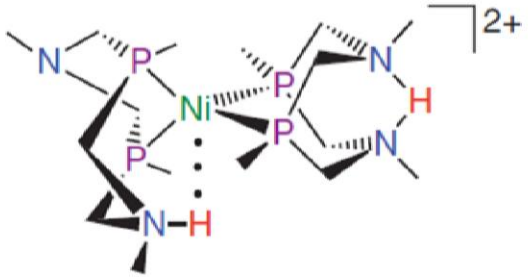

5

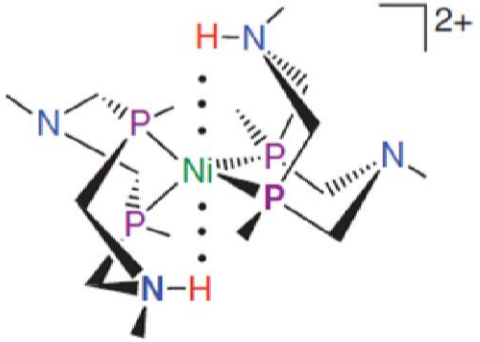

6

Science, 2011,333, 863

Angewandte
Communications

Hydrogen Catalysis

DOI: 10.1002/anie.201108461

Reversible Electrocatalytic Production and Oxidation of Hydrogen at Low Overpotentials by a Functional Hydrogenase Mimic**

Stuart E. Smith, Jenny Y. Yang, Daniel L. DuBois,*

Previous studies in our laboratory have focused on the synthesis and catalytic performance of functional hydrogenase mimics.[6] Our studies have focused on iron,[7] cobalt,[8] and nickel[9] complexes with the diphosphine ligand $P^R_2N^{R'}_2$ shown in Scheme 1, where R is the substituent on phosphorous, and R′ is the substituent on nitrogen. From our experimental and theoretical[10] studies on $[Ni(P^R_2N^{R'}_2)_2]^{2+}$ derivatives, we have established how steric and electronic properties of the R and R′ substituents affect the hydride acceptor and proton acceptor abilities of these complexes. These two quantities determine the free-energy of hydrogen addition to these complexes. The ability to vary these properties by varying substituents on the ligand has led to the design of catalysts that are biased towards hydrogen production[9] or hydrogen oxidation[11] by adjusting the free-energy for hydrogen addition to be either positive or negative, respectively.

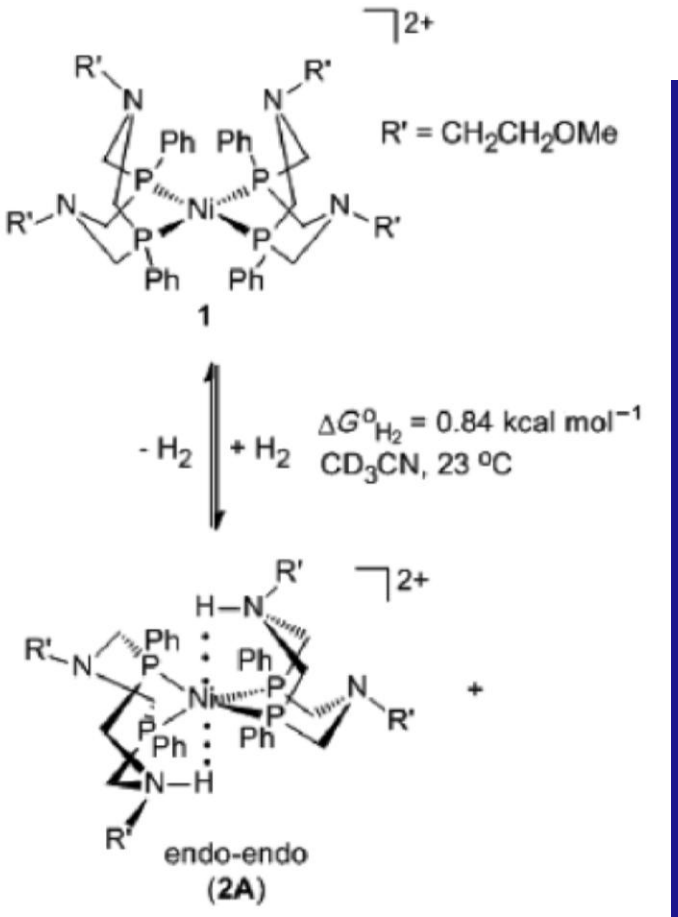

Some Unsolved Problems:

1. **Oxygen sensitivity of catalysts**
2. Self-assembly & self-repair - long term stability
3. Fast rates TOF
4. Low overpotential
5. Interfacing (e.g. to electrodes) – development of linkers
6. Combination with water oxidizing catalysis
7. Combination with (sun) light induced processes (antenna, charge separation etc.)
8. Costs – materials, difficulty of synthesis

Oxygen Inhibition of Hydrogenases

E=+150 mV vs NHE
40ºC, pH 6.0
2500 rpm, 1 bar H_2

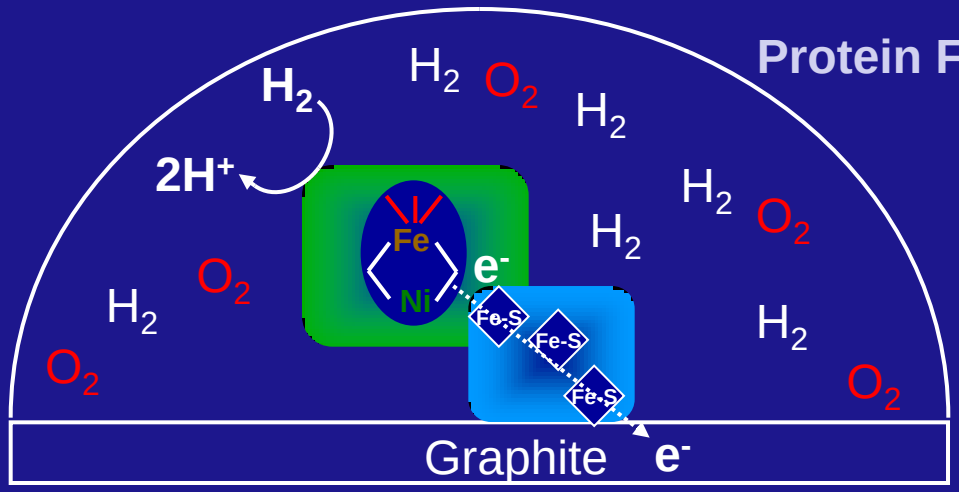

E=+150 mV vs NHE
40ºC, pH 6.0
2500 rpm, 1 bar H_2

[NiFe] Hydrogenase *D. vulgaris* MF

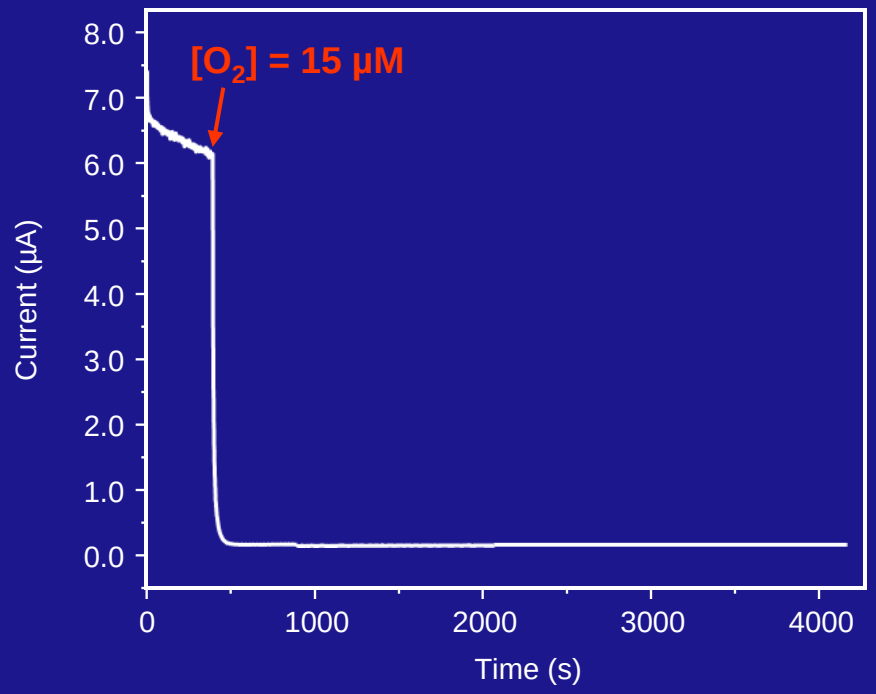

[NiFe] Hydrogenase *A. aeolicus*

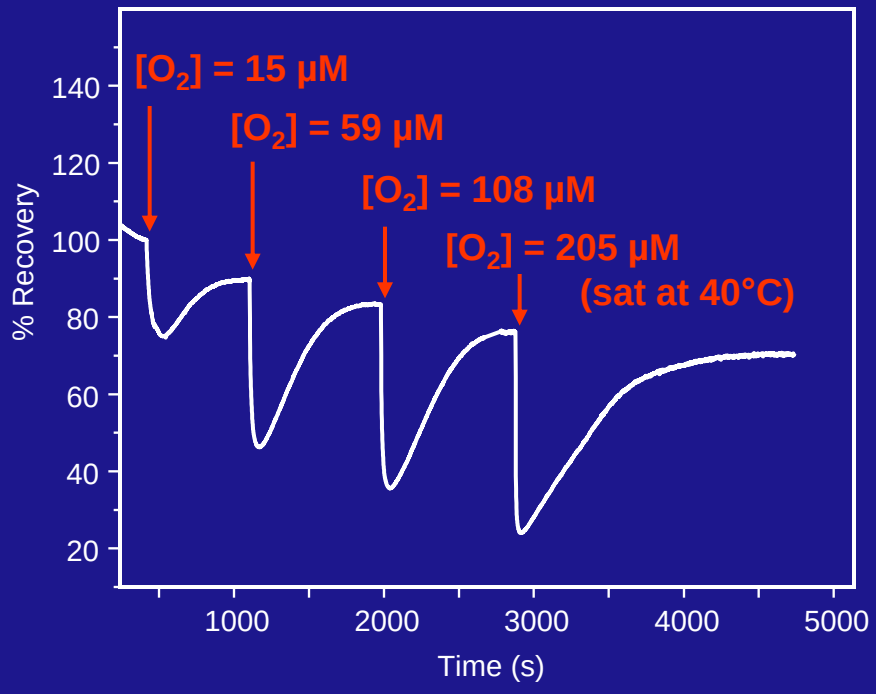

Oxygen Tolerance of [NiFe] Hydrogenases

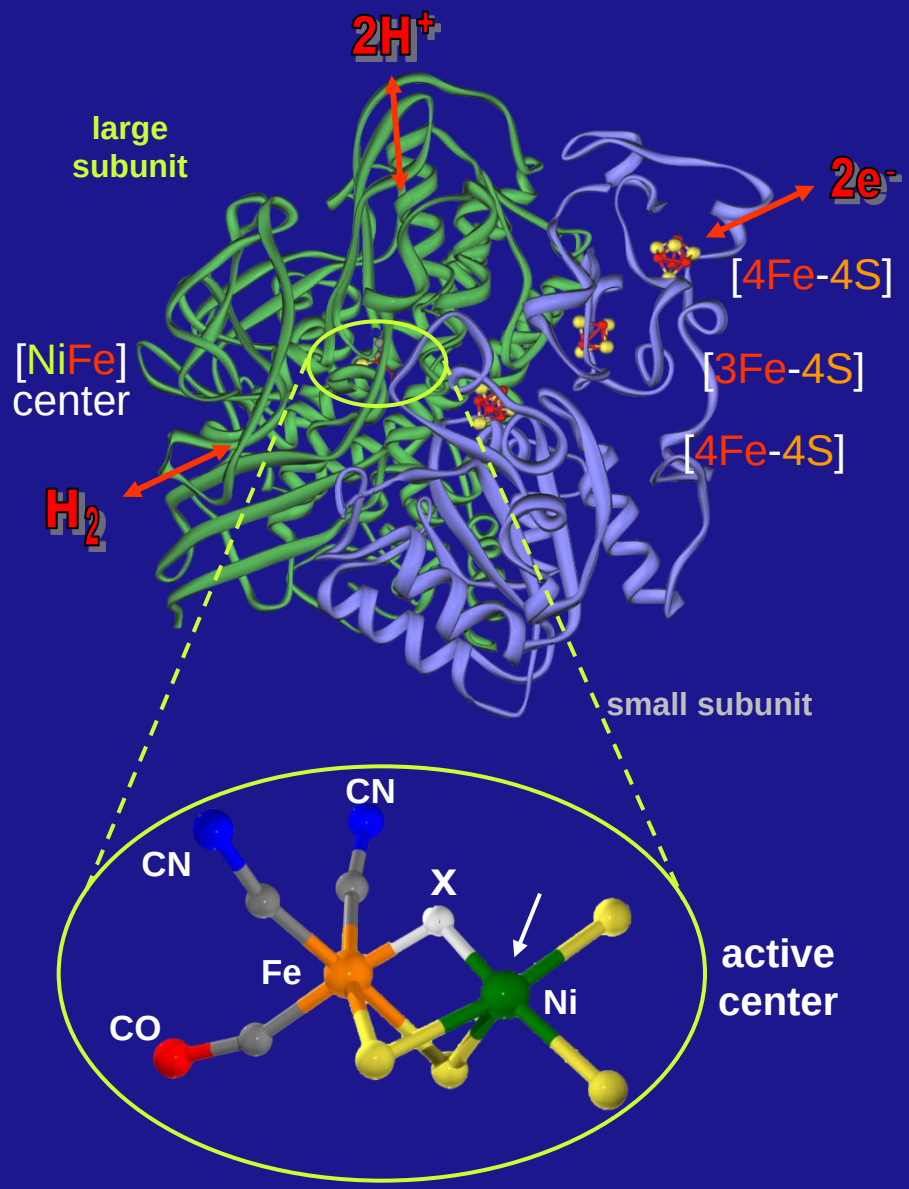

1. Narrower **gas access** channel
2. Blockage of **active site** by additional ligands (CN^-)
3. Modification of redox potentials of the active site and the electron transport components (proximal **4Fe4S-cluster**)

EPR Redox Titration of the FeS Clusters in *A. aeolicus*

4 distinct EPR species

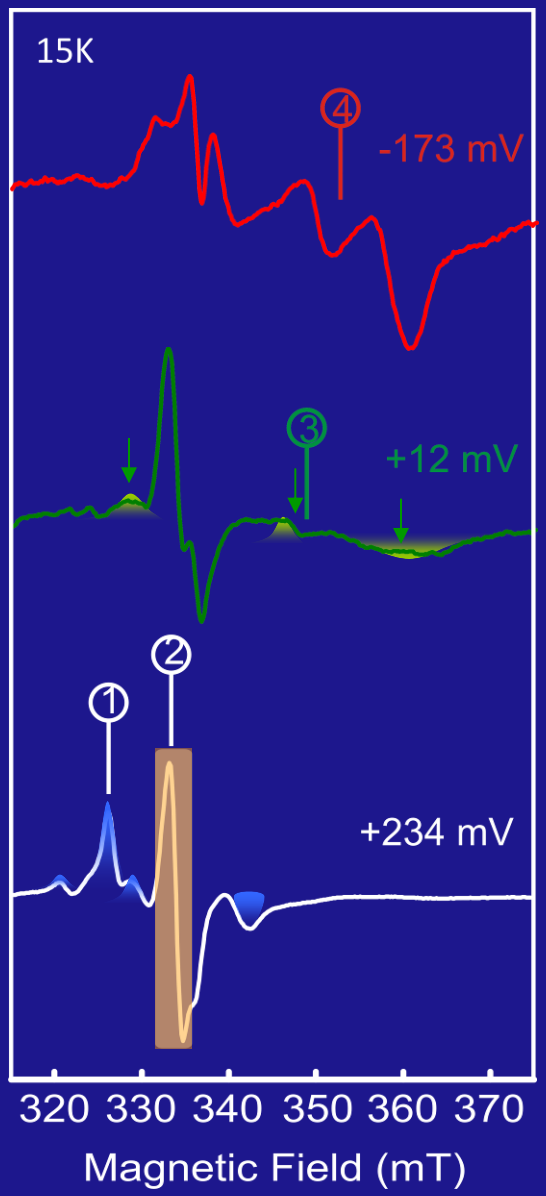

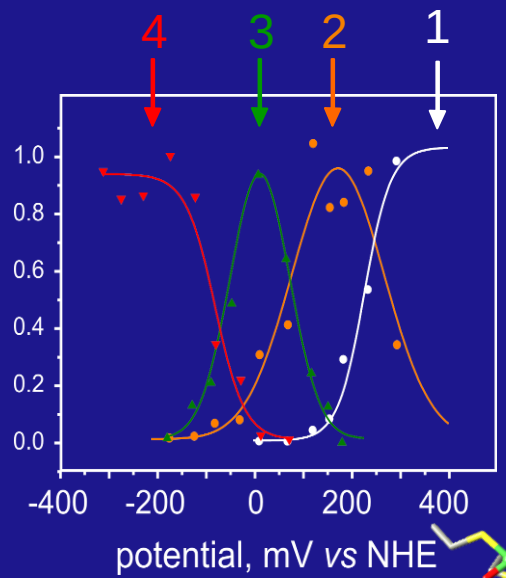

Pandelia et al., PNAS 2011

2 e⁻ (!) **1 e⁻** **1 e⁻**

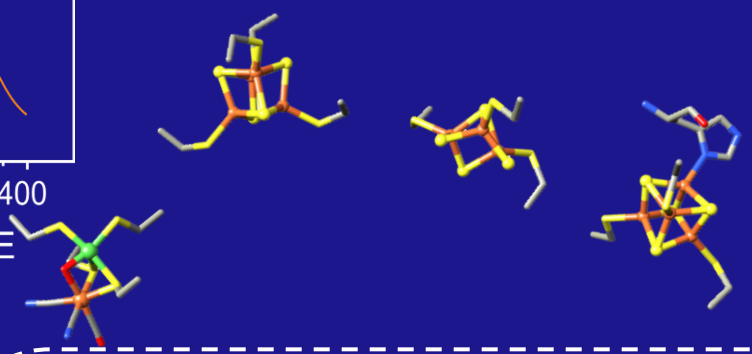

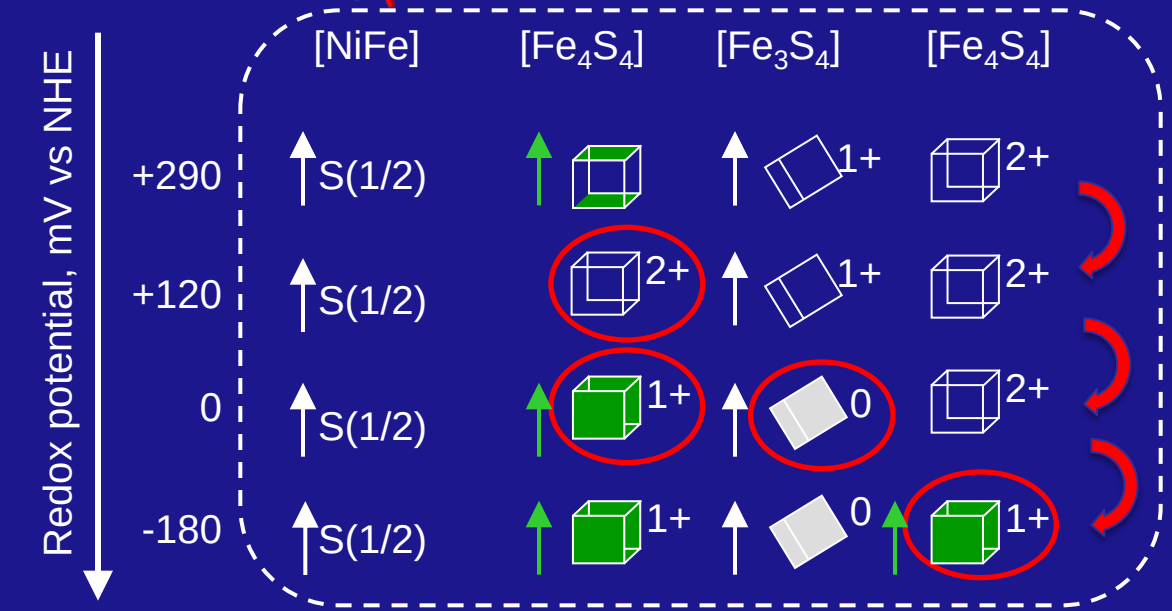

Sequence Alignment Showing Binding of the Proximal FeS Cluster

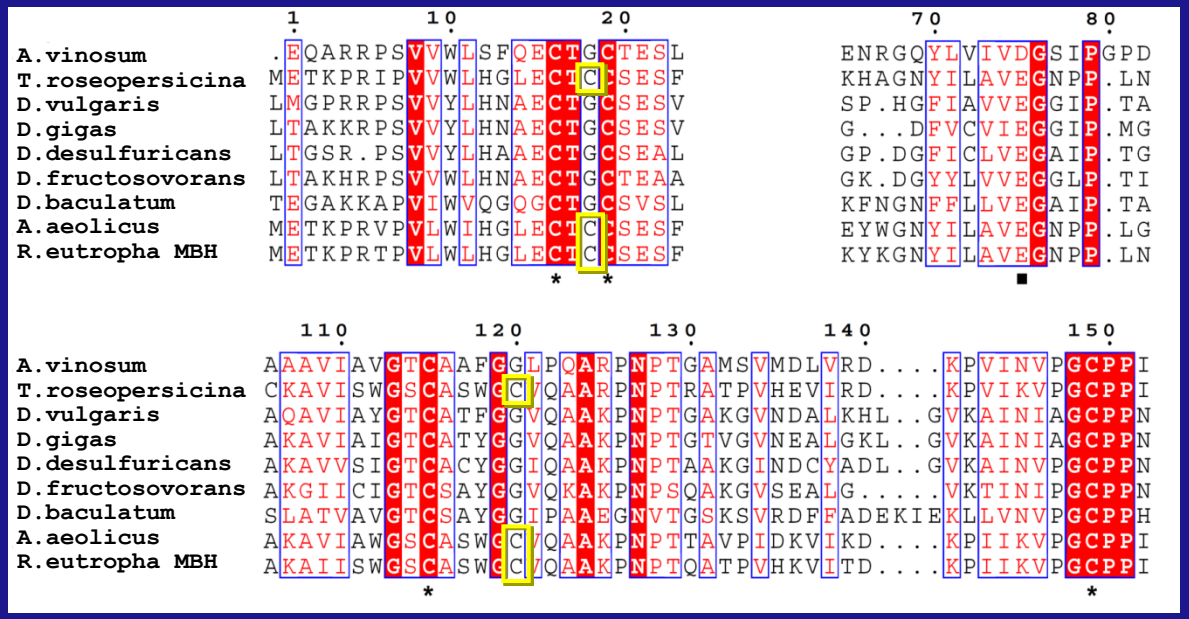

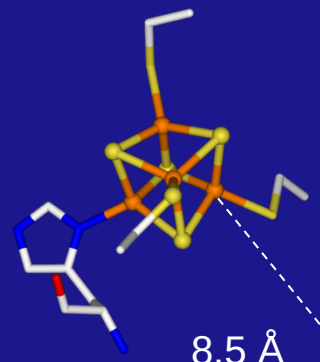

$[Fe_4S_4]$ distal

8.5 Å

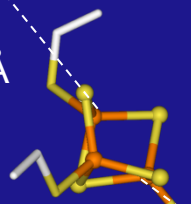

$[Fe_3S_4]$ medial

Electron transfer chain in standard enzymes

9.5 Å

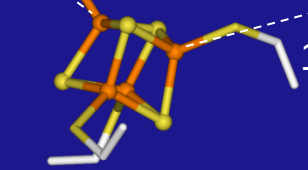

$[Fe_4S_4]$ proximal

10.8 Å

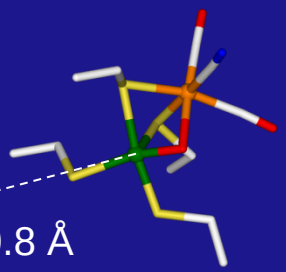

[NiFe] site

Proximal 4Fe4S-cluster in *A. aeolicus*

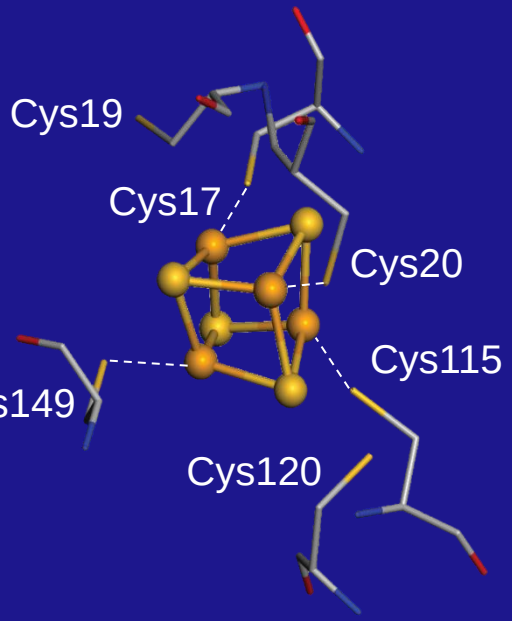

Proximal [4Fe-3S] Cluster: Mössbauer Analysis

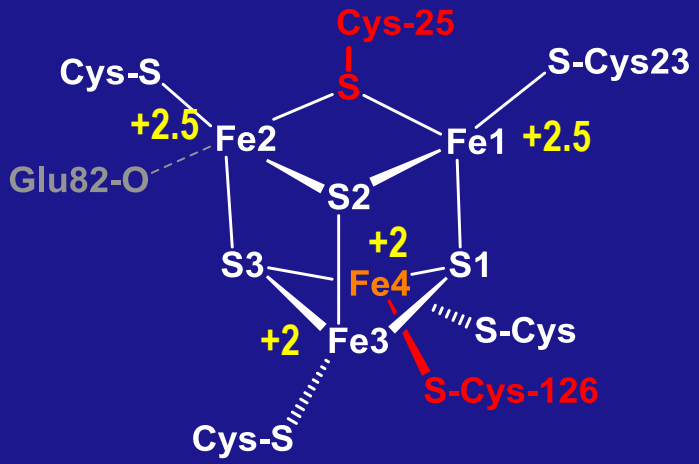

reduced
S_{tot} = 1/2

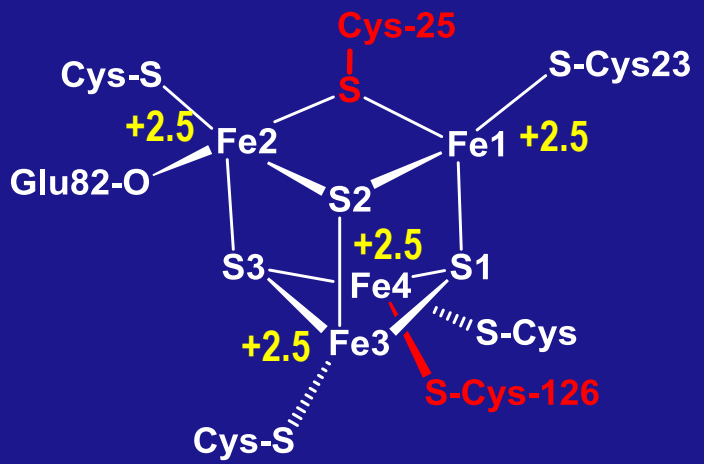

oxidized
S_{tot} = 0

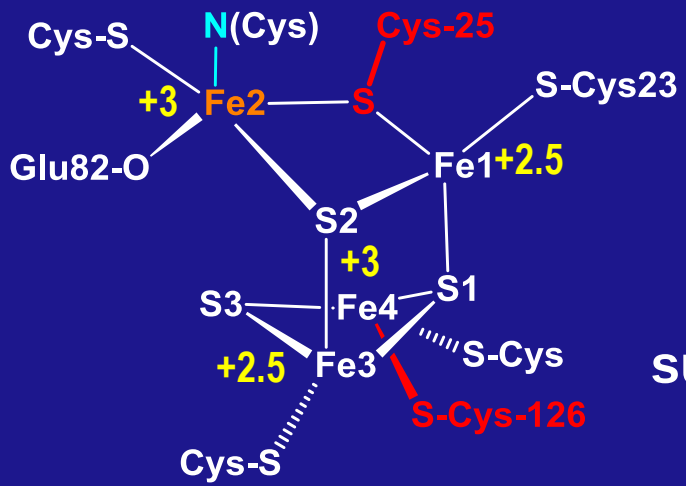

superoxidized
S_{tot} = 1/2

Pandelia et al. (2013)
PNAS

Hydrogenase Catalysis in the Presence of Oxygen

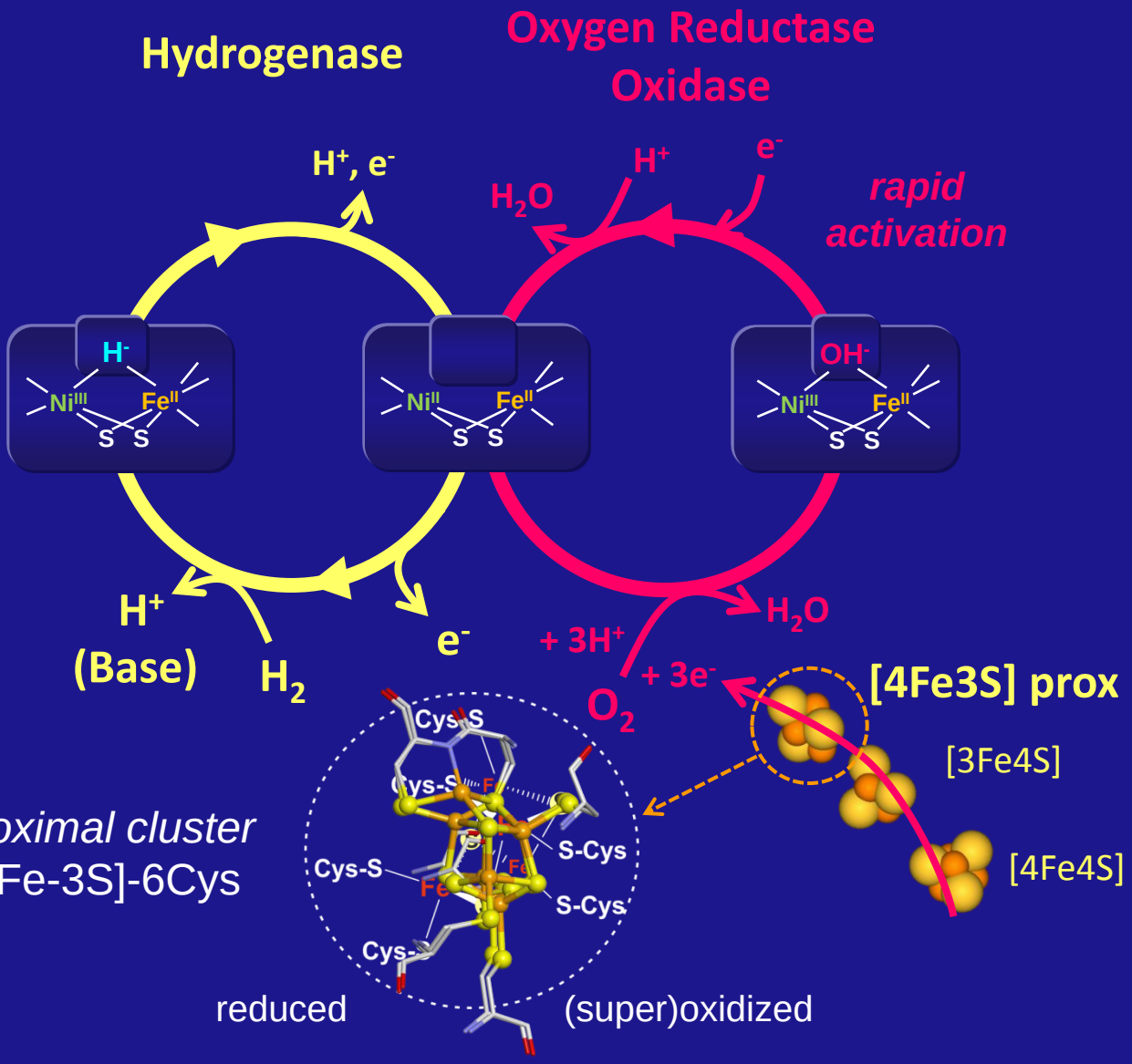

Cracknell et al. *PNAS* (2009); Goris et al. *Nature Chem. Biol.* (2011)

Acknowledgements

Hydrogenases

[NiFe] Hydrogenases and related model systems:


Rüdiger

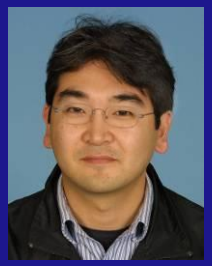
Ogata


Kellers


Pandelia


Flores


van Gastel


Stein


Bill


Fichtner


Shafaat


Nishikawa


Weber

Christof Geßner
Marc Brecht
Stefanie Foerster
Olga Trofanchuk

[FeFe] Hydrogenases and related model systems:


Reijerse


Silakov


Wenk


Erdem


Kamp

Cooperations:

Y. Higuchi (Hyogo)
B. Friedrich (Berlin)
S. Albracht (Amsterdam)
MT. Giudichi-Orticoni (Marseille)
T. Rauchfuss (Urbana, Ill.)

Support:
European Union NEST: SOLAR-H2, Alexander von Humboldt Foundation, Max Planck Society

Acknowledgements

Wateroxidase

Spectroscopy


Kulik


Epel

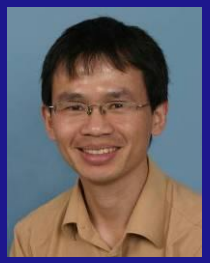
Su


Rapatskiy


Lohmiller


Cox


Pérez Navarro

Crystallography & Preparations


Krause

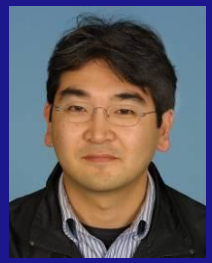
Ogata


Sander

Theory


Neese


Ames


Krewald


Pantazis


Orio

Cooperations

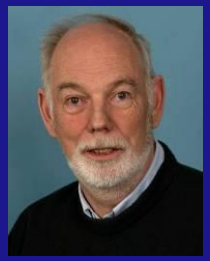
Wieghardt


Weyhermüller


Messinger (Umeå)


Boussac (Saclay)


Rögner (Bochum)


Nowaczyk (Bochum)

Support:

European Union NEST: SOLAR-H2, Alexander von Humboldt Foundation, Max Planck Society


Thank you for your attention!